

Disinfestation of rusty grain beetle (*Cryptolestes ferrugineus*) in stored wheat grain using 50-ohm radio frequency (RF) heating system

A Thesis Submitted to the

College of Graduate and Postdoctoral Studies in
Partial Fulfillment of the Requirements for the Degree of

Master of Science (M.Sc.)

In the

Department of Chemical and Biological Engineering

University of Saskatchewan

By

Roland Macana

©Copyright Roland Macana, April 2019. All rights reserved.

PERMISSION TO USE STATEMENT

In presenting this thesis in partial fulfillment of the requirements for a master of science from the University of Saskatchewan, I agree that the Libraries of this University may make it freely available for inspection. I further agree that permission to copy this thesis in any manner in whole or in part, for scholarly purposes may be granted by Dr. Oon-Doo Baik who supervised my thesis work, or in his absence, by the Dean of the College of Engineering. It is understood that any copying, publications, or use of this thesis or parts thereof for financial gain shall not be allowed without my written permission. It is also understood that due recognition shall be given to me and to the University of Saskatchewan in a scholarly use which may be made of the material in my thesis. Request for permission to copy or to make other use of material in this thesis in whole or part should be addressed to:

Head of the Department of Chemical and Biological Engineering
University of Saskatchewan
3B48 Engineering Building 57 Campus Drive,
Saskatoon, Saskatchewan
Canada S7N 5A9

OR

Dean of the College of Graduate and Postdoctoral Studies
University of Saskatchewan
116 Thorvaldson Building 110 Science Place,
Saskatoon, Saskatchewan
Canada S7N 5C9

GENERAL ABSTRACT

Non-chemical methods were proposed as alternatives for disinfestation of stored grains using fumigants and pesticides. Therefore, this thesis investigated the disinfestation of rusty grain beetle (*Cryptolestes ferrugineus*) in stored wheat grain using electromagnetic energy from 50-ohm radio frequency (RF) heating system. The objectives of this current study were to update the research outcomes of disinfestation using electromagnetic energy; investigate the installation process of the 50-ohm RF heating system; design and fabricate the parallel plate applicator; determine the mortality of rusty grain beetle; estimate parameters of thermal death kinetics during the RF heating of insects in stored grain; compare the quality of wheat grain before and after RF heating; and determine the heating uniformity in the designed applicator. The review showed that using electromagnetic energy for disinfestation might be possible without degrading the quality of the host materials. RF energy for disinfestation, however, was being preferred over microwave energy for its higher selective heating characteristics. The 100% mortality rates of adult rusty grain beetle were found at all moisture contents of the bulk wheat grain at the end temperatures of 70°C and 80°C. It was observed also that the complete mortalities at all life stages of the insects were achieved at 80°C target temperature at three moisture contents (12%, 15%, and 18%) of the bulk wheat samples. The simulated mortalities based on the model were in good agreement with the experimental mortalities. The determined thermal death kinetic parameters, E_a , K_0 , and n were 97,490 J/mol, 6.74×10^{13} 1/s, and 1, respectively. The results showed that disinfestation of insect pests in wheat grain using 50-ohm RF heating did not degrade the quality of the host material significantly. Nevertheless, the RF heating in the applicator was not uniform at all moisture

contents and power levels. The temperature differences between the hottest and coldest spots at different MCs and power levels were 38.6°C at 3 kW, 38.7°C at 5 kW, and 39.1°C at 7 kW (12% MC) and 43°C at 3 kW, 43.6°C at 5 kW, and 41.9°C at 7 kW (18% MC). Non-uniform heating in the RF applicator has been a challenge in disinfestation using electromagnetic energy. Thus, suggestions for future studies were provided to solve the problem of heating uniformity in the applicator and the guidelines for a successful installation of 50-ohm RF heating system for disinfestation of insects in stored agricultural materials.

ACKNOWLEDGMENTS

I would like to express my heartfelt gratitude to my supervisor Professor Oon-Doo Baik for his priceless guidance, encouragement, and unwavering support in various ways during my study. I would like to acknowledge the members of my Graduate Advisory Committee, Professors Lope Tabil, and Venkatesh Meda for helping me and providing me constructive comments during the course of my research work. I am also thankful to Professor Bob Tyler for serving as the external examiner and giving me helpful comments.

I gratefully acknowledge the Saskatchewan Ministry of Agriculture and the Western Grains Research Foundation, Saskatchewan, Canada for their financial support through the Agriculture Development Fund program (ADF #20130219) for this study. I acknowledge also the contributions of the following persons: Rlee Prokopishyn, the electric technician in the Department of Chemical and Biological Engineering at University of Saskatchewan for helping us during the design and installations of the RF system; Ian Armer, the manager of Grain Quality Control Division, Viterra Inc. for providing us grains; Colin Demianyk from Agriculture and Agri-Food Canada for providing us the insects; Connie Briggs, the research officer in the Crop Development Center at University of Saskatchewan for her guidance and assistance for this study in doing some of the quality tests (Milling and baking); and Oliver Broad from Coaxial Power Systems Limited for providing as technical assistance.

Lastly, heartfelt and immeasurable thanks to my dearest wife Rose Ann Macana, daughter Blythe Skyler Macana, friends, and CFC and SFC community for their limitless support and encouragement during my study. To God be the glory! Thanks God! AMDG!

TABLE OF CONTENTS

PERMISSION TO USE STATEMENT	i
GENERAL ABSTRACT	ii
ACKNOWLEDGMENTS	iv
TABLE OF CONTENTS.....	v
LIST OF FIGURES.....	x
LIST OF TABLES	xv
GENERAL INTRODUCTION	1
Outline of the Thesis	3
References.....	4
CHAPTER 1	6
Disinfestation of insect pests in stored agricultural materials using microwave and radio frequency heating: A review	6
1.1 Abstract.....	6
1.2 Introduction	7
1.3 RF and MW disinfestation principles.....	9
1.3.1 Dielectric heating principle	10
1.3.2 Selective heating.....	11
1.4 Dielectric properties of host materials and insect pests	15
1.4.1 Measurement methods	23
1.4.1.1 Open-ended coaxial probe.....	26
1.4.1.2. Dielectric test fixture	27
1.5 Radio frequency and microwave comparison	29
1.5.1 Effect of power and temperature on the exposure time for 100% mortality of different insect pests	34
1.5.2 Quality of host materials after disinfestation	36
1.5.3 Heating uniformity	39
1.6 Disinfestation economics.....	41
1.7 Concluding remarks.....	43
1.8 References	45
CHAPTER 2.....	60

Installation of a pilot-scale 50-ohm radio frequency heating system for controlling insect pests in stored agricultural materials: Applicator design, impedance matching, and RF arcing problem	60
2.1 Abstract.....	60
2.2 Introduction	62
2.3 Materials and methods	65
2.3.1 Parts of 50-ohm RF heating system	65
2.3.2 Applicator design and fabrication	68
2.3.3 Impedance matching	70
2.3.3.1 Automatic matching network.....	71
2.3.3.2 Basic electrical parameters	73
2.3.3.3 Voltage standing wave ratio (VSWR)	74
2.3.4 The arcing and fire problem.....	75
2.4 Results and discussions	76
2.4.1 VSWR of the original configuration of the matching network	76
2.4.2 Capacitance and inductance inside the matching network	76
2.4.3 Addition of inductance to tune the matching network	78
2.4.4 Causes of arcing in the 50-ohm RF applicator	80
2.5 Problems encountered and solutions were provided during the installation of the 50-ohm RF heating system	83
2.5.1 Tuning the system	83
2.5.2 RF leakage	84
2.5 Concluding remarks and suggestions	88
2.6 References	89
CHAPTER 3.....	94
Mortality and thermal death kinetics of rusty grain beetle in stored wheat using a pilot-scale 50-ohm RF heating system	94
3.1 Abstract.....	94
3.2 Introduction	95
3.3 Materials and methods	97
3.3.1 The 50-ohm RF heating system	97
3.3.3 Wheat preparation.....	99
3.3.4 Rusty grain beetle preparation	100

3.3.4 Temperature histories	101
3.3.5 Mortality at all life stages of the insects	101
3.3.6 Thermal death kinetic modeling of rusty grain beetle	102
3.3.7 Data analysis	103
3.4 Results and discussions	104
3.4.1 Temperature histories of wheat grain samples	104
3.4.2 Mortality of rusty grain beetles at different temperature levels	105
3.4.3 Thermal death kinetics	110
3.4.3.1 Best fit kinetic model and its performance.....	110
3.4.3.2 Numerically simulated lethal RF exposure time	113
3.5 Conclusions.....	114
3.6 References	115
CHAPTER 4	119
Effect of 50-ohm RF energy on the quality of stored wheat after disinfestation .	119
4.1 Abstract.....	119
4.2 Introduction	120
4.3 Materials and methods	123
4.3.1 Wheat samples preparation	123
4.3.2 The 50-ohm RF heating system	124
4.3.3 Measurement of the physicochemical properties of wheat grains.....	125
4.3.3.1 Moisture content.....	125
4.3.3.2 Bulk density	126
4.3.3.3 Particle density	126
4.3.3.4 Porosity	128
4.3.3.5 Colour	128
4.3.4 Measurement of baking quality predictors of the wheat samples	130
4.3.4.1 Falling number	130
4.3.4.2 Mixing development time, PKH, and PBW.....	131
4.3.5 Measurements of the milling quality of the wheat samples	132
4.3.6 Data Analysis	134
4.4 Results and discussions	135
4.4.1 Physicochemical properties	135

4.4.1.1 Moisture content, bulk and particle density, and porosity.....	135
4.4.1.2 Colour	137
4.4.2 Germination.....	139
4.4.3 Baking quality predictors	140
4.4.3.1 Falling number	140
4.4.3.2 Mixograph.....	141
4.4.4 Milling quality	144
4.5 Conclusions.....	146
4.6 References	147
CHAPTER 5.....	153
Heating rate and heating uniformity of bulk wheat grain with the designed parallel plate applicator for a pilot-scale 50-ohm RF heating system.....	153
5.1 Abstract.....	153
5.2 Introduction	154
5.3 Materials and methods	156
5.3.1 Wheat samples.....	156
5.3.2 The 50-ohm RF heating system	157
5.3.3 The RF applicator.....	158
5.3.4 Temperature distribution measurement	159
5.3.5 Heating uniformity index calculation	162
5.3.6 Data Analysis	162
5.4 Results and discussion	163
5.4.1 Heating time and the heating rate of wheat grains using a pilot-scale 50-ohm RF heating system	163
5.4.1.1 Under different moisture contents of the wheat sample	163
5.4.1.2 Under different power levels of the RF system.....	164
5.4.2 Typical temperature histories of the bulk wheat samples at different MCs and power levels	164
5.4.3 Temperature distribution in the parallel plate applicator of the 50-ohm RF heating system.....	168
5.4.3.1 Vertical distribution of temperature of bulk wheat samples and its temperature histories at different heights from the bottom of the applicator	168

5.4.3.2 Horizontal distribution of temperature of bulk wheat samples in the applicator and its temperature histories	173
5.4.3.3 Effect of distance from the wall on the temperature distribution of the bulk wheat samples.....	175
5.4.4 Heating uniformity of the applicator.....	176
5.4.4.1 Temperature distribution of bulk wheat samples in the applicator....	176
5.4.4.2 Uniformity index values	180
5.4.4.3 Electric field strength assessment in relation to heating uniformity .	180
5.5 Conclusions and recommendations.....	187
5.6 References.....	188
CHAPTER 6.....	193
General discussion	193
6.1 Disinfestation using electromagnetic energy from a 50-ohm RF heating system.....	193
6.2 General conclusions	194
6.3 General recommendations	196
6.4 References	198

LIST OF FIGURES

Figure 1.1. Dielectric heating principle.....	11
Figure 1.2. Dielectric properties measurement using an open-ended coaxial probe.....	27
Figure 1.3. Dielectric properties measurement using a dielectric test fixture	28
Figure 1.4. Mechanism of measurement using a dielectric test fixture.....	28
Figure 1.5. Microwave (MW) and radio frequency (RF) allocation in the electromagnetic spectrum.....	29
Figure 1.6. The schematic buildup of microwave (MW) applicators: a) Monomode applicator b) Multimode applicator	32
Figure 1.7. The schematic buildup of radio frequency (RF) applicators: a) Stray field electrodes b) Staggered electrodes c) Flat electrodes.....	32
Figure 1.8. Conventional radio frequency (RF) heating system	33
Figure 1.9. 50 Ohm Technology based radio frequency (RF) Heating.....	34
Figure 2.1. 50 Ohm Technology based radio frequency (RF) Heating System...	66
Figure 2.2. The exterior photographs of the RF generator (27.12 MHz, 15 kW).....	66
Figure 2.3. The 50-ohm coaxial cable used for connecting the AMN and RF generator.....	67
Figure 2.4. The exterior photograph of the automatic matching network (AMN).....	67
Figure 2.5. Designed applicator with the auger system: (a) left view (b) right view (c) front view (d) top view.....	69
Figure 2.6. Auger system: (a) Auger (b) Tubular channel (c) Auger inside the tubular channel.....	70
Figure 2.7. Impedance matching between generator and load.....	71
Figure 2.8. The L configuration of the automatic matching network (Coaxial Power Systems Ltd., 2001).....	72
Figure 2.9. Actual photograph inside the matching network	

with L configuration.....	72
Figure 2.10 The network analyzer used for measuring the basic electrical parameters and tuning the system.....	74
Figure 2.11. Coil added between the applicator and matching network.....	79
Figure 2.12. Photographs of the applicator after arcing and fire happened at 11 kW and 27.12 MHz: (a) Applicator (b) Arcing and fire marks (c) Burnt marks between table and hot electrode (d) Showing arcing happened on the edges and corner of the electrodes.....	82
Figure 2.13. Photograph of the applicator with 8-cm lift placed between the tubular channel and table.....	82
Figure 2.14. Coil added with maximum power transfer to the load.....	83
Figure 2.15. Water cooling system connection.....	84
Figure 2.16. Cable melted because of RF leakage.....	85
Figure 2.17. RF shielding (Expanded steel metal).....	86
Figure 2.18. RF shielding photograph (expanded steel metal).....	87
Figure 2.19. RF shielding: (a) Addition of aluminum metal sheet in both sides and (b) Matching network has good contact to the shielding and the ground	87
Figure 3.1. The 50-ohm RF heating system (27.12 MHz, 15 kW): (a) Left view (b) Right view.....	98
Figure 3.2. The technical details of applicator for 50-ohm RF heating system with its hottest spot location.....	99
Figure 3.3. The suction assembly for collecting and counting the insects.....	100
Figure 3.4. The temperature histories of wheat grain at three moisture content levels.....	104
Figure 3.5. Immediate mortality of the insect pests rusty grain beetle at the different temperature levels.....	106
Figure 3.6. Delayed mortalities of insect rusty grain beetle at different temperature levels: (a) 12% MC (b) 15% MC (c) 18% MC. (Note: The experimental data points are connected with simple straight lines for visual presentation).....	107

Figure 3.7. The survival rate of insect pests rusty grain beetle at different temperature levels: (a) 12% MC (b) 15% MC (c) 18% MC.....	112
Figure 4.1. The bags of polypropylene with wheat samples.....	123
Figure 4.2. The 50-ohm RF heating system: (a) Left view (b) Right view (c) Front view (d) Top view.....	124
Figure 4.3. Temperature distribution of the applicator.....	125
Figure 4.4. Bulk density measurement materials.....	126
Figure 4.5. Measurement of particle density using a multi pycnometer.....	127
Figure 4.6. Measurement of the colour of wheat kernels using the spectrophotometer.....	128
Figure 4.7. Germination of wheat kernels procedure (a) Moistened Whatman filter paper in the petri dish (b) Wheat kernels were added (c) Ziploc bag with the samples (d) Inside the chamber (e) Outside the chamber.....	129
Figure 4.8. Falling number determination procedure: (a) UDY Cyclone grinder (b) Moisture content dishes with the ground sample (c) 25 ml distilled water in viscometer tube (d) Weighing samples (e) Samples added into the viscometer tube with distilled water (f) Sample and water are mixed well using Perten Shakermatic automatic sample mixer (g) Stirrer in the viscometer tube placed into the cassette and the cassette was inserted into the boiling water bath of the Perten FN apparatus (h) The stirrer inside the apparatus started to fall down by its own weight.....	131
Figure 4.9. Measurement baking qualities using a mixograph procedure: (a) Wheat flour (b) Weighing (c) RO water (d) Mixing bowl (e) mixing the dough (f) Mixing bowl and the clock (g) Curve on the screen (h) Dough when the run completed.....	132
Figure 4.10. Preparation of samples a day before milling: (a) Grinding the wheat using Wiley (b) Moisture content measurement (c) Tempering the wheat grains.....	133
Figure 4.11. The mills and the shakers: (a) Quadrumat Sr. Flour mill consisting two milling heads, the break side at the right and the reduction side at the left (b) Wheat samples at break side mill (c) Break sieve (d) Reduction sieve.....	133
Figure 4.12. Milling products: (a) Results after the break side mill (b) Bran (c) Break flour (d) Middlings (e) Reduction flour (f) Shorts (g) Weighing scale for weight measurement.....	134
Figure 4.13. The germination rate of 50-ohm RF treated wheat kernels with three levels of MC at different temperature levels and the controls.....	140

Figure 4.14. Comparison of falling number (FN) of wheat grain treated and untreated with RF energy at different temperature.....	142
Figure 5.1. Wheat samples placed in the polypropylene bag before RF heating.....	157
Figure 5.2. 50-ohm RF heating system.....	158
Figure 5.3. RF parallel plate applicator.....	159
Figure 5.4. Three sections of the applicator for temperature distribution measurement.....	160
Figure 5.5. Three sections of the applicator with 21 points in total for temperature monitoring (a) Right (b) Middle (c) Left.....	161
Figure 5.6. The temperature histories of wheat samples at 3 power levels (7 kW, 5 kW, and 3 kW) and 2 MCs (12% and 18%).....	166
Figure 5.7. The average temperature at different power levels and 2 MCs on the temperature histories of wheat samples.....	167
Figure 5.8. Visual presentation of measurement points of the vertical distribution of temperature at different sections of the applicator: (a) Left, (b) Middle, and (c) Right.....	169
Figure 5.9. Effect of height from the hot electrode on temperature profile at 12% MC of wheat sample.....	171
Figure 5.10. Effect of height from the hot electrode on temperature profile at 18% MC of wheat sample.....	172
Figure 5.11. Effect of horizontal distance from the feed point on the temperature profile at 12% MC of the wheat samples at 7 kW.....	174
Figure 5.12. Temperature distribution of bulk wheat samples in the RF applicator at 7 kW and 12% MC.....	178
Figure 5.13. Temperature distribution of bulk wheat samples in the RF applicator at 7 kW and 18% MC.....	179
Figure 5.14. The intensity of the electric field between the parallel plate electrodes in the applicator (a) no sample, (b) sample was placed at the bottom (ground electrode), (c) sample was placed at the center of the applicator.....	182
Figure 5.15. Visual presentation of the location the hottest and coldest spot of the applicator: (a) Hottest spot location at the right section of the applicator (b) View of the left section of the applicator outside the tubular channel (c) Inside	

look of the tubular channel pointing the coldest spot at the left section of the applicator.....184

Figure 5.16. Temperature distribution of wheat samples at 12% MC treated at 7 kW RF power in the applicator: (a) Right (b) Middle (c) Left.....185

Figure 5.17. Temperature distribution of wheat samples at 18% MC treated at 7 kW RF power in the applicator: (a) Right (b) Middle (c) Left.....186

LIST OF TABLES

Table 1.1. Dielectric loss factor ratio between insect pests and agricultural material at specific moisture content and temperature range at different frequency levels.....	14
Table 1.2. Dielectric properties of agricultural material at a specific moisture content and temperature range at different frequency levels.....	17
Table 1.3. Dielectric properties of target insect pest at a specific moisture content and temperature range at different frequency levels.....	19
Table 1.4. Effect of temperature on the dielectric properties of agricultural materials at 27.12 MHz.....	21
Table 1.5. Effect of temperature on the dielectric properties of insect pests at 27.12 MHz.....	22
Table 1.6. Effect of moisture content on the dielectric properties of agricultural materials at 27.12 MHz.....	24
Table 1.7. Quality of the host material not significantly affected by dielectric heating with a 100% mortality rate.....	38
Table 2.1. VSWR, capacitance, and inductance of copper coil (loop diameter= 40 mm, wire diameter= 6mm) at 27.12 MHz and 50-ohm impedance at different number of turns.....	77
Table 2.2. Results of the addition of copper coil to tune the matching network.....	79
Table 2.3. Causes of arcing at different situations of the applicator and power levels of the RF generator: Unrounded, rounded, no gap, 8-cm gap, and burn marks.....	81
Table 3.1. The performance of the kinetic model in predicting the mortalities of the adult rusty grain beetle at different moisture content levels (12%, 15%, and 18%) treated by 50-ohm RF heating system.....	111
Table 3.2. Numerically simulated RF exposure time with 100%, 99%, 95%, and 90% mortality rate at three moisture content levels (12%, 15%, and 18%).....	113
Table 4.1. Physicochemical properties of the 50-ohm RF treated and untreated wheat samples at three levels of MC and temperature.....	136
Table 4.2. Assessment of the colour of wheat grains after RF heating at different temperature and moisture content levels.....	138
Table 4.3. MDT, PKH, and BWP at different temperature and moisture content levels of wheat grain after RF heating.....	143

Table 4.4. Milling quality of wheat grain at different temperature and moisture content levels treated by 50-ohm RF energy.....	145
Table 5.1. The heating rate and RF heating time at three MCs (12%, 15%, and 18%) at different power levels.....	163
Table 5.2. Effect of power from the RF generator on the heating rate and heating time when the target temperature is 85°C and the sample initial temperature is 24 °C.....	164
Table 5.3. The regression models for the temperature of the bulk wheat sample in the hottest spot as a function of RF heating time at different power levels.....	167
Table 5.4. Vertical temperature distribution of bulk wheat samples at 2 power levels (12% and 18%) at 7 kW.....	170
Table 5.5. Temperature distribution at the horizontal of bulk wheat samples treated at 7 kW and 2 moisture content levels (12% and 18%).....	173
Table 5.6. Temperature distribution as a function of distance from the wall of the tubular channel at 7 kW and 12% MC of the wheat samples.....	175
Table 5.7. The temperature difference between the hottest and coldest spot in the designed applicator for 50-ohm RF heating system at different power levels and 2 MCs (12% and 18%).....	177
Table 5.8. Heating uniformity of the designed applicator for 50-ohm RF heating system at 7 kW and 2 MCs (12% and 18%).....	180

GENERAL INTRODUCTION

In 2017, wheat (29,984,200 metric tonnes) was the largest in terms of crop production in Canada, followed by canola (21,328,000 metric tonnes) and corn (14,095,300 metric tonnes) (Statistics Canada 2018). Wheat contributes \$11 billion per year to Canada's economy (NRCC 2013) and in 2012, Canada was one of the top seven wheat producing countries worldwide (FAO 2014). For the dollar value of wheat exported in 2017, Canada (US\$5.1 billion) ranked third globally, which was next to the United States (US\$6.1 billion) and Russia (US\$5.8 billion) (Workman 2018). However, the infestation by insect pests in wheat grain, which decreases the value of wheat in terms of both quality and quantity, has been a serious problem during storage. The annual losses for grains worldwide because of insect pests were in the range of 9% to 20% (Hou et al. 2016). In addition, during marketing and trading, the presence of insect pests was not allowed due to the phytosanitary and quarantine protocols that have been established worldwide by regulatory agencies (Hou et al. 2016). A common insect pest present in stored wheat is the rusty grain beetle. It is the most serious pest of stored grain in Canada and can be found worldwide. Both the larvae and adults damage the kernels and eat the germ (Canadian Grain Commission 2013). Traditional methods for controlling insect pests use chemicals (fumigants and pesticides). Nevertheless, there has a negative effect on the environment. For example, using fumigants (methyl bromide) can damage the ozone layer (UNEP 2006). In addition, pesticides leave chemical residues in products (Wang et al. 2007a; Govindasamy et al. 1997). Therefore, non-chemical methods have been proposed as alternatives to fumigants and pesticides.

Radio frequency (RF) heating is a non-chemical, and electromagnetic-based method for disinfestation, which relies on the interaction of materials (insects and host materials) and electromagnetic waves. The advantage of this method is fast, volumetric, and selective heating. The electromagnetic based methods (radio frequency and microwave) have been studied in past years as alternatives to chemical disinfestation. RF heating was preferred for disinfestation over microwave heating due to its higher selective heating effect and greater penetration depth (Macana and Baik 2017). The 50-ohm RF heating system is a modern type of RF technology and it is more advantageous than conventional RF heating for disinfestation because of its installation flexibility and maximum power transfer to the load. However, despite its advantages, there have been a limited number of installations and applications globally and none in disinfestation due to a lack of knowledge in using this technology.

Therefore, the main objective of this study was to investigate the disinfestation of rusty grain beetle in stored wheat grain using a pilot-scale, 50-ohm RF heating system. The following were the specific objectives to achieve the main goal:

- 1) to update the recent research outcomes of disinfestation using electromagnetic energy (microwave and radio frequency;
- 2) to investigate the installation process of the 50-ohm RF heating system;
- 3) to design and fabricate the parallel plate applicator for a pilot-scale, 50-ohm RF heating system;
- 4) to determine the mortality of rusty grain beetles in stored wheat grain;

- 5) to estimate parameters of thermal death kinetics during the RF heating of insects in stored grain;
- 6) to compare the quality of wheat grain before and after 50-ohm RF disinfestation; and
- 7) to determine the heating rate and temperature distribution of bulk wheat samples at different RF power levels, along with wheat grain moisture contents in the designed applicator.

Outline of the thesis

This thesis is based on a collection of journal papers and is comprised of six chapters. The first chapter is a critical review of the disinfestation of insect pests in stored agricultural materials using microwave and radio frequency heating (specific objective 1). This chapter was published in Food Reviews International, 34(5) 483-510. The second chapter is about the installation of a pilot-scale, 50-ohm radio frequency heating system for controlling insect pests in stored agricultural materials: applicator design, impedance matching and RF arcing problem (specific objectives 2 and 3). The third chapter determined the mortality and thermal death kinetics of the rusty grain beetle in stored wheat using a pilot-scale, 50-ohm RF heating system (specific objectives 4 and 5). The fourth chapter deals with the effect of 50-ohm RF energy on the quality of stored wheat after disinfestation (specific objective 6). The fifth chapter determined the heating rate and heating uniformity of bulk wheat grain with the designed parallel plate applicator for a pilot-scale 50-ohm RF heating system (specific objective 7). Chapter two to five will be submitted for publication. The sixth chapter integrated all of the findings found in the

previous five chapters. The general conclusions and recommendations for future studies also were provided in this chapter.

References

Canadian Grain Commission. 2013. Eight common insect pests. Accessed on March 9, 2017 at <http://www.grainscanada.gc.ca/storage-entrepot/8cip-8irc-eng.htm>

Food and Agriculture Organization (FAO). 2014. World top wheat production. Accessed on March 8, 2017 at <http://faostat.fao.org/site/339/default.aspx>

Govindasamy, R., J. Italia and C. Liptak. 1997. Quality of agricultural produce: consumer preferences and perceptions. New Jersey Agricultural Experiment Station, P-02137-1-97, http://www.cook.rutgers.edu/~agecon/pub/qual_ag.pdf.

Hou, L., J. Johnson and S. Wang. 2016. Radio frequency heating for postharvest control of pests in agricultural products: a review. *Postharvest Biology and Technology* 113: 106–118.

Macana, R.J. and O.D. Baik. 2017. Disinfestation of insect pests in stored agricultural materials using microwave and radio frequency heating: A review, *Food Reviews International* 34(5): 483-510.

National Research Council Canada (NRC). 2013. The Canadian wheat alliance factsheet. Accessed on March 9, 2017 at http://www.nrc-cnrc.gc.ca/eng/news/releases/2013/wheat_nrc_factsheet.html

Statistics Canada. 2017. Estimated areas, yield, production, average farm price and total farm value of principal field crops, in metric and imperial units. Accessed on November 6, 2018 at <https://www150.statcan.gc.ca/t1/tbl1/en/tv.action?pid=3210035901>

UNEP. 2006. Handbook for the Montreal protocol on substances that deplete the ozone layer. 7th ed. Nairobi, Kenya: United Nations Environmental Program, Ozone Secretariate.

Wang, S., M. Monzon, J.A. Johnson, E.J. Mitcham and J. Tang. 2007a. Industrial-scale radio frequency treatments for insect control in walnuts I: heating uniformity and energy efficiency. *Postharvest Biol. Technol.*, 45, 240–246.

Workman, D. 2019. Wheat exports by country. Accessed on January 17, 2019 at <http://www.worldstopexports.com/wheat-exports-country/>

CHAPTER 1

Disinfestation of insect pests in stored agricultural materials using microwave and radio frequency heating: A review

Published, *Food Reviews International* 34 (2017) 483-510.

Contribution of this paper to the overall study

This chapter updated the recent research outcomes of disinfestation using electromagnetic energy (radio frequency and microwave) (specific objective 1). This involved the discussion and analysis of the principles of RF- and MW- assisted disinfestation and their effect on the mortality of various insect species, quality of the host materials, and heating uniformity; effects of frequency, temperature and moisture content on the dielectric properties of the insects and host materials; measurement methods of dielectric properties; and, economics of disinfestation. The journal article for this chapter was drafted by myself.

1.1 Abstract

This chapter gives a comprehensive review of the disinfestation of insects in stored agricultural materials using radio frequency and microwave heating. It covers RF and MW disinfestation principles; measurement methods and effects of the operating parameters

on dielectric properties; comparison between RF and MW and their effect on the mortality of different insects, quality of the host materials after disinfestation; heating uniformity; and disinfestation economics. This review shows that RF and MW disinfestation are useful without affecting the quality of the host materials. However, RF heating is preferred over MW heating for its higher selective heating characteristic.

Keywords: Radio frequency; Microwave; Disinfestation; Insect pests; Grains; Dielectric properties

1.2 Introduction

Disinfestation of insect pests from host materials is a critical issue in marketing and trading of grain products. Traditional methods include the use of fumigants and insecticides that can be toxic to human health and the environment (Birla et al. 2008). Exporting of agricultural commodities is one of the important parts of the economy of most countries all over the world. Countries must meet the importing countries maximum residue limits for fumigants or pesticides. Thus, the best approach would be to use a chemical-free technique for disinfestation. Conventional heating is a traditional method which is chemical free but it takes a large amount of energy and possibly introduces thermal degradation of grain quality.

Radio frequency (RF) and microwave (MW) heating are disinfestation methods that are electromagnetic-based and chemical-free. They rely on the interactions between electromagnetic energy and materials. Under electromagnetic exposure, the heating rate and power generation of the insect pests and host materials depend on

their dielectric properties, electric field intensity, and their thermal properties (Ling et al. 2015). Thus, the dielectric properties of the insects and host materials are helpful to consider in evaluating the potential for practical selective heating using RF and MW energy. One of the factors affecting the power dissipation and heating rate of the insect pests and host materials is their dielectric loss factor (Shrestha and Baik 2013). The higher the dielectric loss factor of the material, the higher the power that is generated, and thus a higher heating rate. Comparison of the dielectric loss factors of the materials (insects and grains) is a rough estimation of selective heating due to neglecting the thermal properties and electric field intensity of the materials. In addition, heat conduction from hotter insect bodies to colder grains also should be considered for a more realistic estimation of selective heating.

RF and MW heating have several advantages over thermal gradient driven conventional heating methods. The advantages are that they are non-contact, volumetric and rapid heating methods (Shrestha et al. 2013; Manickavasagan et al. 2006; Tang et al. 2000). The first study using this method in disinfestation was reported 86 years ago by Headlee and Burdette (1929) and later studies have been summarized in a fair number of reviews (Hou et al. 2016; Marra et al. 2009; Wang and Tang 2001; Nelson 1996, 1966; Ark and Parry 1940); however, there is still a need to update the recent research outcomes of disinfestation using MW and RF heating for the past 15 years.

Therefore, the objective of this review was to summarize, analyze, and provide an up-to-date overview of the disinfestation of insect pests in stored agricultural products

using RF and MW heating. Especially this review will serve as planning for industrialization of disinfestation using RF and MW heating and it includes RF and MW energy disinfestation principles (ionic polarization, dipole rotation, and selective heating); effects of operating parameters (frequency, temperature, and moisture content) on dielectric properties of agricultural materials and insect pests and measurement methods of dielectric properties; comparison between RF and MW and their effect on the mortality of different insect pests, quality of the host materials, and heating uniformity; and economics of disinfestation. In addition, suggestions are given for further research directions for the improvement of RF and MW disinfestation of insect pest from the host materials.

1.3 RF and MW disinfestation principles

For disinfestation of insects from host materials, two principles need to be understood; the first is dielectric heating and the second is selective heating. Dielectric heating involves radio frequency (RF) and microwave (MW) heating. RF and MW energy heat wet materials such as insects and host materials in bulk by two heating mechanisms, ionic polarization and dipole rotation (Morris 2011). Selective heating is another factor to be considered for its importance in heating the insect pests selectively with electromagnetic energy to their fatal temperature while keeping the host material at a moderate temperature. In this principle, the pest insects are killed first before the physicochemical properties of host materials (grains) are thermally degraded to a significant extent.

1.3.1 Dielectric heating principle

One of the important principles contributing to MW and RF heating is ionic polarization (Figure 1.1). Ions move at an accelerated pace when subjected to the alternating electric field generated by MW and RF energy. The resulting collision causes an increase in temperature. Two opposite charges or ions (+ and -) of salt, for example, may be separated when dissolved in biological material. When subjected to the alternating electric field, separated charges or ions move back and forth. The friction created by the moving charges results in dielectric heating (Piyasena et al. 2003). Another mechanism is dipole rotation, which is a major contributor to dielectric heating (Figure 1.1). A water molecule is a polar structure: the centroid of the negative oxygen ion does not coincide with the centroid of the hydrogen positive charge. The polar structure of water is equivalent to a pair of equal and opposite charges separated by a small distance; this is called a dipole. The dipoles of water molecules rotate to follow the alternating electric field. These rapidly rotating molecules cause friction leading to temperature rise (Piyasena et al. 2003).

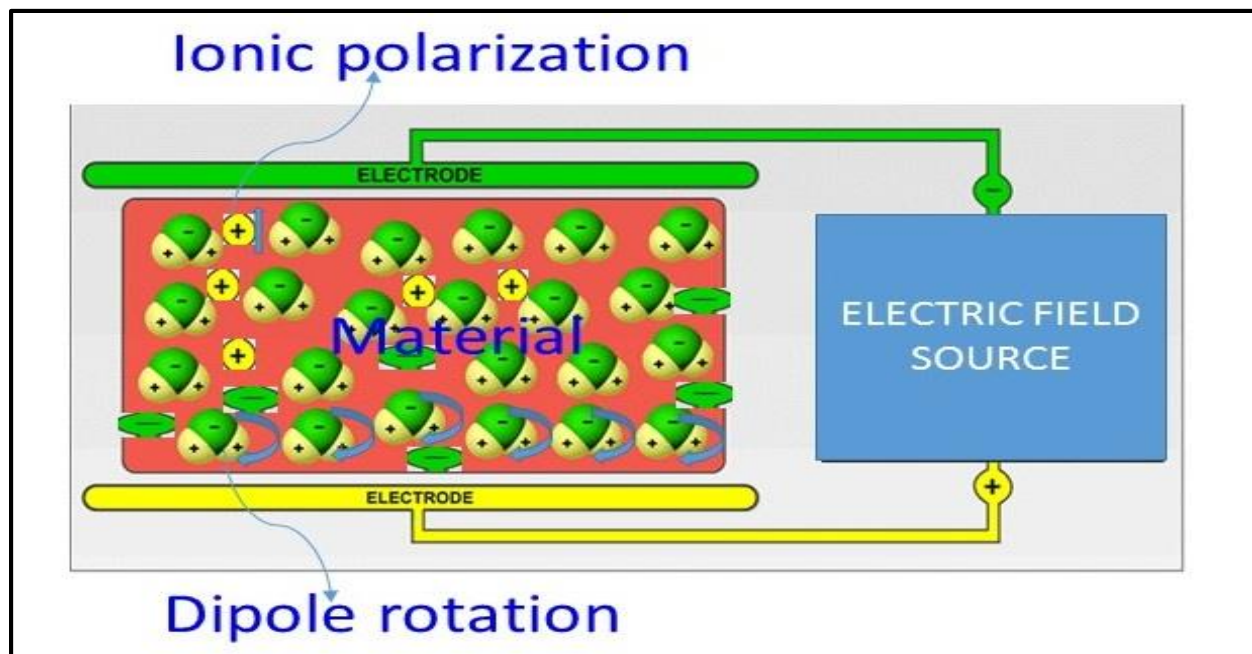


Figure 1.1. Dielectric heating principle (Modified from Radio Frequency Inc. (Radio frequency Inc. 2015).

1.3.2 Selective heating

The idea of selective heating was first proposed in 1972 by Nelson and Charity (1972). In 2003, Wang et al. (2003) published the theoretical and experimental demonstration of this concept and in 2015, Huang et al. (2015) studied this with computer simulation.

Selective heating is required to heat the insect pests to their fatal temperature while keeping the agricultural host material at a moderate temperature. Thus, pest insects will be killed first, before any significant thermal degradation of agricultural host materials.

Selective heating is a function of the ratios of power dissipation and heating rate of the insect body to the host materials. The power dissipation ratio can be related to the

dielectric loss factor ratio and the power dissipation ratio can be related to the rate of increase of temperature, as shown in Eqs. (1.1) (Choi and Konrad 1991), (1.2) (Shrestha and Baik 2013), and (1.3) (Shrestha and Baik 2013). Among all the factors affecting the power dissipation ratio, the dielectric loss factor ratio has more impact on the rate of increase of temperature (Shrestha and Baik 2013). The higher the dielectric loss factor of the material, the higher the power that is generated, thus resulting in a higher rate of temperature increase.

$$P_{avg} = 5.563 \times 10^{-11} f E^2 \varepsilon'' = \rho C_p \frac{\Delta T}{\Delta t} \quad (1.1)$$

From Eq. (1.1), at a constant frequency, the power dissipation ratio (P_{ih}) and the rate of increase of temperature (T_{tih}) between the insect and the host material can be derived as shown in Eqs. (1.2) and (1.3).

$$P_{ih} = \frac{E_i^2 \varepsilon_i''}{E_h^2 \varepsilon_h''} \quad (1.2)$$

$$T_{tih} = \frac{(\frac{\Delta T}{\Delta t})_i}{(\frac{\Delta T}{\Delta t})_h} = \left(\frac{E_i^2 \varepsilon_i''}{E_h^2 \varepsilon_h''} \right) \left(\frac{\rho_h C_{ph}}{\rho_i C_{pi}} \right) \quad (1.3)$$

Here, P_{avg} is the average power density (W/m^3), C_p is the specific heat of the material ($J/kg-^\circ C$), ρ is the density of the material (kg/m^3), E is the electric field intensity (V/m), f is the frequency (Hz), Δt is the time duration (s), ΔT is the temperature rise in the material ($^\circ C$), ε'' is the dielectric loss factor, and the subscripts i and h denote insect and host material, respectively.

Table 1.1 shows ranges in dielectric loss factor ratios between insects and agricultural materials, with their corresponding frequencies, temperatures, and moisture contents. It shows that the dielectric loss factor ratios between insect pest and agricultural material are greater than 1 at different frequency and temperature ranges. It means that insect pests have greater dielectric loss factors than those of their corresponding agricultural host materials. At a constant frequency of 27.12 MHz and temperature ranges from 20°C to 60°C, the range of the dielectric loss factor ratio between Mediterranean fruit fly and nectarine is 1.62 to 2.34, chestnut weevil and chestnut is 1.78 to 4, codling moth and golden delicious apple is 1.98 to 2.18, codling moth and red delicious apple is 2.59 to 2.86, codling moth and grape is 1.18 to 1.27, codling moth and walnut is 793.67 to 852.17, and Mediterranean fruit fly larvae and peach is 1.63 to 1.66. At 27.12 MHz and temperature ranges from 15°C to 75°C, the range of the dielectric loss factor ratio between rusty grain beetle and wheat is 11.23 to 22.30. The higher value means that there is a large increase in temperature of insect pest bodies compared to the host materials. For example, considering dielectric heating only, the Mediterranean fruit fly body temperature increases 162% to 234% times faster than the nectarine temperature, and the rusty grain beetle body temperature increases 2085% to 2230% times faster than does the temperature of wheat. These may have potential benefits in heating the insect pests selectively with radio frequency energy at 27.12 MHz to their lethal temperature while keeping the host material at moderate temperature. It shows that selective heating is possible for Mediterranean fruit fly in nectarine and peach at

27.12 MHz, rusty grain beetle in wheat at 27.12 MHz, weevil in chestnut at 10 to 4500 MHz, and codling moth in golden and red delicious apple, grape, and walnut at 27 to 1800 MHz because their dielectric loss factor ratios are greater than 1. Thus, results in higher power dissipation in the insects compared to that within the agricultural materials, hence the insects were heated faster than the agricultural materials (Shrestha and Baik 2013). When the dielectric loss factor ratio between the insect and the host material is less than 1, there might be more chance to have thermal degradation of the host materials before pest insects are killed. However, in most cases, the dielectric loss factor ratio between the host material and pest insects is greater than 1. This feasibility check for selective heating with dielectric loss factor ratio is only a rough estimation, without considering heat conduction from hotter insect bodies to surrounding host materials during RF heating. Furthermore, as stated earlier, the heating rate and power generation of insects and host materials also are dependent on electric field intensity and the thermal properties of the materials.

1.4 Dielectric properties of host materials and insect pests

Dielectric constant (ϵ') and dielectric loss factor (ϵ'') are important dielectric properties of host materials and insect pests. They are helpful information to evaluate practical and potential selective heating using MW and RF energy. The dielectric loss factor is a measure of how well a material converts electromagnetic energy into heat energy, while the dielectric constant is the ability of a medium to store electrical energy (Shrestha et al. 2013). As stated earlier, the dielectric properties of agricultural materials and insect pests are one of the important factors in selective heating using MW and RF energy and can be affected by the frequency of electromagnetic waves, temperature,

moisture content, density and composition of the materials (Hou et al. 2016; Barba and Lamberti 2013; Peng et al. 2013; Solyom et al. 2013; Hossan and Dutta 2012; Nelson and Trabelsi 2012; Boldor et al. 2004; Nelson 2010, 2003; Piyasena et al. 2003; Berbert et al. 2002, 2001; Inoue et al. 2002; Ryynanen 1995; Engelder and Buffler 1991; Nelson and Charity 1972). Tables 1.2 and 1.3 summarize the effect of frequency on the dielectric properties of agricultural materials and insect pests for studies conducted over the past 15 years. In general, at a constant temperature and moisture content, the dielectric constant and dielectric loss factor of the agricultural materials and insect pests decreased with increasing frequency. For example, at a constant temperature of 60°C and constant moisture content, the dielectric constant of chestnut (45.3% moisture content) and chestnut weevil (62.2% moisture content) at 10 MHz, 27.12 MHz, 40.68, and 915 MHz are 190.6, 57.7, 44.1, and 20.1, respectively, and 159.2, 70.9, 61.2, and 39.8, respectively, while the dielectric loss factors of chestnut and chestnut weevil at four levels of frequencies are 366.9, 158.1, 114.21, and 9.52, respectively, and 763.9, 281.1, 206.7, and 13.3, respectively. A decreasing trend in dielectric constant and dielectric loss factor with an increasing frequency also is seen in black-eyed pea, mung bean, mango, cherry, grape, orange, avocado, cherimoya, longan, macadamia nut, passion fruit, pear, pineapple, persimmon, and white sapote, and in insect pests such as codling moth, Indian meal moth, Mexican fruit fly, navel orange worm, medfly egg and larvae, melon fly, and oriental fruit fly. It is very clear that the dielectric properties of agricultural materials and insect pests in the radio frequency range (10 MHz, 27.12 MHz, and 40.68 MHz) are higher compared to those in the microwave range (915 MHz, 1800 MHz, 2450 MHz, and 4500 MHz).

Table 1.2. Dielectric properties of agricultural material at a specific moisture content and temperature range at different frequency levels.

Agricultural Material	Temperature (°C)	Moisture Content (% Wet base)	Dielectric Constant								Dielectric loss factor								Reference
			10 MHz	27.12 MHz	40.68 MHz	915 MHz	1800 MHz	2450 MHz	4500 MHz	10 MHz	27.12 MHz	40.68 MHz	915 MHz	1800 MHz	2450 MHz	4500 MHz			
Almond	20	3	----	5.7	5.9	1.7	3.4	----	----	----	0.6	1.0	5.7	2.9	----	----	Wang et al. 2003		
	to		to	to	to	to	to	to	to	to	to	to	to	to	to				
	60		----	6.0	6.3	3.4	5.8	----	----	----	1.2	1.5	6.4	3.5	----	----			
Apple	15	----	----	66.9	61.9	57.7	----	57.7	----	----	118.3	77.4	8.7	----	7.5	----	Zhu et al. 2012		
	to		to	to	to	to	to	to	to	to	to	to	to	to	to				
	95	----	----	83.3	81.5	78.2	----	76.0	----	----	358.3	233.6	12	----	14.8	----			
Apple (Golden delicious)	20	86	----	66.5	66.4	65.6	60.1	----	----	----	120.4	80.5	8.2	6.7	----	----	Wang et al. 2003		
	to		to	to	to	to	to	to	to	to	to	to	to	to	to				
	60		----	72.5	72.6	74.3	67.4	----	----	----	234.1	157.4	8.7	9.9	----	----			
Apple (Red delicious)	22	3.8	----	----	----	1.7	----	1.7	----	----	----	----	0.1	----	0.07	----	Feng et al. 2002		
	to		to	to	to	to	to	to	to	to	to	to	to	to	to				
	60	87.5	----	----	----	32.8	----	30.8	----	----	----	----	9.1	----	7.5	----			
Apple (Red delicious)	20	87	----	66.8	66.8	67.1	62.0	----	----	----	92.0	61.1	8.9	6.7	----	----	Wang et al. 2003		
	to		to	to	to	to	to	to	to	to	to	to	to	to	to				
	60		----	74.6	74.7	77.0	70.4	----	----	----	178.6	119.9	10.0	10.8	----	----			
Apricots	20	----	----	33.9	32.3	19.7	17.6	----	----	----	11.8	10.6	7.1	6.3	----	----	Alfaifi et al. 2003		
	to		to	to	to	to	to	to	to	to	to	to	to	to	to				
	60	----	----	40.8	38.9	26.2	23.2	----	----	----	37.4	28.9	10.2	10.0	----	----			
Avocado	20	----	----	115.7	92.7	57.8	56.4	----	----	----	699.6	477.2	27.4	19.0	----	----	Wang et al. 2008		
	to		to	to	to	to	to	to	to	to	to	to	to	to	to				
	60	----	----	140.5	105.4	59.9	58.7	----	----	----	1422.0	965.1	47.8	27.7	----	----			
Black-eyed pea	20	8.8	----	3.4	3.33	2.84	----	----	----	----	0.24	0.26	0.24	----	----	----	Vadivambal et al. 2013		
	to		to	to	to	to	to	to	to	to	to	to	to	to	to				
	60	20.9	----	13.86	12.78	7.62	----	----	----	----	6.06	5.10	2.08	----	----	----			
Cherimoya	20	----	----	68.4	64.5	48.7	55.7	----	----	----	238.5	163.4	25.4	17.0	----	----	Wang et al. 2013		
	to		to	to	to	to	to	to	to	to	to	to	to	to	to				
	60	----	----	72.1	68.9	62.0	59.0	----	----	----	480.6	325.6	31.5	18.3	----	----			
Cherry	20	88	----	89.8	78.5	64.1	62.8	----	----	----	293.0	198.5	16.4	14.1	----	----	Wang et al. 2003		
	to		to	to	to	to	to	to	to	to	to	to	to	to	to				
	60		----	91.4	85.0	73.7	70.9	----	----	----	565.4	381.8	20.4	16.0	----	----			
Chestnut	20	45.3	69.7	31.2	26.6	14.6	----	12.4	10.8	101.5	45.9	33.9	5.2	----	4.6	4.8	Guo et al. 2011		
	to		to	to	to	to	to	to	to	to	to	to	to	to	to				
	60		190.6	57.7	44.1	20.1	----	18.8	17.1	366.9	158.1	114.21	9.52	----	6.9	6.9			
Chickpea	20	7.9	----	2.96	2.86	2.51	2.43	----	----	----	0.16	0.2	0.15	0.19	----	----	Guo et al. 2008		
	to		to	to	to	to	to	to	to	to	to	to	to	to	to				
	90	20.9	----	71.59	60.14	26.43	23.80	----	----	----	248.25	182.28	14.96	10.39	----	----			
Dates	20	----	----	27.2	25.5	12.0	9.8	----	----	----	10.1	9.0	5.7	5.1	----	----	Alfaifi et al. 2003		
	to		to	to	to	to	to	to	to	to	to	to	to	to	to				
	60	----	----	35.0	32.9	18.3	15.1	----	----	----	26.9	20.0	7.5	7.1	----	----			
Figs	20	----	----	37.7	35.7	21.3	19.1	----	----	----	14.4	13.1	8.9	8.0	----	----	Alfaifi et al. 2003		
	to		to	to	to	to	to	to	to	to	to	to	to	to	to				
	60	----	----	46.5	44.2	29.1	25.7	----	----	----	42.2	32.7	10.8	11.1	----	----			
Grape	20	88	----	89.0	80.8	63.7	63.7	----	----	----	202.4	137.8	12.1	10.7	----	----	Wang et al. 2003		
	to		to	to	to	to	to	to	to	to	to	to	to	to	to				
	60		----	96.5	82.7	72.7	72.1	----	----	----	401.1	273.3	15.5	12.6	----	----			
Grape	15	----	----	66.9	61.2	56.5	----	56.2	----	----	181.5	118.7	12.4	----	10.5	----	Zhu et al. 2012		
	to		to	to	to	to	to	to	to	to	to	to	to	to	to				
	95	----	----	82.5	80.7	76.3	----	72.5	----	----	568.9	371.1	18.7	----	16.7	----			

Agricultural Material	Temperature (°C)	Moisture Content (% Wet base)	Dielectric Constant							Dielectric loss factor							Reference
			10 MHz	27.12 MHz	40.68 MHz	915 MHz	1800 MHz	2450 MHz	4500 MHz	10 MHz	27.12 MHz	40.68 MHz	915 MHz	1800 MHz	2450 MHz	4500 MHz	
Longan	20	----	----	69.7	65.0	58.3	57.6	----	----	----	230.1	156.5	13.3	11.7	----	----	Wang et al. 2013
	to	to	to	to	to	to	to	to	to	to	to	to	to	to	to	to	
Macadamia nut kernel	60	----	----	75.2	73.8	68.2	66.3	----	----	----	431.4	293.3	16.0	14.1	----	----	Zhu et al. 2012
	25	3	----	4.3	4.2	5.1	5.4	----	----	----	0.3	0.4	0.8	0.8	----	----	
Mango	to	to	to	to	to	to	to	to	to	to	to	to	to	to	to	to	Sosa-Morales et al. 2009
	100	24	----	29.2	19.3	16.3	15.7	----	----	----	173.5	119.3	8.5	5.9	----	----	
Mung bean	20	86.26	----	78.9	73.1	65.0	62.9	----	----	----	250.1	161.5	13.8	12.9	----	----	Jiao et al. 2011
	to	to	to	to	to	to	to	to	to	to	to	to	to	to	to	to	
Orange	60	10.2	----	83.1	79.8	74	70.9	----	----	----	466.0	300.5	17.5	14.7	----	----	Wang et al. 2003
	20	to	----	3.23	3.15	2.61	----	----	----	----	0.23	0.24	0.34	----	----	----	
Orange	to	22.3	----	to	to	to	to	to	to	to	to	to	to	to	to	to	Zhu et al. 2012
	60	88	----	27.50	24.46	13.01	----	----	----	----	21.8	17.28	4.34	----	----	----	
Orange	20	----	----	75.8	69.9	63.2	62.7	----	----	----	223.3	151.6	16.5	12.2	----	----	Wang et al. 2013
	to	to	to	to	to	to	to	to	to	to	to	to	to	to	to	to	
Passion fruit	60	----	----	84.0	81.0	72.9	72.5	----	----	----	418.4	282.8	18.7	14.8	----	----	Zhu et al. 2012
	15	----	----	60.9	55.5	54.0	----	53.7 to	----	----	191.5	125.1	12.6	----	10.3	----	
Pear	to	to	to	to	to	to	to	75.4	to	to	to	to	to	to	to	to	Wang et al. 2013
	95	----	----	84.7	82.8	78.3	----	----	----	----	569.5	370.6	18.5	----	17.0	----	
Persimmon	20	----	----	82.7	73.5	54.2	52.9	----	----	----	264.1	179.7	15.0	12.8	----	----	Zhu et al. 2012
	to	to	to	to	to	to	to	to	to	to	to	to	to	to	to	to	
Pineapple	60	----	----	96.6	77.7	59.7	57.8	----	----	----	523.9	356.3	19.6	14.0	----	----	Wang et al. 2013
	15	----	----	60.0	57.9	56.2	----	55.6 to	----	----	152.6	99.8	10.4	----	8.6	----	
Pineapple	to	to	to	to	to	to	to	74.8	to	to	to	to	to	to	to	to	Zhu et al. 2012
	95	----	----	82.7	81.7	77.8	----	----	----	----	474.8	309.6	15.6	----	16.1	----	
Prunes	20	----	----	75.4	71.0	66.0	64.1	----	----	----	207.5	179.7	21.1	11.2	----	----	Alfaifi et al. 2003
	to	to	to	to	to	to	to	to	to	to	to	to	to	to	to	to	
Raisins	60	----	----	79.8	77.6	73.2	70.3	----	----	----	401.3	356.3	15.9	15.3	----	----	Alfaifi et al. 2003
	15	----	----	61.1	53.4	49.2	----	48.9 to	----	----	231.1	151.0	13.8	----	10.7	----	
Walnut	to	to	to	to	to	to	to	74.9	to	to	to	to	to	to	to	to	Shrestha et al. 2013
	95	----	----	86.7	83.5	77.9	----	----	----	----	617.2	402.5	19.8	----	16.9	----	
Walnut	20	----	----	40.6	38.7	24.2	22.0	----	----	----	17.2	15.7	10.8	10.0	----	----	Wang et al. 2003
	to	to	to	to	to	to	to	to	to	to	to	to	to	to	to	to	
Wheat	60	----	----	48.9	47.2	34.2	31.8	----	----	----	47.8	38.4	11.3	11.7	----	----	Wang et al. 2013
	20	----	----	21.9	20.2	7.8	4.6	----	----	----	8.1	7.4	3.8	3.1	----	----	
White Sapote	to	to	to	to	to	to	to	to	to	to	to	to	to	to	to	to	Wang et al. 2013
	60	----	----	33.8	31.9	15.2	11.5	----	----	----	11.4	10.6	7.2	6.5	----	----	
Walnut	20	3	----	4.9	4.8	2.1	2.1 to	----	----	----	0.3	0.5	1.8	1.0	----	----	Wang et al. 2003
	to	to	to	to	to	to	3.7	to	to	to	to	to	to	to	to	to	
Walnut	60	----	----	5.3	5.2	3.8	----	----	----	----	0.6	0.7	2.9	1.8	----	----	Wang et al. 2003
	20	----	----	4.9	4.8	2.1	2.8	----	----	----	0.3	0.5	1.8	1.0	----	----	
Wheat	to	to	to	to	to	to	to	to	to	to	to	to	to	to	to	to	Shrestha et al. 2013
	60	----	----	5.3	5.2	3.8	3.7	----	----	----	0.6	0.7	2.8	1.7	----	----	
White Sapote	15	12	----	3.82	----	----	----	----	----	----	0.07	----	----	----	----	----	Wang et al. 2013
	to	to	to	to	to	to	to	to	to	to	to	to	to	to	to	to	
White Sapote	75	18	----	5.97	----	----	----	----	----	----	0.93	----	----	----	----	----	Wang et al. 2013
	20	----	----	69.1	64.9	52.8	55.5	----	----	----	258.6	176.0	24.0	14.5	----	----	
White Sapote	to	to	to	to	to	to	to	to	to	to	to	to	to	to	to	to	Wang et al. 2013
	60	----	----	76.0	73.6	62.6	64.0	----	----	----	470.8	319.4	26.2	16.8	----	----	

Table 1.3. Dielectric properties of target insect pest at a specific moisture content and temperature range at different frequency levels.

Insect pest	Temperature (°C)	Moisture Content (% Wet base)	Dielectric Constant							Dielectric loss factor							Reference
			10 MHz	27.12 MHz	40.68 MHz	915 MHz	1800 MHz	2450 MHz	4500 MHz	10 MHz	27.12 MHz	40.68 MHz	915 MHz	1800 MHz	2450 MHz	4500 MHz	
Chestnut weevil	20	62.2	93.1	53.5	49.0	35.1	----	32.4	29.8	481.3	183.5	124.9	11.0	----	9.8	11.3	Guo et al. 2011
	to 60		to 159.2	to 70.9	to 61.2	to 39.8	to ----	to 37.0	to 34.7	to 763.9	to 281.1	to 206.7	to 13.3	to ----	to 11.9	to 15.7	
Codling moth	20	74	----	71.5	63.9	44.6	41.6	----	----	----	238.1	163.3	11.7	11.7	----	----	Wang et al. 2003
	to 60		to ----	to 84.5	to 71.5	to 47.9	to 44.5	to ----	to ----	to ----	to 511.3	to 349.1	to 13.4	to 10.6	to ----	to ----	
Indian-meal moth	20	74	----	81.3	69.1	37.2	35.3	----	----	----	210.9	149.0	13.4	10.6	----	----	Wang et al. 2003
	to 60		to ----	to 113.0	to 90.4	to 39.9	to 37.5	to ----	to ----	to ----	to 397.4	to 280.7	to 19.9	to 12.8	to ----	to ----	
Mexican fruit fly	20	74	----	90.3	71.2	44.5	43.0	----	----	----	343.9	230.9	17.5	13.3	----	----	Wang et al. 2003
	to 60		to ----	to 141.2	to 111.5	to 48.5	to 47.0	to ----	to ----	to ----	to 582.1	to 414.5	to 29.4	to 16.5	to ----	to ----	
Navel orange worm	20	74	----	80.2	68.6	42.2	40.0	----	----	----	307.8	212.6	16.1	12.7	----	----	Wang et al. 2003
	to 60		to ----	to 99.4	to 80.1	to 44.5	to 42.2	to ----	to ----	to ----	to 562.7	to 386.7	to 24.0	to 15.5	to ----	to ----	
Codling moth	20	----	----	73.8	63.9	44.6	41.6	----	----	----	238.1	163.3	11.7	11.7	----	----	Wang et al. 2003
	to 60	to ----	to ----	to 84.5	to 71.5	to 47.9	to 44.5	to ----	to ----	to ----	to 511.3	to 349.1	to 19.1	to 14.2	to ----	to ----	
Medfly egg	20	----	----	107.6	85.8	46.4	44.8	----	----	----	235.1	168.5	15.6	11.9	----	----	Wang et al. 2013
	to 60	to ----	to ----	to 158.1	to 116.1	to 47.4	to 45.7	to ----	to ----	to ----	to 463.5	to 329.9	to 22.7	to 14.0	to ----	to ----	
Medfly larvae	20	----	----	98.4	83.1	48.8	46.7	----	----	----	341.8	237.4	19.2	14.4	----	----	Wang et al. 2013
	to 60	to ----	to ----	to 134.5	to 105.8	to 49.5	to 48.4	to ----	to ----	to ----	to 703.3	to 485.4	to 29.3	to 18.7	to ----	to ----	
Melon fly	20	----	----	104.7	89.8	57.3	54.4	----	----	----	379.7	261.5	19.8	16.1	----	----	Wang et al. 2013
	to 60	to ----	to ----	to 141.1	to 108.7	to 59.0	to 55.8	to ----	to ----	to ----	to 772.3	to 529.3	to 31.3	to 20.7	to ----	to ----	
Mexican fruit fly	20	----	----	90.3	71.2	44.5	43.0	----	----	----	343.9	230.9	17.5	13.3	----	----	Wang et al. 2013
	to 60	to ----	to ----	to 141.2	to 111.5	to 48.5	to 47.0	to ----	to ----	to ----	to 585.2	to 414.5	to 29.4	to 16.5	to ----	to ----	
Oriental fruit fly	20	----	----	99.3	83.3	50.8	48.1	----	----	----	399.1	274.5	19.3	14.9	----	----	Wang et al. 2013
	to 60	to ----	to ----	to 137.7	to 104.3	to 52.8	to 49.9	to ----	to ----	to ----	to 820.6	to 563.7	to 32.6	to 21.1	to ----	to ----	
Rusty grain beetle	15	49.6	----	6.41	----	----	----	----	----	----	1.46	----	----	----	----	----	Shrestha et al. 2013
	to 75		to ----	to 25.14	to ----	to ----	to ----	to ----	to ----	to ----	to 20.74	to ----	to ----	to ----	to ----	to ----	

This also shows in the dielectric loss factor ratio between agricultural materials and insect pests in Table 1.1, as there are higher dielectric loss factor ratios of insect pest to host materials in the radio frequency range compared to those in the microwave range. Therefore, at frequencies between 27.12 MHz and below, there is the largest dielectric loss factor ratio of the material and insects. This suggests a greater potential for selective heating of insect pests from agricultural materials in an RF system at these conditions.

Tables 1.4 and 1.5 show the effect of temperature on the dielectric properties of agricultural materials and insect pests. In general, the dielectric constant and dielectric loss factor of agricultural materials and insect pests increased with increasing temperature at a given frequency and constant moisture content. For example, at constant frequency of 27.12 MHz and moisture content at five temperature levels (20°C, 30°C, 40°C, 50°C, and 60°C) in Table 1.4, the dielectric constant and dielectric loss factors of chestnut are 31.2 at 20°C, 32.9 at 30°C, 38.8 at 40°C, 46.6 at 50°C, and 57.7 at 60°C, and 45.9 at 20°C, 55.3 at 30°C, 77.9 at 40°C, 115.2 at 50°C, and 158.1 at 60°C, respectively. In Table 1.5, the dielectric constants and dielectric loss factors of chestnut weevil are 53.3 at 20°C, 58.3 at 30°C, 65.5 at 40°C, 68.6 at 50°C, and 70.9s at 60°C, and 183.5 at 20°C, 205.1 at 30°C, 229.2 at 40°C, 253.7 at 50°C, and 281.1 at 60°C, respectively. The increasing trend in dielectric constant means that those agricultural materials and insect pests absorbed more electromagnetic energy as their temperature increased (Hou et al. 2016; Hossan and Dutta 2012). The dielectric loss factors of most agricultural materials and insects increased with temperature due to increased ionic conductivity as a result of reduced viscosity at high temperatures (Wang et al. 2008; Tang et al. 2002).

Table 1.4. Effect of temperature on the dielectric properties of agricultural materials at 27.12 MHz.

Agricultural material	Moisture content (% Wet base)	Dielectric constant					Dielectric loss factor					Reference
		20°C	30°C	40°C	50°C	60°C	20°C	30°C	40°C	50°C	60°C	
Almond	3	5.9	5.7	5.8	5.8	6.0	1.2	0.6	0.6	0.6	0.7	Wang et al. 2003
Apple (GD)	86	72.5	71.3	69.7	68.1	66.5	120.4	143.9	171.8	202.2	234.1	Wang et al. 2003
Apple (RD)	87	74.6	72.7	70.6	68.7	66.8	92.0	109.1	130.7	153.8	178.6	Wang et al. 2003
Apricots	----	33.9	35.9	37.4	39.1	40.8	11.8	14.8	19.9	28.7	37.4	Alfaifi et al. 2013
Avocado	75-87	115.7	123.7	131.6	137.9	140.5	699.6	814.3	951.6	1136.2	1422.0	Wang et al. 2013
Black-eyed pea	8.8	3.4	3.43	3.51	3.62	3.84	0.24	0.25	0.27	0.28	0.31	Vadivambal et al. 2008
Black-eyed pea	20.9	8.9	9.5	9.86	11.2	13.86	2.44	2.65	3.06	3.94	6.06	Vadivambal et al. 2008
Cherimoya	75-87	71.5	72.1	68.4	72.0	70.0	238.5	283.1	339.1	406.4	480.6	Wang et al. 2013
Cherry	88	91.2	91.4	91.0	89.6	89.8	293.0	363.1	440.1	501.9	565.4	Wang et al. 2003
Chestnut	45.3	31.2	32.9	38.8	46.6	57.7	45.9	55.3	77.9	115.2	158.1	Guo et al. 2011
Chickpea	7.9	2.99	3.16	3.23	3.44	3.94	0.16	0.26	0.16	0.19	0.32	Guo et al. 2008
Chickpea	20.9	4.50	4.79	6.35	11.43	23.26	0.81	0.99	2.14	7.85	28.66	Guo et al. 2008
Dates	----	27.2	29.3	31.0	33.0	35.0	10.1	11.9	15.0	20.6	26.9	Alfaifi et al. 2013
Figs	----	37.7	39.6	42.3	44.8	46.5	14.4	17.6	23.8	32.7	42.2	Alfaifi et al. 2013
Grape	88	89.0	90.3	91.9	93.8	96.5	202.4	242.6	291.4	345.3	401.1	Wang et al. 2003
Longan	75-87	75.2	73.5	71.6	69.7	67.5	230.1	276.1	326.4	377.7	431.4	Wang et al. 2013
Mango	86.26	83.1	81.7	80.5	79.8	78.9	250.1	293.5	346.4	404.6	466.0	Sosa-Morales et al. 2009
Mung bean	10.2	3.23	3.38	3.53	3.75	4.15	0.23	0.24	0.26	0.28	0.37	Vadivambal et al. 2008
Mung bean	22.3	10.98	11.56	13.83	18.92	27.50	4.16	4.64	6.75	11.83	21.8	Vadivambal et al. 2008
Orange	88	84.0	82.2	80.2	78.0	75.8	223.3	267.9	318.0	367.7	418.4	Wang et al. 2003
Passion fruit	75-87	82.7	84.9	88.1	91.6	96.6	264.1	310.7	373.6	441.2	523.9	Wang et al. 2013
Persimmon	75-87	79.8	79.1	77.6	76.6	75.4	207.5	247.9	295.6	346.4	401.3	Wang et al. 2013
Prunes	----	40.6	42.8	44.4	46.6	48.9	17.2	20.5	25.4	34.4	47.8	Alfaifi et al. 2013
Raisins	----	21.9	24.8	28.0	31.2	33.8	8.1	8.9	9.8	10.6	11.4	Alfaifi et al. 2013
Walnut	3	4.9	5.0	5.1	5.2	5.3	0.6	0.5	0.4	0.3	0.4	Wang et al. 2003
White sapote	75-87	76.0	75.4	75.5	74.5	69.1	258.6	307.1	369.9	433.1	470.8	Wang et al. 2013
		25°C	40°C	60°C	80°C	100°C	25°C	40°C	60°C	80°C	100°C	
Macadamia nut	3	4.3	4.3	4.5	4.7	5.1	0.3	0.4	0.4	0.4	0.6	Zhu et al. 2012
Macadamia nut	24	20.6	21.6	22.9	25.5	29.2	47.5	61.7	81.0	113.1	173.5	Zhu et al. 2012
		15°C	30°C	45°C	60°C	75°C	15°C	30°C	45°C	60°C	75°C	
Wheat	12	3.82	4.11	4.28	4.66	5.10	0.13	0.09	0.07	0.09	0.19	Shrestha et al. 2013
Wheat	18	4.46	4.77	5.16	5.77	5.95	0.17	0.21	0.34	0.66	0.93	Shrestha et al. 2013

Table 1.5. Effect of temperature on the dielectric properties of insect pests at 27.12 MHz.

Insect pest	Moisture content (% Wet base)	Dielectric constant					Dielectric loss factor					Reference
		20°C	30°C	40°C	50°C	60°C	20°C	30°C	40°C	50°C	60°C	
Chestnut weevil	62.2	53.5	58.3	65.5	68.6	70.9	183.5	205.1	229.2	253.7	281.1	Guo et al. 2011
Codling moth	74	71.5	71.5	73.8	79.3	84.5	238.1	277.8	332.4	422.5	511.3	Wang et al. 2003
Indian-meal moth	----	81.3	85.8	94.4	103.7	113.0	210.9	244.1	268.7	314.0	397.4	Wang et al. 2003
Mexican fruit fly	----	90.3	105.1	117.4	128.7	141.2	343.9	384.7	446.1	521.8	582.1	Wang et al. 2003
Navel orange worm	----	80.2	83.6	87.7	92.8	99.4	307.8	359.7	419.4	480.3	562.7	Wang et al. 2003
Medfly egg	----	107.6	118.9	131.8	143.7	158.1	235.1	278.5	334.1	392.8	463.5	Wang et al. 2013
Medfly larvae	----	98.4	106.7	115.2	124.7	134.5	341.8	414.2	495.8	589.0	703.3	Wang et al. 2013
Melon fly	----	104.7	109.2	115.1	123.4	141.1	379.7	438.8	520.1	624.7	772.3	Wang et al. 2013
Oriental fruit fly	----	99.3	104.1	110.6	121.4	137.7	399.1	460.8	541.6	664.4	820.6	Wang et al. 2013

In increasing the temperature, the viscosity of most fluids decreases due to a reduction in cohesive forces. This increases the mobility of ions, which in turn creates more charges on the electrodes, resulting in higher dielectric loss factors (Shrestha and Baik 2013).

Table 1.6 shows the effect of the moisture content of agricultural materials on their dielectric properties. In general, the dielectric constant and dielectric loss factors of agricultural materials at a given frequency with the constant temperature increased with increasing moisture content. For example, at 27.12 MHz and a constant temperature of 20°C with four moisture contents (8.8%, 12.7%, 16.8%, and 20.9%), the dielectric constant and dielectric loss factors of black-eyed pea are 3.4 at 8.8%, 3.60 at 12.7%, 3.64 at 16.8%, and 8.90 at 20.9%, and 0.24 at 8.8%, 0.33 at 12.7%, 0.40 at 16.8%, 2.44 at 20.9%, respectively. The dielectric constants and dielectric loss factors of agricultural materials increased with increasing moisture content because the materials absorbed more electromagnetic energy as moisture content increased and water dipoles became more mobile, which increases ionic conductivity (Okos et al. 1992).

1.4.1 Measurement methods

The dielectric properties of agricultural materials and insect pests have been most commonly measured using the open-ended coaxial probe method and the dielectric test fixture method. The open-ended coaxial probe technique allows measurement of dielectric properties over the frequency range of 30 MHz to 4500 MHz in various fruits, nut products, legumes, grains, and insects (Wang et al. 2013, 2005, 2003; Zhu et al. 2012; Jiao et al. 2011; Guo et al. 2011, 2008; Sosa-Morales et al. 2009; Feng et al. 2002; Ikediala et al. 2000). The dielectric test fixture technique measures the dielectric properties in the radio frequency range of 75 kHz to 30 MHz.

Table 1.6. Effect of moisture content on the dielectric properties of agricultural materials at 27.12 MHz.

Agricultural material	Temperature (°C)	Dielectric constant				Dielectric loss factor				Reference
		8.8%	12.7%	16.8%	20.9%	8.8%	12.7%	16.8%	20.9%	
Black-eyed pea	20	3.4	3.60	3.64	8.90	0.24	0.33	0.40	2.44	Jiao et al. 2011
	30	3.43	3.75	3.82	9.50	0.25	0.38	0.47	2.65	Jiao et al. 2011
	40	3.51	4.07	4.18	9.86	0.27	0.47	0.60	3.06	Jiao et al. 2011
	50	3.62	4.59	4.98	11.22	0.28	0.64	0.91	3.94	Jiao et al. 2011
	60	3.84	5.50	6.67	13.86	0.31	0.97	1.67	6.06	Jiao et al. 2011
Chickpea		7.9%	11.4%	15.8%	20.9%	7.9%	11.4%	15.8%	20.9%	
	20	2.99	2.96	3.16	3.23	0.16	0.18	0.35	0.81	Guo et al. 2008
	30	3.16	3.03	3.94	4.79	0.26	0.15	0.39	0.99	Guo et al. 2008
	40	3.23	3.22	4.70	6.35	0.16	0.13	0.62	2.14	Guo et al. 2008
	50	3.44	3.60	6.98	11.43	0.19	0.20	1.71	7.85	Guo et al. 2008
	60	3.94	4.37	11.47	23.26	0.32	0.40	5.08	28.66	Guo et al. 2008
	70	4.86	6.00	19.76	39.19	0.58	1.06	14.75	73.33	Guo et al. 2008
	80	6.81	9.01	33.55	36.51	1.38	3.06	38.66	145.88	Guo et al. 2008
	90	11.20	15.35	51.92	71.59	4.27	9.41	86.42	248.25	Guo et al. 2008
Macadamia nut		3%	6%	12%	18%	3%	6%	12%	18%	
	25	4.3	5.3	9.3	16.7	0.3	0.8	5.7	22.8	Zhu et al. 2012
	40	4.3	5.6	10.2	18.1	0.4	0.9	7.9	30.9	Zhu et al. 2012
	60	4.5	6.1	11.1	19.8	0.4	1.2	11.0	42.4	Zhu et al. 2012
	80	4.7	6.6	12.2	21.6	0.4	1.7	15.9	57.7	Zhu et al. 2012
	100	5.1	7.4	13.8	24.7	0.6	2.9	26.0	94.5	Zhu et al. 2012
Mung bean		10.2%	14.4%	18.2%	22.3%	10.2%	14.4%	18.2%	22.3%	
	20	3.23	4.21	5.77	10.98	0.23	0.43	1.06	4.16	Jiao et al. 2011
	30	3.38	4.15	5.88	11.56	0.24	0.47	1.10	4.64	Jiao et al. 2011
	40	3.53	4.50	6.48	13.83	0.26	0.54	1.40	6.75	Jiao et al. 2011
	50	3.75	5.17	7.88	18.92	0.28	0.75	2.18	11.83	Jiao et al. 2011
	60	4.15	6.07	10.36	27.50	0.37	1.11	3.81	21.8	Jiao et al. 2011
Wheat		12%	15%	18.2%		12%	15%	18.2%		
	15	3.82	4.03	4.46	----	0.13	0.12	0.17	----	Shrestha et al. 2013
	30	4.11	4.48	4.77	----	0.09	0.12	0.21	----	Shrestha et al. 2013
	45	4.28	4.91	5.16	----	0.07	0.17	0.34	----	Shrestha et al. 2013
	60	4.66	5.51	5.77	----	0.09	0.35	0.66	----	Shrestha et al. 2013
	75	5.10	5.97	5.95	----	0.19	0.60	0.93	----	Shrestha et al. 2013

For more accurate measurement, the former method requires the sample surface to be brought in close contact with the probe, while the latter makes sure the sample is uniformly distributed in the bottom half of the fixture. Therefore, it is hard to directly measure the dielectric properties of stored agricultural materials and insects because most of the stored agricultural materials and insects have irregular shapes and are small. For these reasons, numerous studies reduced the size of the sample before the measurement of dielectric properties to minimize the void fraction of bulk samples. For example, chickpea and chestnut were ground into flour, chestnut weevil and cowpea weevil were ground into a semi-dry paste, fruits were blended into a paste, nuts were blended into a powder, and codling moth, Indian meal moth, Mexican fruit fly, and navel orange worm were blended into a slurry. Some were compressed to match the true density of the material (Wang et al. 2013, 2005, 2003; Zhu et al. 2012; Jiao et al. 2011; Guo et al. 2011, 2008; Sosa-Morales et al. 2009; Ikediala et al. 2000). However, the dielectric properties of the materials produced by the two methods are just an effective (apparent) value because of some void space in the bulk samples. The true (actual) value of dielectric properties of the material in dielectric heating is important to know but most of the time the effective value in bulk is more useful. For example, if we know the dielectric loss factor of the bulk material, then we can estimate the temperature increase of the bulk material. Otherwise, if we know the true dielectric loss factor and include electric field intensity and the thermal properties of the material, we can calculate the heating rate as if there were no pores in the sample. However, in reality, most of the time samples are in bulk. In order to calculate the heating rate of the bulk sample, we have to use the effective

value of the dielectric loss factor for practical selective heating evaluation using MW and RF energy.

1.4.1.1 Open-ended coaxial probe

The technique of using an open-ended coaxial probe (Figure 1.2) measures the dielectric properties of the sample based on its reflection coefficient. The active probe tip that touches the sample is connected to the analyzer. The analyzer gives the reflection coefficient of the material and calculates its dielectric constant using equation (1.4) (de los Santos et al. 2003) and the dielectric loss factor using equation (1.5) (de los Santos et al. 2003).

$$\varepsilon' = \frac{1}{Af} \left[\frac{-2\Gamma''}{(1+\Gamma')^2 + \Gamma''^2} \right] \quad (1.4)$$

$$\varepsilon'' = \frac{1}{Af} \left[\frac{1 - \Gamma'^2 - \Gamma''^2}{(1+\Gamma')^2 + \Gamma''^2} \right] \quad (1.5)$$

Here, Γ' and Γ'' are reflection coefficient data automatically transferred from the network analyzer to the computer, f is the measuring frequency, A is determined by the characteristic impedance of the analyzer ($Z_0 = 50 \Omega$) and the dimensions of the sample $A = 2\varepsilon_0 \frac{\pi^2 r^2}{t} Z_0$, where ε_0 is the dielectric permittivity of free space, r is the radius, and t is the thickness of the sample.

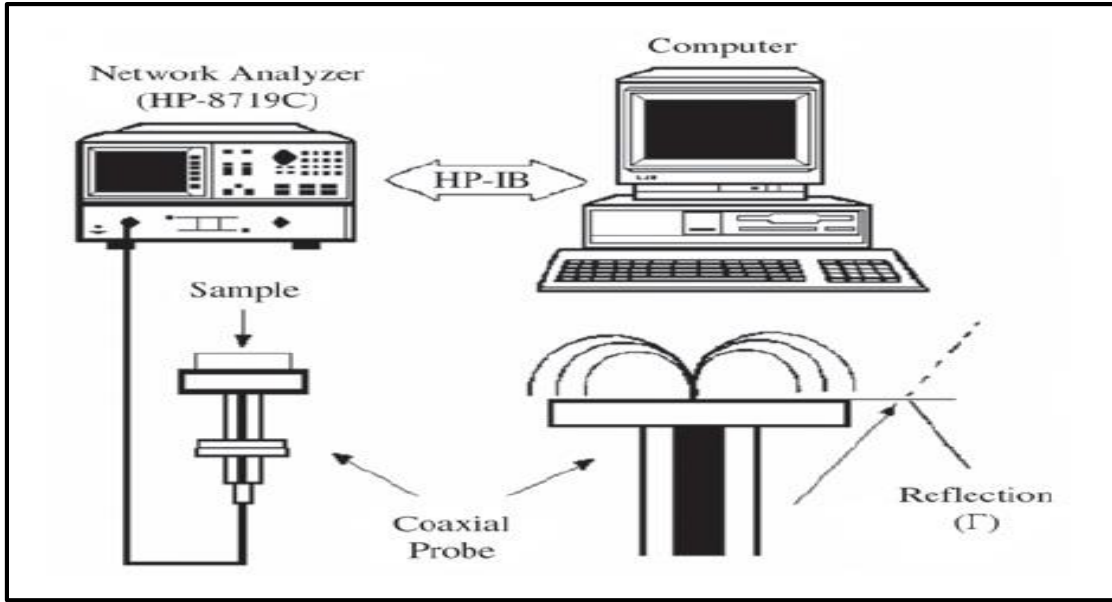


Figure 1.2. Dielectric properties measurement using an open-ended coaxial probe (de los Santos et al. 2003).

1.4.1.2. Dielectric test fixture

Figures 1.3 and 1.4 illustrate the mechanism for measuring the dielectric loss factor of a material using the dielectric test fixture (Shrestha and Baik, 2013). The sample is equally spread onto the bottom half of the dielectric test fixture. The fixture is tightly closed, and its inlet and outlet are sealed from the inside to prevent moisture escaping from the fixture. The fixture is connected to the Conductance (L), Capacitance (C), and Resistance (R) meter (LCR meter), which measures the conductance, capacitance, and resistance of the sample and calculates the dielectric constant using equation (1.6) (Von Hippel 1954; Agilent Technologies 2000) and the dielectric loss factor using equation (1.7) (Von Hippel 1954; Agilent Technologies 2000).

$$\epsilon' = tC_p/A\epsilon_0 \quad (1.6)$$

$$\epsilon'' = t/2\pi f A\epsilon_0 R_p \quad (1.7)$$

Here, t is the electrode gap (m), A is the electrode area (m^2), f is the frequency (MHz), ϵ_0 is the permittivity of free space or vacuum (8.854×10^{-12} F/m), C_p is the parallel capacitance, and R_p is the parallel resistance (Ω).

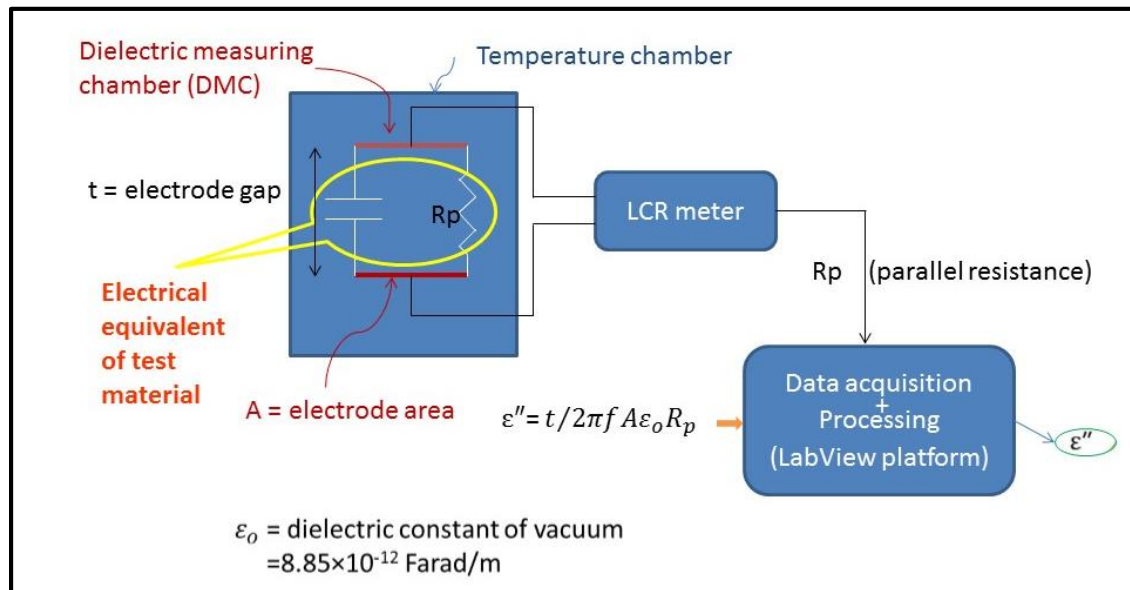


Figure 1.3. Mechanism of measurement using a dielectric test fixture (Shrestha and Baik 2013).

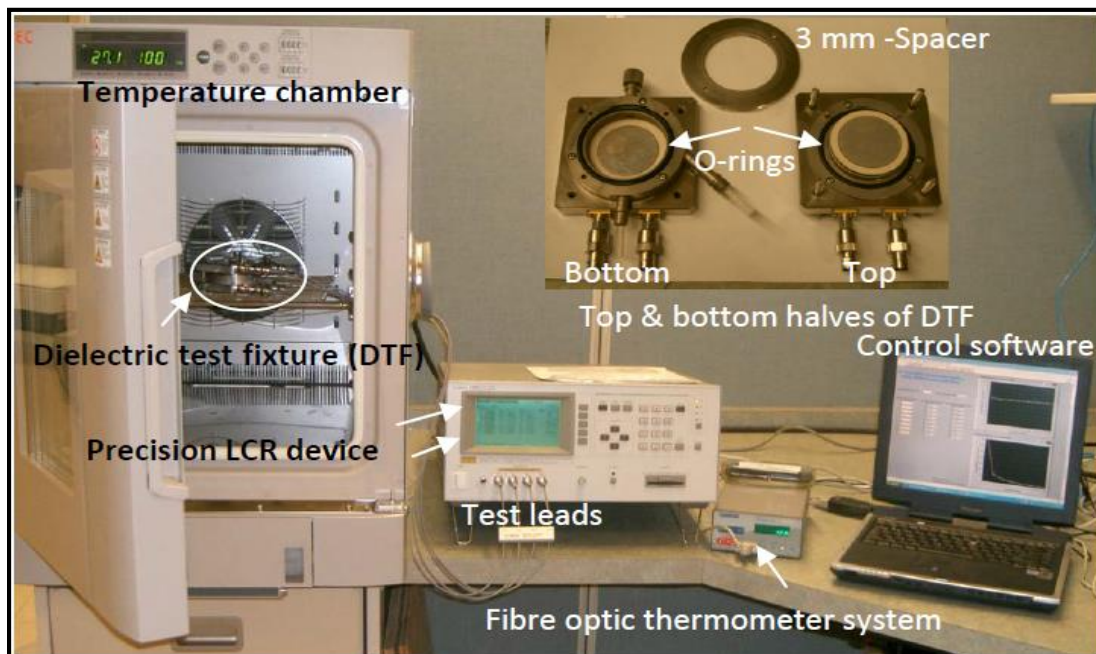


Figure 1.4. Dielectric properties measurement using a dielectric test fixture (Shrestha and Baik 2013).

1.5 Radio frequency and microwave comparison

Radio frequency (RF) and microwave (MW) radiation are parts of the electromagnetic spectrum (Figure 1.5). The term radio frequency involves frequencies between 1 and 100 MHz and microwave involves frequencies above 500 MHz (Metaxas and Meredith 1988). The US Federal Communications Commission (FCC), which is the responsible regulatory agency for the out-of-band emissions from medical, scientific, domestic, and industrial applications in the United States, has allocated the following frequencies for industrial applications: 13.56 MHz, 27.12 MHz, 40.68 MHz for RF applications and 915 MHz, 2450 MHz, 5800 MHz and 24125 MHz for MW applications (Wang et al. 2011).

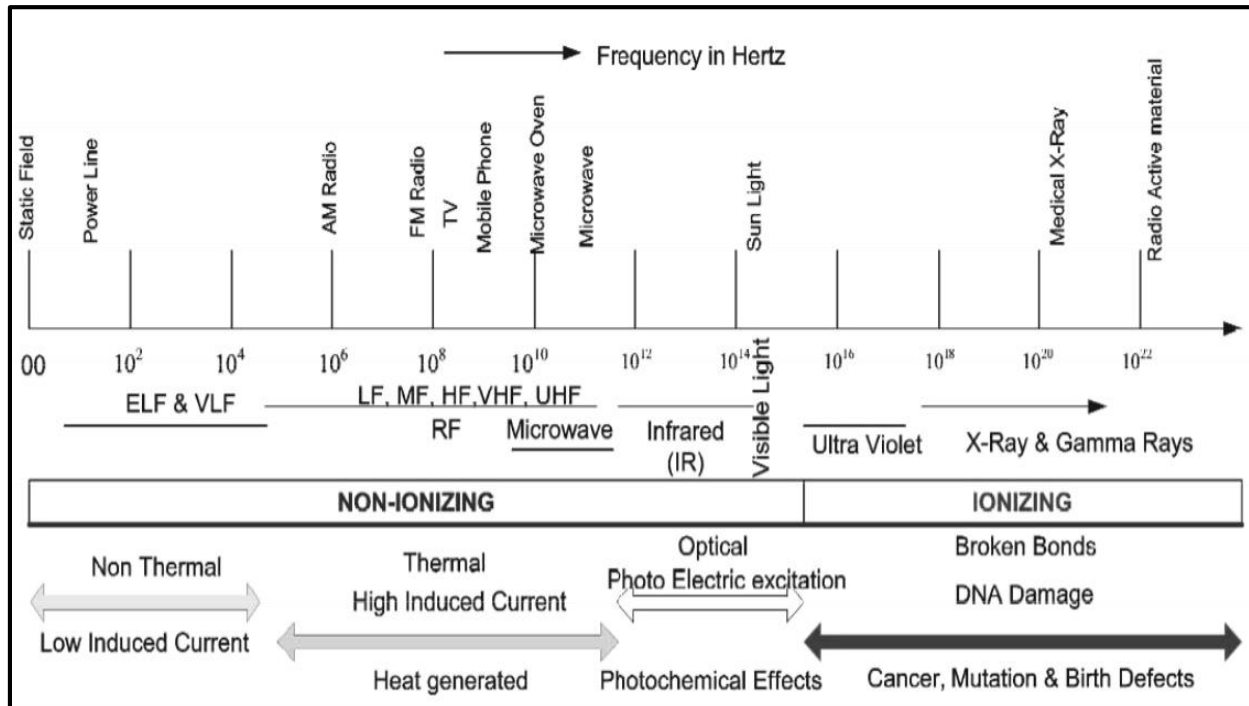


Figure 1.5. Microwave (MW) and radio frequency (RF) allocation in the electromagnetic spectrum (Wang et al. 2011).

The frequencies of 27.12 MHz (RF) and 2450 MHz (MW) are commonly used for industrial applications (Das et al. 2014; Manickavasagan et al. 2013; Purohit et al. 2013; Shrestha and Baik 2013; El-Naggar et al. 2011; Singh et al. 2011; Wang et al. 2010, 2007a, 2007b, 2002, 2001; Vadivambal et al. 2010; Tiwari et al. 2008; Lagunas-Solar et al. 2007; Birla et al. 2005). In the case of RF heating, 27.12 MHz has been popularly used because it offers a good compromise between low frequency (13.56 MHz) and high frequency (40.68 MHz) problems in RF heating. Of the three frequencies (13.56 MHz, 27.12 MHz, and 40.68 MHz), 13.56 MHz has the most uniform voltage distribution and the highest penetration depth, followed by 27.12, and 40.68 MHz (Shrestha and Baik 2013; Shrestha et al. 2013; Mehdizadeh 2010). The low frequency (13.56 MHz) also produces the highest electric field strength (voltage/cm) in the air surrounding the material that can easily cause air ionization and breakdown (arcing) (Mehdizadeh 2010). The high frequency (40.68 MHz) produces the lowest electric field strength (voltage/cm) in the air surrounding the material and is far from the arcing limit, but high-frequency heating is associated with important problems during operation. The first problem is high long-term maintenance costs due to cooling problems and the shorter life of various components at high frequency (Koral 2008). Another issue is that the less uniform voltage distribution associated with high-frequency heating results in problems in heating uniformity (Koral 2008). The 27.12 MHz radio frequency provides a good compromise that neutralizes the problems associated with the low and high frequencies. In addition, 27.12 MHz has the highest permitted frequency band of operations (± 163 kHz). The bands of operations for 13.56 MHz and 40.68 MHz are only ± 7 kHz and ± 20 kHz, respectively (Koral 2008). Moreover, for MW heating, of

the four frequencies (915 MHz, 2450 MHz, 5800 MHz, and 24125 MHz) allocated for industrial applications, 2450 MHz is the frequency most popularly used because it is the same frequency as that used in domestic microwave ovens (Jankowski and Reszke 2011).

Furthermore, over the past 15 years, microwave heating has been used for disinfestation of walnut, wheat, chickpea, pigeon pea, green gram, corn, barley, rye, date fruit, mung bean, and soil (Das et al. 2014; Jian et al. 2014; Manickavasagan et al. 2013; Purohit et al. 2013; El-Naggar et al. 2011; Singh et al. 2011; Vadivambal et al. 2010, 2008; Mavrogiannopoulos et al. 2000) and radio frequency heating for disinfestation of wheat, rice, apple, black-eyed peas, mung beans, chickpeas, lentils, cherry, orange, persimmon, walnut, almond, coffee bean, pistachios, rapeseeds, corn, macadamia, soybeans, and chestnut (Alfaifi et al. 2016, 2014; Kong et al. 2016; Ling et al. 2016; Yu et al. 2016; Zhou et al. 2016, 2015; Huang et al. 2015; Zhang et al. 2015; Hou et al. 2015; Shrestha et al. 2013; Pan et al. 2012; Jiao et al. 2016, 2015, 2011; Wang et al. 2014a, 2014b, 2013, 2010, 2008, 2007a, 2007b, 2006a, 2006b, 2005, 2003, 2002, 2001; Tiwari et al. 2008; Lagunas-Solar et al. 2007; Monzon et al. 2007; Birla et al. 2005, 2004; Mitcham et al. 2004; Ikediala et al. 2002). The results of these studies show that both RF and MW heating may be used for disinfestation. Many studies, however, have shown that RF heating is preferred over MW heating for controlling insect pests in host materials (Shrestha et al. 2013; Guo et al. 2010; Wang et al. 2011, 2003; Nelson 1996). This preference is due to the greater penetration depth and stronger selective heating effects of RF heating compared to MW heating. The penetration depth of RF heating is measured in metres whereas the penetration depth of MW heating is measured in centimetres.

The main components of a dielectric heating system are the generator and applicator. The generator is the source of the alternating charges going to the applicator. The applicator consists of two electrodes (- and +) in RF heating and it is where the materials (grains and insects) are heated. In disinfestation, the design of the applicator is very important. Five applicator configurations are used in dielectric heating for industrial applications: monomode and multimode applicators in MW heating (Figure 1.6) and plate, staggered, and stray field electrodes in RF heating (Figure 1.7). Full descriptions of these applicators and the differences between them were given by Wang et al (2011).

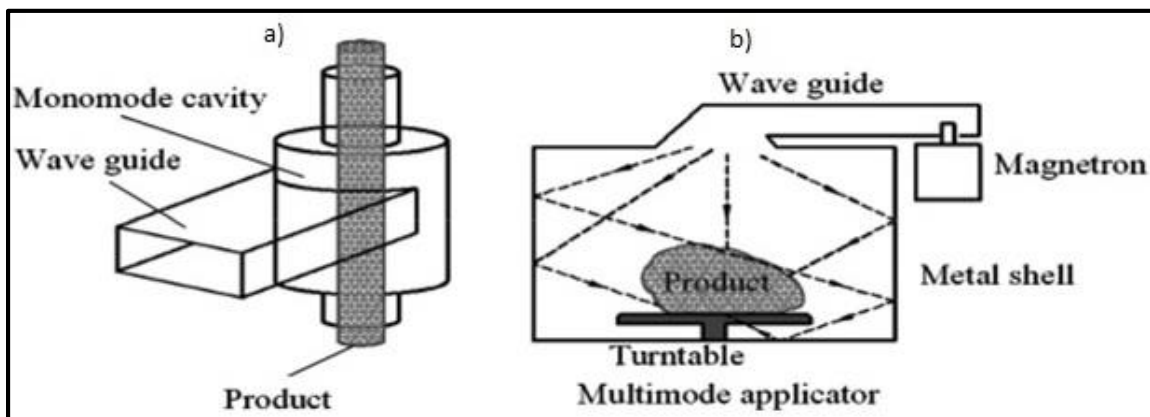


Figure 1.6. Schematic buildup of microwave (MW) applicators: a) Monomode applicator b) Multimode applicator (Wang et al. 2011).

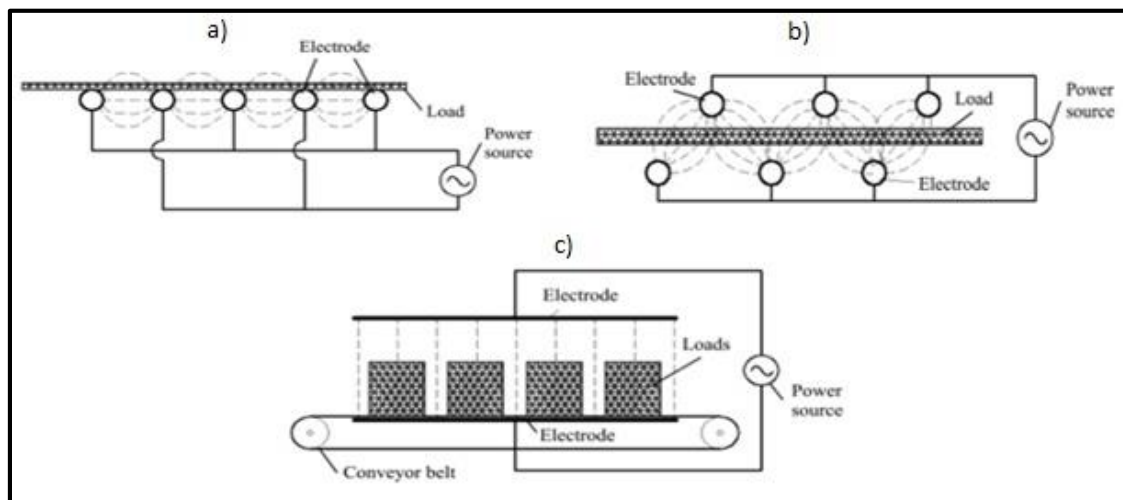


Figure 1.7. Schematic buildup of radio frequency (RF) applicators: a) Stray field electrodes b) Staggered electrodes c) Flat electrodes (Wang et al. 2011).

According to Wang et al. (2011), there are two types of RF heating systems used in the industry: conventional (Figure 1.8) and 50-ohm technology-based (Figure 1.9). In the conventional RF heating system, power is generated by a standard oscillator circuit using triode tubes. The applicator consists of an electrode system (hot and ground) in which the material (load) is heated. The electrodes and load constitute a tuned circuit coupled inductively to the output circuit of the generator. The 50-ohm dielectric heating system has the same principle heating as the conventional system of radio frequency heating. The advantage of this system includes locational flexibility as a coaxial cable can separate the RF generator and applicator, and maximum power output and fine power control by the matching network (Jones and Rowley 1996).

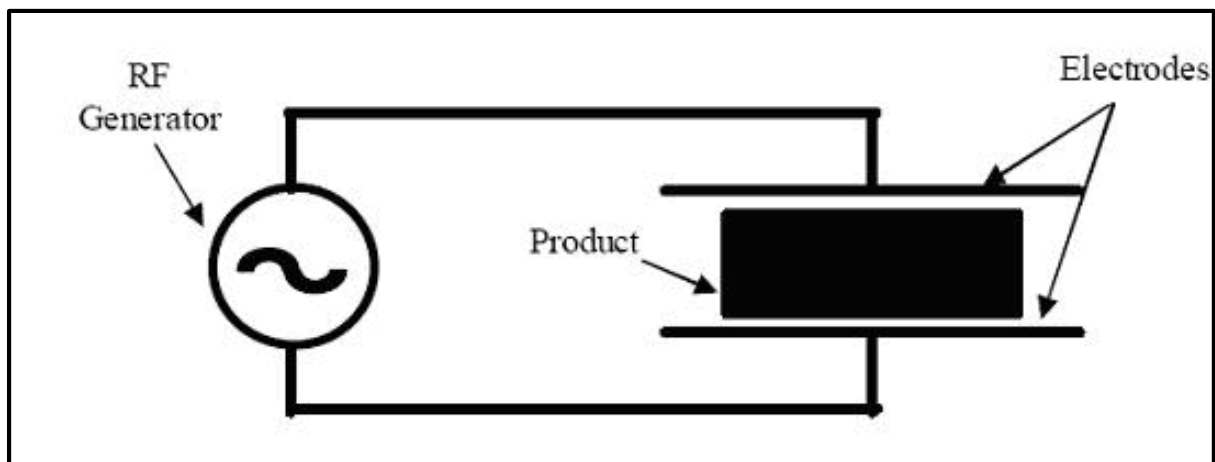


Figure 1.8. Conventional radio frequency (RF) heating system (Koral 2004).

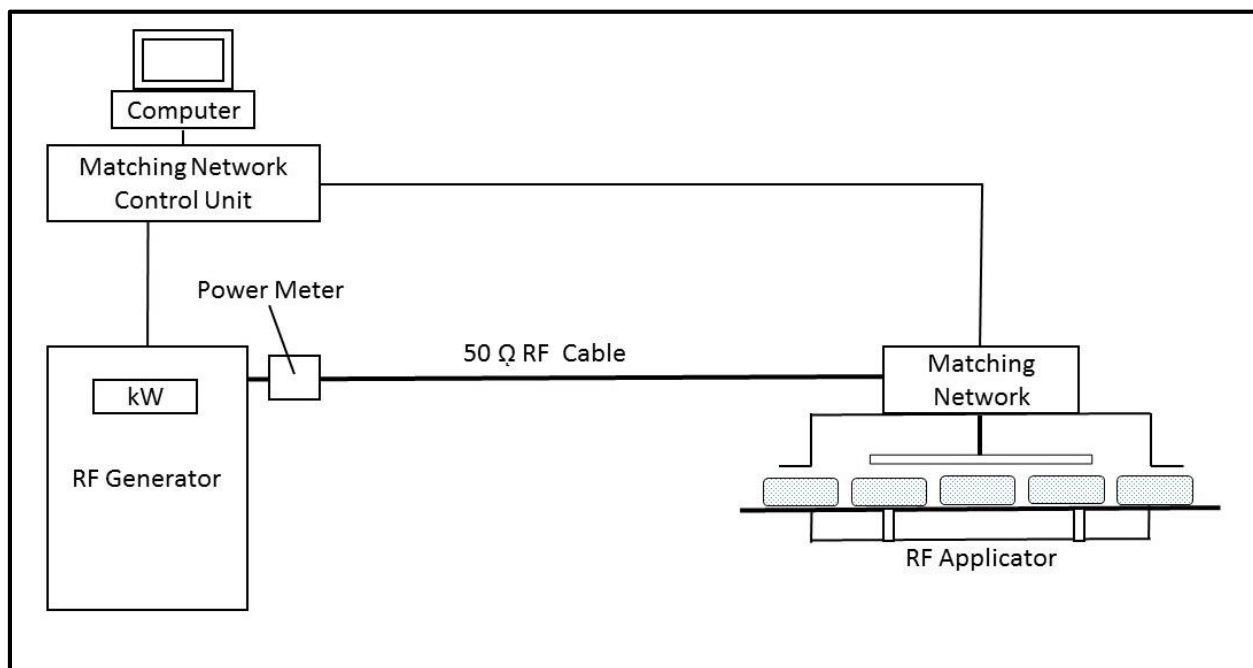


Figure 1.9. 50-ohm Technology based radio frequency (RF) Heating System (Adapted from Jones and Rowley 1996).

1.5.1 Effect of power and temperature on the exposure time for 100% mortality of different insect pests

Power-time and temperature-time relationships can be useful for identifying the best combination for achieving 100% mortality of insects using RF and MW heating without damaging the quality of the host material. Inadequate combinations of these relationships result in degradation of the quality of the material or failure to kill 100% of the insects. A significant number of studies have investigated the effect of the power level on the exposure time required to reach 100% mortality of insect pests. In general, the results show that the exposure time required pests increases when the power level decreases. This is logical because the amount of heat energy required to kill the insect is directly related to the product of power and time. For example, the exposure times required to achieve 100% mortality of *Collosobruchus chinenses* at five different power

levels (700 W, 560 W, 420 W, 280 W, and 140 W) in the case of chickpeas are 100 s, 160 s, 200 s, 240 s, and 300 s, respectively. In the case of pigeon peas, the exposure times required are 90 s, 140 s, 180 s, 240 s, and 280 s, respectively. In the case of green grams, the exposure times required are 70 s, 120 s, 160 s, 240 s, and 300 s respectively (Singh et al. 2011). However, the research shows that other properties also are affected. For example, as the power increased, the viability and germination of chickpeas, pigeon peas, and green grams decreased. These findings suggest that the power-time relationship is important in identifying the best combinations for killing the insects without degrading the quality of the host material. The need for increased exposure time when power is decreased also has been demonstrated in the disinfestation of *Sitophilus zeamais*, *Tribolium castaneum* and *Plodia interpunctella* in stored corn (Vadivambal et al. 2010), the disinfestation of *Tribolium castaneum*, *Cryptolestes ferrugineus*, and *Sitophilus granaries* in barley and rye (Vadivambal et al. 2008), the disinfestation of *Tribolium castaneum* and *Oryzaephilus surinamensis* in stored dates (Manickavasagan et al. 2013), and the disinfestation of cowpea weevil in mung beans (Purohit et al. 2013). To summarize, lower power levels require longer heating times, and higher power levels require shorter heating times.

Another important factor in the mortality of insect pests is the temperature of insect pest. All of the following studies have used the surface temperature of insect pests and it was considered an indicator of the insect pest's body temperature. The method of measuring the surface temperature was not accurate because the RF and MW heating was stopped and the surface temperature was measured using a thermal video camera and fiber optic temperature sensors. There might be an effect of cooling after stopping

the heating. On the other hand, it might be reasonable to assume that the surface temperature of the insect is similar to the insect body temperature because the insects are tiny and heated volumetrically, which means uniform heating. To evaluate the effect of temperature on the mortality of insect pests, disinfestation of wheat, walnut, and rice at different average surface temperatures was studied using microwave and radio frequency energy (El Nagggar et al. 2011; Lagunas-Solar et al. 2007; Wang et al. 2007b, 2001). The results of their studies showed when the temperature increased, the exposure time for 100% mortality rate of insect pests decreased. For example, with the disinfestation of confused flour beetle and rice moth in wheat, a 100% mortality rate for confused flour beetle was achieved in 50 s at 50°C and when the temperature was increased to 55°C, the time was shortened to 20 s. For rice moth, a 100% mortality rate was obtained in 20 s at 50°C. When the temperature was decreased to 40°C, the exposure time required to achieve 100% mortality increased to 50 s (El-Nagggar and Mikhael 2011). These results indicate that lower temperatures require longer heating times, and higher temperatures require shorter heating times. The relationship is obvious because the temperature is directly related to power.

1.5.2 Quality of host materials after disinfestation

RF and MW heating are promising methods for disinfestation. They offer two main advantages over conventional methods: volumetric heating and rapid heating. Conventional heating methods heat the material from the surface and heat penetrates the material slowly, whereas RF and MW heating heat the surface and the inside of the material at the same time. Because of this rapid penetration of the material heated, many researchers have investigated the quality of the host materials after RF and MW

disinfestation. Overall, the research has found that most properties of the host material are not significantly affected by RF or MW heating (Table 1.7). For example, when investigating the effect of MW heating on the instrumental texture (hardness, adhesiveness, springiness, cohesiveness, and chewiness), sensory attributes, and surface colour of dates, Manickavasagan et al. (2013) found no changes in these properties after MW treatment. These findings suggest that MW heating is acceptable for controlling insect pests in stored dates. Various researchers have investigated the quality of the host material after dielectric heating of a number of commodities. This research also found that the quality of the host material was not affected. Example include: the milling and cooking quality of chickpeas, pigeon peas, and green grams (Singh et al. 2011), the protein, fibre, fat, carbohydrates, ash, and milling quality of wheat (Shrestha et al. 2013; El-Naggar and Mikhael 2011), the moisture content and milling quality of rice (Lagunas-Solar et al. 2007), the weight, moisture content, germination, and colour of legumes (Wang et al. 2010), the firmness, acidity, soluble solids, and colour of oranges (Birla et al. 2005), the weight, firmness, soluble solids, titratable acidity, colour, and calyx browning of persimmon (Tiwari et al. 2008; Monzon et al. 2007), and the water activity, shell characteristics, sensory qualities, rancidity, kernel colour, peroxide value and free fatty acids of walnuts (Das et al. 2014; Wang et al. 2007b, 2002). This large body of research proves that dielectric heating does not damage the quality of the host materials. Some properties, however, were found to be slightly affected by dielectric heating but the changes were minor. The changes noted were the colour, peroxide value, and free fatty acid levels of walnuts (Das et al. 2014), the germination of wheat grains (El-Naggar and Mikhael 2011), the volatile flavour profiles of oranges (Birla et al. 2005), the moisture

Table 1.7. Quality of the host material not significantly affected by dielectric heating with 100% mortality rate.

Samples	Quality parameters (not significantly affected)	Frequency	Reference
Chickpea	Milling and cooking	2450 GHz	Singh et al. 2011
Pigeon pea	Milling and cooking	2450 GHz	Singh et al. 2011
Green gram	Milling and cooking	2450 GHz	Singh et al. 2011
Date Fruit	Hardness, adhesiveness, springiness, cohesiveness, chewiness, sensory attributes, and surface colour	2450 GHz	Singh et al. 2011
Wheat	Falling numbers; yield of flour, bran, and shorts; and PBW	27.12 MHz	Shrestha et al. 2013
Wheat	Protein, fiber, fat, carbohydrates, and ash	2450 GHz	El-Naggar and Mikhael 2011
Rice	Moisture content and milling quality of the rice	27.12 MHz	Lagunas-Solar et al. 2007
legumes	Weight loss, moisture content, germination, and colour	27.12 MHz	Wang et al. 2010
Oranges	Firmness, acidity, total soluble solids, and colour	27.12 MHz	Birla et al. 2005
Persimmon Persimmon	Weight, firmness, soluble solid content, and titratable acidity of the fruit	27.12 MHz	Monzon et al. 2007
	Soluble solids, titratable acidity, peel and pulp colour, and calyx browning of persimmons	27.12 MHz	Tiwari et al. 2008
Walnuts	Water activity	2450 GHz	Das et al. 2014
Walnuts	Shell characteristics, sensory qualities, and rancidity	27.12 MHz	Wang et al. 2002
Walnuts	Kernel colour, peroxide values and fatty acid values	27.12 MHz	Wang et al. 2007

content of in-shell walnuts and almond shells (Gao et al. 2010; Wang et al. 2002), and the flour protein, mixing-development-time, mean-peak-height, colour, and moisture content of wheat (Shrestha et al. 2013). Although these changes in quality are not significant, they are still important to note. There are, however, circumstances where a change in quality is desirable. For example, moisture content loss is beneficial to grains that are to be dried for storage. In this example, RF heating can be said “to kill two birds (disinfestation and drying) with one stone”.

In summary, MW and RF heating for disinfestation is clearly feasible and does not sacrifice the quality of the host material. Furthermore, the selective heating and heating

uniformity made possible by MW and RF heating do not damage the quality of the host materials. When using selective heating, 100% of the insects will be killed when the insects' fatal temperature is applied, but the host materials can be maintained at a lower temperature that does not significantly affect the quality of the host materials. When using uniform heating, it is possible to avoid degrading the quality of the host materials.

1.5.3 Heating uniformity

Global heating uniformity in the disinfestation of insect pests from host materials using dielectric heating is very important. However, one of the important challenges in dielectric heating disinfestation is minimizing the temperature difference between the hot and cold spots in the bulk samples for more uniform heating. Non-uniform heating in dielectric heating happens because of the non-uniform distribution of the electromagnetic field. Non-uniformity increases the chance of insect pests surviving (Jian et al. 2014). Insect pests have the ability to escape to the colder spots (Shrestha et al. 2013). Many studies have reported the non-uniform distribution of temperature when using MW and RF radiation in heating fruits (orange, apple, grapefruit, peach, and avocado), mixed beans (black-eyed peas, mung beans, chickpeas, and lentils), disinfesting codling moth in in-shell walnuts, three grain insects (*Sitophilus zeamais*, *Tribolium castaneum* and *Plodia interpunctella*) in corn, and *Cryptolestes ferrugineus* in wheat (Jian et al. 2014; Shrestha et al. 2013; Jiao et al. 2011; Birla et al. 2008; Vadivambal et al. 2010; Wang et al. 2001). Thus, non-uniform heating of the system is a significant challenge for successful disinfestation using MW and RF heating.

Many studies have tried to improve heating uniformity in RF and MW systems. Some of these studies on RF heating added hot air, saline water, and movements of the

conveyor to improve heating uniformity (Zhou et al. 2016, 2015; Jiao et al. 2015a, 2015b; Wang et al. 2013, 2010, 2007a; Pan et al. 2012; Gao et al. 2010; Mitcham et al. 2004; Ikediala et al. 2002). For example, Pan et al. (2012) studied RF heating uniformity of coffee beans under four conditions: RF heating only, RF heating with conveyor belt speeds of 0.89 m per minute, RF heating with conveyor belt movement and forced hot air at 48°C, and RF heating with conveyor belt movement, hot air, and holding for 10 minutes. To determine whether RF heating uniformity was improved, heating uniformity indexes of the four conditions were compared. Heating uniformity index is defined as the ratio of the rise in the standard deviation to the mean of the product temperatures over the heating time. RF heating only had a heating uniformity index at the surface of 0.109, RF heating with conveyor belt speed of 0.89 m per minute had 0.105, RF heating with a conveyor belt movement and forced hot air at 48°C had 0.073, and RF heating with conveyor belt movement, hot air, and holding for 10 minutes had 0.030. The results show that movement and hot air improved RF heating uniformity, resulting in a reduced heating uniformity index (Pan et al. 2012). Some studies on MW heating improved heating uniformity by improving the uniformity of the electromagnetic field in the MW cavity and improving the uniformity of MW energy absorption by displacing the material (Li et al. 2011). According to Li et al. (2011), improving the uniformity of electromagnetic field in a cavity can be done by increasing the number of MW power ports, using various MW sources with different allowed frequencies, installing a mode stirrer, applying pulse MW heating, arranging for a mobile MW radiator, or designing the size and shape of the MW cavity. Atong (2006) improved heating uniformity by displacing the material. The author designed a continuous belt MW dryer that moves the material as the conveyor belt moves

across the cavity, increasing the number of MW generators, and adjusting the output power (Li et al. 2011).

In summary, the design of the heating system has a significant effect on the heating uniformity during RF or MW disinfestation. Another suggestion for more uniform heating for both MW and RF disinfestation is by using computer simulation to design more globally uniform heating of the system (Alfaifi et al. 2016; Chen et al. 2016, 2015; Huang et al. 2016a, 2016b, 2015a, 2015b) Computer simulation can be used to determine the electric field formation and temperature of the system theoretically. Simulation can investigate different parameters such as the position, shape, and size of both the heating system and the materials. After a series of simulations, the optimum design of an applicator and the proper selection of the input and operating parameters can be determined.

1.6 Disinfestation economics

Radio frequency and microwave disinfestation are chemical free and offer many advantages compared to pesticides, fumigants, and conventional heating. However, one of the problems in using RF and MW heating for disinfestation of insect pests from host materials is the initial cost of the technology. Nelson (1996) mentioned that the cost of the equipment to disinfest insect pest from stored grains is too high to justify RF and MW disinfestation as a practical means. However, economic factors have changed over the past years. The capital cost per kW of power output has dropped significantly. The fall in cost will be like the case of the microwave in 1993; it was very expensive (\$3000 to \$4000) (Das and Curlee 1993), but now it is affordable (\$50 to \$200). Furthermore, the initial cost will be paid over time because the RF and MW heating operating cost is cheaper than

conventional disinfestation methods. Despite its advantages, the current RF and MW heating applications for disinfestation and other commercial application are priced competitively in comparison with other methods (Lagunas-Solar et al. 2006).

Shrestha et al. (2013) calculated the relative cost for RF disinfestation of wheat stored in a medium-sized bin, with a capacity of 8750 bushels, based on the findings from their study of disinfesting rusty grain beetle from stored wheat. The operating cost of treating that volume of wheat using RF energy was much cheaper compared to fumigants and pesticides: \$25 for RF heating, and based on their preliminary research, \$250 to \$2500 for the chemical cost plus the operating cost. Lagunas-Solar et al. (2006, 2005) calculated the operating cost of fishmeal disinfection and rough rice disinfestation using RF energy, as \$3.20 per ton for fishmeal and \$1.35 per ton for rough rice. The costs were much lower than for chemical alternatives (about \$15 to \$20 per ton) or conventional heating (about \$25 per ton) (Lagunas-Solar et al. 2006). Langlinais (1989) compared the cost of controlling weevils in rice using fumigation and MW energy. It was found that the MW disinfestation cost was only 6.3 cents/CWT (one hundred pounds) and the fumigation cost was 11 cents/CWT (Rajagopal 2009). Halverson et al. (1999) estimated the cost of controlling stored-product insects using RF heating. The results showed that the RF disinfestation operating cost was 0.67\$/t and was lower than the \$2 treatment cost of 1 ton of grain using chemicals (Rajagopal 2009; Zajtzev et al. 2001). Rajagopal (2009) calculated the cost of disinfestation of stored grain insects using MW energy. He found that the operational cost to disinfest 1 ton of wheat using MW energy was cheaper than the cost of Malathion to kill insects in wheat. The MW operating cost was \$0.75/t while Malathion treatment cost was \$1.19/t. RF and MW disinfestation seem to be promising

alternatives to fumigation and pesticides for disinfestation of insect pests from the host material despite their high capital cost.

1.7 Concluding remarks

Disinfestation of insect pests from host materials using RF and MW energy is possible without affecting host material quality significantly. Radio frequency heating has greater penetration depth, higher energy efficiency, and a higher selective heating effect than MW heating. The dielectric properties of agricultural materials and insects increased with increasing temperature and MC and decreased with frequency. The large dielectric loss factor ratios between agricultural materials and insects showed potential for practical selective heating of insects in agricultural host materials using MW and RF energy. However, the largest dielectric loss factor ratio is in the radio frequency range between 27 MHz and below. Thus, RF heating is preferred for disinfestation. This feasibility check for selectivity of heating using the dielectric loss factor ratio is only a rough estimation without considering the electric field intensity and the thermal properties of the insect pests and host materials, and heat conduction from hotter insect bodies to colder host grains.

Many studies showed that RF heating has several advantages over conventional heating, because RF heating is volumetric, fast, and chemical-free. However, there is still a need for further studies to solve problems in the disinfestation of insect pests from host agricultural materials using RF heating technology. Based on our comprehensive review and speculation, the following can be suggested. First, for the non-uniform heating of the system, investigators can work on the proper design of applicators, reflecting on operating

parameters (frequency, output power, and residence time), and the dielectric properties of host materials and insect pests. Second, for mixing of non-uniformly heated materials and continuous processing, some accessories in the heating system that can move and stir the material while it is being subjected to RF heating, such as an RF-transparent auger transport system, can be developed. Third, to improve selective heating of the insect pests, the use of a high power RF heating system can be tested to see whether a high power system can reduce conductive heat transfer from hotter insect bodies to colder grains by reducing RF heating time (residence time). Fourth, it is suggested to use of computer simulation to understand and quantify the impacts of electric field formation and temperature of the samples with different configurations and positions of electrodes, shapes, size, and quantity of host grains, the orientation of grains and insects. Fifth, for process optimization and grain quality control, researchers can investigate the kinetics of thermal mortality versus the kinetics of grain quality change during RF-assisted disinfestation. Sixth, for a more realistic and practical feasibility test, a selective heating index should be developed, considering all the factors affecting the rate of temperature increase and the power dissipation ratio of the sample, such as the conductive heat transfer from hotter insects to colder grains in terms of a variety of insects, moisture content and quantity, dielectric properties and thermal properties of the insect pests and grains, and electric field intensity. Lastly, for practical and effective application of RF heating technology to disinfestation of insect pests from host agricultural materials, the cost and energy efficiency of the technology need to be evaluated in the development phase of the technology.

1.8 References

Agilent Technologies. 2000. Model #16452. In Liquid Test Fixture Manual; Agilent Technologies: Palo Alto, CA.

Alfaifi, B., J. Tang, B. Rasco, S. Wang and S. Sablani. 2016. Computer simulation analyses to improve radio frequency (RF) heating uniformity in dried fruits for insect control. *Innovative Food Science and Emerging Technologies* 37: 125-137.

Alfaifi, B., J. Tang, Y. Jiao, S. Wang, B. Rasco, S. Jiao and S. Sablani. 2014. Radio frequency disinfestation treatments for dried fruit: model development and validation. *Journal of Food Engineering* 120: 268-276.

Alfaifi, B., S. Wang, J. Tang, B. Rasco, S. Sablani and Y. Jiao. 2013. Radio frequency disinfestation treatments for dried fruit: Dielectric properties. *Food Science and Technology* 50: 746-754.

Ark, P. and W. Parry. 1940. Application of high-frequency electrostatic fields in agriculture. *The Quarterly Review of Biology* 15: 172-191.

Atong, D. 2006. Drying of a slip casting for tableware product using microwave continuous belt dryer. *Drying Technology* 24(5): 589-594.

Barba, A. and G. Lamberti. 2013. Dielectric properties of pineapple as function of temperature and water content. *International Journal of Food Science and Technology* 48: 1334–1338.

Berbert, P., D. Queiroz and E. Melo. 2002. Dielectric properties of common bean. *Biosystems Engineering* 83: 449–462.

Berbert, P., D. Queiroz, E. Sousa, M. Molina, E. Melo and L. Faroni. 2001. Dielectric properties of parchment coffee. *Journal of Agricultural Engineering Research* 80: 65-80.

Birla, S., S. Wang, J. Tang and G. Tiwari. 2008. Characterization of radio frequency heating of fresh fruits influenced by dielectric properties. *Journal of Food Engineering* 89: 390-398.

Birla, S.L., S. Wang, J. Tang and G. Hallman. 2004. Improving heating uniformity of fresh fruit in radio frequency treatments for pest control. *Postharvest Biology and Technology* 33: 205-217.

Birla, S.L., S. Wang, J. Tang, J.K. Fellman, D.S. Mattinson and S. Lurie. 2005. Quality of oranges as influenced by potential radio frequency heat treatments against Mediterranean fruit flies. *Postharvest Biology and Technology* 38: 66-79.

Boldor, D., J. Sanders and J. Simunovic. 2004. Dielectric properties of in-shell and shelled peanuts at microwave frequencies. *Transaction of the ASAE* 47: 1159–1169.

Chen, L., K. Wang, W. Li and S. Wang. 2015. A strategy to simulate radio frequency heating under mixing conditions. *Computers and Electronics in Agriculture* 118: 100-110.

Chen, L., Z. Huang, K. Wang, W. Li and S. Wang. 2016. Simulation and validation of radio frequency heating with conveyor movement. *Journal of Electromagnetic Waves and Applications* 30(4): 473-491.

Choi, C. and A. Konrad. 1991. Finite element modeling of the RF heating process. *IEEE Transactions on Magnetics* 27: 4227-4230.

Das, I., N.G. Shah and G. Kumar. 2014. Properties of walnut influenced by short time microwave treatment for disinfestation of insect infestation. *Journal of Stored Products Research* 59: 152-157.

Das, S. and T.R. Curlee. 1993. An assessment of the cost of microwave sintering ceramic tiles for armor applications: Phase 1 report. Oak Ridge National Laboratory, Oak Ridge Tennessee 37831.

De los Santos, J., D. Garcia and J. Eiras. 2003. Dielectric characterization of materials at microwave frequency range. *Materials Research* 6: 1980-5373.

El-Naggar, S. and A. Mikhael. 2011. Disinfestation of stored wheat grain and flour using gamma rays and microwave heating. *Journal of Stored Products Research* 47: 191-196.

Engelder, D. and C. Buffler. 1991. Measuring dielectric properties of food products at microwave frequencies. *Microwave World* 12: 6-15.

Feng, H., J. Tang and R. Cavalieri. 2002. Dielectric properties of dehydrated apples as affected by moisture and temperature. *Transaction of the ASAE* 45: 129–135.

Gao, M., J. Tang, Y. Wang, J. Powers and S. Wang. 2010. Almond quality as influenced by radio frequency heat treatments for disinfestation. *Postharvest Biology and Technology* 58: 225-231.

Guo, W., G. Tiwari, J. Tang and S. Wang. 2008. Frequency, moisture and temperature-dependent dielectric properties of chickpea flour. *Biosystems Engineering* 101: 217-224.

Guo, W., S. Wang, G. Tiwari, J. Johnson and J. Tang. 2010. Temperature and moisture dependent dielectric properties of legume flour associated with dielectric heating. *LWT Food Science Technology* 43: 193–201.

Guo, W., X. Wu, X. Zhu and S. Wang. 2011. Temperature-dependent permittivities of chestnut and chestnut weevil from 10 to 4500 MHz. *Biosystems Engineering* 110: 340–347.

Halverson, S., T. Phillips, T. Bigelow, G. Mbata and M. Payton. 1999. The control of various species of stored-product insects with EHF energy. Annual International Research Conference on Methyl Bromide Alternatives and Emissions Reductions. San Diego California. November 1-4.

Headlee, T. and R. Burdette. 1929. Some facts relative to the effect of high frequency radio waves on insect activity. *Journal of the New York Entomological Society* 37: 59-64.

Hossan, M. and P. Dutta. 2012. Effects of temperature dependent properties in electromagnetic heating. *International Journal of Heat Mass Transfer* 55: 3412-3422.

Hou, L., J. Hou, Z. Li, J. Johnson and S. Wang. 2015. Validation of radio frequency treatments as alternative non-chemical methods for disinfesting chestnuts. *Journal of Stored Products Research* 63: 75-79.

Hou, L., J. Johnson and S. Wang. 2016. Radio frequency heating for postharvest control of pests in agricultural products: A review. *Postharvest Biology and Technology* 113: 106-118.

Huang, Z., B. Zhang, F. Marra and S. Wang. 2016. Computational modelling of the impact of polystyrene containers on radio frequency heating uniformity improvement for dried soybeans. *Innovative Food Science and Emerging Technologies* 33: 365-380.

Huang, Z., F. Marra and S. Wang. 2016. A novel strategy for improving radio frequency heating uniformity of dry food products using computational modeling. *Innovative Food Science and Emerging Technologies* 34: 100-111.

Huang, Z., H. Zhu, R. Yan and S. Wang. 2015. Simulation and prediction of radio frequency heating in dry soybeans. *Biosystems Engineering* 129: 34-47.

Huang, Z., L. Chen and S. Wang. 2015. Computer simulation of radio frequency selective heating of insects in soybeans. *International Journal of Heat and Mass Transfer* 90: 406-417.

Ikediala, J., J. Tang, S. Drake and L. Neven. 2000. Dielectric properties of apple cultivars and codling moth larvae. *Transaction of the ASAE* 43: 1175-1184.

Ikediala, J.N., J.D. Hansen, J. Tang, S.R. Drake and S. Wang. 2002. Development of a saline water immersion technique with RF energy as a postharvest treatment against codling moth in cherries. *Postharvest Biology and Technology* 24: 209-211.

Inoue, C., Y. Hagura, M. Ishikawa and K. Suzuki. 2002. The dielectric property of soybean oil in deep-fat frying and the effect of frequency. *Food Science* 67: 1126-1129.

Jankowski, K.J. and E. Reszke. 2011. Microwave induced plasma analytical spectrometry. *Royal Society of Chemistry* 12: 1-248.

Jian, F., D.S. Jayas, N.D.G. White, P.G. Fields and N. Howe. 2014. An evaluation of insect expulsion from wheat samples by microwave treatment for disinfestation. *Biosystems Engineering* 130: 1-12.

Jiao, S., J. Johnson, J. Tang, G. Tiwari and S. Wang. 2011. Dielectric properties of cowpea weevil, black-eyed peas and mung beans with respect to the development of radio frequency heat treatments. *Biosystems Engineering* 108: 280–291.

Jiao, S., J. Tang, J.A. Johnson, G. Tiwari and S. Wang. 2011. Determining radio frequency heating uniformity of mixed beans for disinfestation treatments. *Transactions of the ASABE* 54: 1847- 1855.

Jiao, S., Y. Zhong and Y. Deng. 2016. Hot air-assisted radio frequency heating effects on wheat and corn seeds: quality change and fungi inhibition. *Journal of Stored Research* 69: 265-271.

Jiao, S., Y. Deng, Y. Zhong, D. Wang and Y. Zhao. 2015. Investigation of radio frequency heating uniformity of wheat kernels by using the developed computer simulation model. *Food Research International* 71: 41-49.

Jiao, Y., H. Shi, J. Tang, F. Li and S. Wang. 2015. Improvement of radio frequency (RF) heating uniformity on low moisture foods with polyetherimide (PEI) blocks. *Food Research International* 74: 106-114.

Jones, P. and A. Rowley. 1996. Dielectric drying. *Drying Technology* 14: 1063-1098.

Kong, L., M. Zhang, Y. Wang, B. Adhikari and Z. Yang. 2016. Evaluation of heating uniformity in radio frequency heating systems using carrot and radish. *International Agrophysics* 30: 465-473.

Koral, T. 2008. Radio frequency dielectric heating re-emerges as an effective process in the food industry. International Microwave Power Institute (IMPI). Paper presented at the IMPI 42nd Annual Microwave Symposium in New Orleans. June 25-27, 2-14.

Koral, Tony. 2004. Radio frequency heating and post-baking. Accessed on June15, 2016 at <http://www.strayfield.co.uk/biscuit.htm>.

Lagunas-Solar, M., N. Zeng, T. Esser, et al. 2005. Disinfection of fishmeal with radio frequency heating for improved quality and energy efficiency. *Journal of the Science of Food and Agriculture* 85: 2273-2280.

Lagunas-Solar, M., N. Zeng, T. Essert, T. Truong and C. Piña. 2006. Radio frequency power disinfests and disinfest food, soils and wastewater. *California Agriculture* 60: 192-199.

Lagunas-Solar, M.C., Z. Pan, N.X. Zeng, T.D. Truong, E. Khir and K.S.P. Amaratunga. 2007. Application of radio frequency power for non-chemical disinfestations of rough rice with full retention of quality attributes. *Applied Engineering in Agriculture* 23: 647–654.

Langlinais, S. 1989. Economics of microwave treated rice for controlling weevils. ASABE. ASAE Paper No. 893544.

Li, Z., R. Wang and T. Kudra. 2011. Uniformity issue in microwave drying. *Drying Technology* 29: 652-660.

Ling, B., G. Tiwari and S. Wang. 2015. Pest control by microwave and radio frequency energy: dielectric properties of stone fruit. *Agronomy for Sustainable Development* 35: 233–240.

Ling, B., G. Tiwari and S. Wang. 2015. Pest control by microwave and radio frequency energy: dielectric properties of stone fruit. *Agronomy for Sustainable Development* 35: 233-240.

Ling, B., L. Hou, R. Li and S. Wang. 2016. Storage stability of pistachios as influenced by radio frequency treatments for postharvest disinfestations. *Innovative Food Science and Emerging Technologies* 33: 357-364.

Manickavasagan A., D.S. Jayas and N.D.G. White. 2006. Non-Uniformity of Surface Temperatures of Grain after Microwave Treatment in an Industrial Microwave Dryer. *Drying Technology: An International Journal* 24: 1559-1567.

Manickavasagan, A., P.M.K. Alahakoon, T.K. Al-Busaidi, S. Al-Adawi, A.K. Al-Wahaibi, A.A. Al-Reesi, R. Al-Yahyai and D.S. Jayas. 2013. Disinfestation of stored dates using microwave energy. *Journal of Stored Products Research* 55: 1-5.

Marra, F., L. Zhang and J. Lyng. 2009. Radio frequency treatment of foods: Review of recent advances. *Journal of Food Engineering* 91: 497-508.

Mavrogianopoulos G.N., A. Frangoudakis and J. Pandelakis. 2000. Energy Efficient Soil Disinfestation by Microwaves. *J. agric. Engng Res.* 75: 149 -153.

Mehdizadeh, M. 2010. Microwave/RF applicators and probes for material heating, sensing, and plasma generation. Elsevier Science. ISBN-13:978-0-8155-1592-0, 1-389.

Metaxas, R. and R. Meredith. 1988. *Industrial Microwave Heating*. Herts, U.K.: Peter Peregrinus Ltd.

Mitcham, E.J., R.H. Veltman, X. Feng, E. De Castro, J.A. Johnson, T.L. Simpson, W.V. Biasi, S. Wang and J. Tang. 2004. Application of radio frequency treatments to control insects in in-shell walnuts. *Postharvest Biology and Technology* 33: 93-100.

Monzon, M.E., B. Biasi, E.J. Mitcham, S.J. Wang, J.M. Tang and G. Hallman. 2007. Effect of radiofrequency heating on the quality of 'Fuyu' persimmon fruit as a treatment for control of the Mexican fruit fly. *HortScience* 42: 125-129.

Morris, S. 2011. Food and package engineering. Wiley- Blackwell.

Nelson, S. 1966. Electromagnetic and sonic energy for insect control. *Transaction of the ASAE* 9: 398-403.

Nelson, S. 1996. Review and assessment of radio-frequency and microwave energy for stored-grain control. *Transactions of the ASAE* 39: 1475-1484.

Nelson, S. 2003. Frequency- and temperature-dependent permittivities of fresh fruits and vegetables from 0.01 to 1.8 GHz. *Transactions of the ASAE* 46: 567–576.

Nelson, S. 2005. Dielectric spectroscopy of fresh fruit and vegetable tissues from 10 to 1800 MHz. *Journal of Microwave Power and Electromagnetic Energy* 40: 31–47.

Nelson, S. 2010. Fundamentals of dielectric properties measurements and agricultural applications. *Journal of Microwave Power and Electromagnetic Energy* 44: 98-113.

Nelson, S. and L. Charity. 1972. Frequency dependence of energy absorption by insects and grain in electric fields. *Transactions of the ASAE* 6: 1099-1102.

Nelson, S. and S. Trabelsi. 2012. Factors influencing the dielectric properties of agricultural and food materials. *Journal of Microwave Power Electromagnetic Energy* 46: 93-107.

Okos, M., G. Narsimhan, R. Singh and A. Weitnauer. 1992. Food dehydration. In *Handbook of Food Engineering*, 437–562. D. R. Heldman and D. B. Lund, eds. New York, N.Y.: Marcel Dekker, Inc.

Pan, L., S. Jiao, S. Wang, L. Gautz and T. Kang. 2012. Developing radio frequency postharvest treatment protocol for disinfesting coffee beans. *Transactions of the ASABE* 55: 2293-2300.

Peng, J., J. Tang, Y. Jiao, S. Bohnet and D. Barrett. 2013. Dielectric properties of tomatoes assisting in the development of microwave pasteurization and sterilization processes. *LWT—Food Science Technology* 54: 367–376.

Piyasena, P., C. Dussault, T. Koutchma, H.S. Ramaswamy and G.B. Awuah. 2003. Radio Frequency Heating of Foods: Principles, Applications and Related Properties—A Review. *Critical Reviews in Food Science and Nutrition* 43: 587-606.

Purohit, P., D.S. Jayas, B.K. Yadav, V. Chelladurai, P.G. Fields and N.D.G. White. 2013. Microwaves to control *Callosobruchus maculatus* in stored mung bean (*Vigna radiata*). *Journal of Stored Products Research* 53: 19-22.

Radio Frequency Inc. 2015. How RF heating works. Accessed on June 24, 2016 at <http://www.macrowave.com/rftech.html>

Rajagopal, V. 2009. Disinfestation of stored grain insects using microwave energy (Doctoral Dissertation). University of Manitoba. <http://mspace.lib.umanitoba.ca/bitstream/handle/1993/3152/Disinfestation%20of%20stored%20grain%20insects%20using%20microwave%20energy.pdf?sequence=1> (Last accessed February 8, 2017).

Ryynanen, S. 1995. The electromagnetic properties of food materials: a review of the basic principles. *Journal of Food Engineering* 26: 409-429.

Shrestha, B. and O.D. Baik. 2013. Radio frequency selective heating of stored-grain insects at 27.12 MHz: A feasibility study. *Biosystems Engineering* 114: 195-204.

Shrestha, B., D. Yu and O.D. Baik. 2013. Elimination of *Crystolestes ferrugineus* in wheat by radio frequency dielectric heating at different moisture contents. *Progress in Electromagnetics Research* 139: 517-538.

Singh, R., K.K. Singh and N. Kotwaliwale. 2011. Study on disinfestation of pulses using microwave technique. *Journal of Food Science and Technology* (July–August 2012) 49: 505–509.

Sipaghioglu, O. and S. Barringer. 2003. Dielectric properties of vegetables and fruits as a function of temperature, ash, and moisture content. *Journal of Food Science* 68: 234–239.

Solyom, K., S. Kraus, R. Mato, V. Gaukel, H. Schuchmann and M. Cocero. 2013. Dielectric properties of grape marc: effect of temperature, moisture content and sample preparation method. *Journal of Food Engioneering* 119: 33-39.

Sosa-Morales, M., G. Tiwari, S. Wang, J. Tang, A. Lopez-Malo and H. Garcia. 2009. Dielectric heating as a potential post-harvest treatment of disinfesting mangoes. I: Relation between dielectric properties and ripening. *Biosystems Engineering* 103: 297–303.

Tang, J., H. Feng and M. Lau. 2002. Microwave heating in food processing. In: *Advances in Agricultural Engineering* (Young X; Tang J; Zhang C; Xin W eds). Scientific Press, New York.

Tang, J., J. Ikediala, S. Wang, J. Hansen and R. Cavalieri. 2000. High-temperature-short-time thermal quarantine methods. *Postharvest Biology and Technology* 21: 129-145.

Tiwari, G., S. Wang, S.L. Birla and J. Tang. Effect of water-assisted radio frequency heat treatment on the quality of 'Fuyu' persimmons. *Biosystems Engineering* 100: 227-234.

Vadivambal R., D.S. Jayas and N.D.G. White. 2008. Mortality of stored-grain insects exposed to microwave energy. *Transactions of the ASABE* 51: 641-647.

Vadivambal, R., O.F. Deji, D.S. Jayas and N.D.G. White. 2010. Disinfestation of stored corn using microwave energy. *Agriculture and Biology Journal of North America* 1: 18-26.

Von Hippel, A. 1954. *Dielectric Properties and Waves*. NY, USA: John Wiley & Sons.

Wang, K., L. Chen, W. Li and S. Wang. 2015. Evaluating the top electrode voltage distribution uniformity in radio frequency systems. *Journal of Electromagnetic Waves and Applications* 29(6): 763-773.

Wang, S. and J. Tang. 2001. Radio frequency and microwave alternative treatments for insect control in nuts: a review. *Agricultural Engineering Journal* 2001 10: 105-120.

Wang, S., A. Monzon, J.A. Johnson, E.J. Mitcham and J. Tang. 2007. Industrial-scale radio frequency treatments for insect control in walnuts I: Heating uniformity and energy efficiency. *Postharvest Biology and Technology* 45: 240-246.

Wang, S., G. Tiwari, S. Jiao, J.A. Johnson and J. Tang. 2010. Developing postharvest disinfestation treatments for legumes using radio frequency energy. *Biosystems Engineering* 105: 341-349.

Wang, S., J. Tang, J. Johnson and R. Cavalieri. 2013. Heating uniformity and differential heating of insects in almonds associated with radio frequency energy. *Journal of Stored Products Research* 55: 15-20.

Wang, S., J. Tang, T. Sun, E.J. Mitcham, T. Koral and S.L. Birla. 2006. Considerations in design of commercial radio frequency treatments for postharvest pest control in in-shell walnuts. *Journal of Food Engineering* 77: 304-312.

Wang, S., J. Tang, J. Johnson, E. Mitcham, J. Hansen, G. Hallman, S. Drake and Y. Wang. 2003. Dielectric properties of fruits and insect pests as related to radio frequency and microwave treatments. *Biosystems Engineering* 85: 201–212.

Wang, S., J. Tang, J.A. Johnson, E. Mitcham, J.D. Hansen, R.P. Cavalieri, J. Bower and B. Biasi. 2002. Process protocols based on radio frequency energy to control field and storage pests in in-shell walnuts. *Postharvest Biology and Technology* 26: 265-273.

Wang, S., J. Tang, R. Cavalieri and D. Davis. 2003. Differential heating of insects in dried nuts and fruits associated with radio frequency and microwave treatments. *Transactions of the ASAE* 46(4): 1175-1182.

Wang, S., J. Yue, B. Chen and J. Tang. 2008. Treatment design of radio frequency heating based on insect control and product quality. *Postharvest Biology and Technology* 49: 417-423.

Wang, S., J. Yue, J. Tang and B. Chen. 2005. Mathematical modelling of heating uniformity for in-shell walnuts subjected to radio frequency treatments with intermittent stirrings. *Postharvest Biology and Technology* 35: 97-107.

Wang, S., J.N. Ikediala, J. Tang, J.D. Hansen, E. Mitcham, R. Mao and B. Swanson. 2001. Radio frequency treatments to control codling moth in in-shell walnuts. *Postharvest Biology and Technology* 22: 29-38.

Wang, S., M. Monzon, J.A. Johnson, E.J. Mitcham and J. Tang. 2007. Industrial-scale radio frequency treatments for insect control in walnuts II: Insect mortality and product quality. *Postharvest Biology and Technology* 45: 247-253.

Wang, S., M. Monzon, Y. Gazit, J. Tang, E. Mitcham and J. Armstrong. 2005. Temperature-dependent dielectric properties of selected subtropical and tropical fruit and associated insect pests. *Transaction of the ASAE* 48: 1873– 1881.

Wang, S., S.L. Birla, J. Tang and J.D. Hansen. 2006. Postharvest treatment to control codling moth in fresh apples using water assisted radio frequency heating. *Postharvest Biology and Technology* 40: 89-96.

Wang, Y., L. Zhang, J. Johnson, M. Gao, J. Tang, J. Powers and S. Wang. 2014. Developing hot air-assisted radio frequency drying for in-shell macadamia nuts. *Food Bioprocess Technology* 7: 278-288.

Wang, Y., L. Zhang, M. Gao, J. Tang and S. Wang. 2014. Pilot-scale radio frequency of macadamia nuts: heating and drying uniformity. *Drying Technology* 32(9): 1052-1059.

Wang, Y., L. Zhang, M. Gao, J. Tang and S. Wang. Temperature-and moisture-dependent dielectric properties of Macadamia nut kernels. *Food Bioprocessing Technology* 6: 2165–2176.

Wang, Y., Y. Li, S. Wang, L. Zhang, M. Gao and J. Tang. 2011. Review of dielectric drying of foods and agricultural products. *International Journal of Agricultural and Biological Engineering* 4: 1 –19.

Yu, D., B. Shrestha and O.D. Baik. 2016. Radio frequency (RF) control of red flour beetle (*Tribolium castaneum*) in stored rapeseeds (*Brassica napus* L.). *Biosystems Engineering* 151: 248-260.

Zajtzev, B., V. Bomko, V. Rashkovan, A. Kobetz, B. Rudiak, L. Bazyma, A. Basteeve, M. Lesnykh, O. Mishchenko, V. Zhuravlev and E. Marinina. 2001. RF installation for the grain disinfestation. *Questions of Atomic Science and Technology* 38(3): 118-120.

Zhang, P., H. Zhu and S. Wang. 2015. Experimental evaluations of radio frequency heating in low-moisture agricultural products. *Emirates Journal of Food and Agriculture* 27(9): 662-668.

Zhou, L. and S. Wang. 2016. Industrial-scale radio frequency treatments to control *Sitophilus oryzae* in rough, brown, and milled rice. *Journal of Stored Products Research* 68: 9-18.

Zhou, L. and S. Wang. 2016. Verification of radio frequency heating uniformity and *Sitophilus oryzae* control in rough, brown, and milled rice. *Journal of Stored Products Research* 65: 40-47.

Zhou, L., B. Ling, A. Zheng, B. Zhang and S. Wang. 2015. Developing radio frequency technology for postharvest insect control in milled rice. *Journal of Stored Products Research* 62: 22-31.

Zhu, X., W. Guo and X. Wu. 2012. Frequency and temperature dependent dielectric properties of fruit juices associated with pasteurization by dielectric heating. *Journal of Food Engineering* 109: 258–266.

CHAPTER 2

Installation of a pilot-scale 50-ohm radio frequency heating system for controlling insect pests in stored agricultural materials: Applicator design, impedance matching, and RF arcing problem

To be submitted for journal publication.

Contribution of this paper to the overall study

This chapter tackles the installation process of the 50-ohm RF heating system for disinfestation of insect pests in stored agricultural materials (specific objective 2). It also discusses the design and fabrication of the parallel plate applicator for a pilot-scale 50-ohm RF heating system (specific objective 3). All the experiments in this chapter were conducted and a journal manuscript is being drafted by myself.

2.1 Abstract

Radio frequency (RF) technology has been studied as an alternative to chemical methods for disinfestation of insect pests in stored agricultural materials. The 50-ohm RF

heating system is an advanced type of RF technology and offers many advantages compared to the former (conventional RF: Type C oscillator). However, with its advantages, there have been a limited number of installations and applications globally, and none in disinfestation due to a lack of knowledge in using this technology. Therefore, this chapter deals with the application of a pilot-scale using 50-ohm RF heating system for the first time in insect disinfestation. The following were discussed for a successful installation of this technology: 1) the understanding of a 50-ohm RF heating system with comprehensive discussion of its components, especially the design and fabrication of the RF applicator; 2) impedance matching with respect to basic electrical parameters [voltage standing wave ratio (VSWR), inductance, capacitance, impedance, and frequency] for maximum power applied to the load; and 3) an inclusive discussion of problems encountered such as arcing and fire during operation. In addition, suggestions are given for the successful installation of a pilot-scale, 50-ohm RF heating system for disinfestation of stored agricultural materials.

2.2 Introduction

Insect pests are a major concern during storage of agricultural materials worldwide. Infestation with these pests decreases the value of the materials due to losses of its quantity and quality. For cereal grains, for example, the annual losses worldwide because of insect pests are in the range of 9% to 20% (Hou et al. 2016; Huang et al. 2015b; Azab et al. 2013). Furthermore, an infestation of insect pests in stored grains during marketing and trading is doable but a serious problem. Regulatory agencies for phytosanitary and quarantine protocols have been established worldwide to prevent the presence of insect pests through marketing channels (Hou et al. 2016). This problem had been solved using chemical methods (fumigants and pesticides). However, in the end, pests developed resistance to the chemicals and during exportation, residual limits for fumigants and pesticides were implemented. Moreover, the application of fumigation has been restricted since 2005 because the gas used for fumigation (methyl bromide) can damage the ozone layer (UNEP 2006). In addition, pesticides leave chemical residues in the products (Wang et al. 2007a; Govindasamy et al. 1997). This residue contaminates the materials (grains) have consumed. Therefore, farmers, traders, the government of each country, and researchers are looking for alternatives to chemical disinfestation. A non-chemical method would be the best alternative for disinfestation. Conventional heating is a non-chemical method and it was thought to have solved the problem. Nevertheless, the process takes a long time to achieve the fatal temperature of pests and can lead to degradation of the quality of the material because of slow heating by thermal diffusion (Hou et al. 2016).

Dielectric heating [radio frequency (RF) or microwave (MW)] is another non-chemical method that has been studied as an alternative to chemical disinfestation. A number of review papers (Macana and Baik, 2017; Hou et al. 2016; Marra et al. 2009; Wang and Tang, 2001; Nelson, 1996, 1966; Ark and Parry, 1940) have summarized the results of those studies. This method relies on the interaction of electromagnetic energy and materials. Radio frequency and MW heating offer several advantages over other methods: fast, non-contact, and volumetric heating. However, RF heating is preferred over MW heating for disinfestation because of its greater penetration depth and selective heating effect (Macana and Baik, 2017; Shrestha et al. 2013; Wang et al. 2011, 2003; Guo et al. 2010; Nelson, 1996).

There are two types of RF heating systems: conventional heating system (Type C oscillator) and 50-ohm RF technology (more advanced) (Macana and Baik 2017; Wang et al. 2011). Both types of RF system work similarly. They both have similar primary parts: generator (source of electromagnetic energy) and applicator (where the material is heated). However, the 50-ohm RF system has advantages over the former. First, its applicator can be separated from the generator by a 50-ohm coaxial cable, in contrast to the conventional where the generator is attached to the applicator and cannot be separated. This could be an advantage for flexibility in movement and location. Another advantage is the modern-type RF system has a higher power efficiency because of the automatic matching network (AMN). The AMN is an additional part of the modern type RF system which helps to ensure maximum power is applied to the load. Finally, the modern-type RF system has a stable frequency and is harmonic free, whereas the former has a lack of frequency stability and harmonic output (Koral 2014). This might cause

interference by the signal in other applications, such as telecommunications and broadcasting. Despite the advantages of the 50-ohm RF heating system, no applications have been developed for disinfestation. All of the studies reported for disinfestation have been done using conventional RF heating system (Macana and Baik, 2017; Shrestha et al. 2013; Shrestha and Baik, 2013; Lagunas-Solar et al. 2007). The conventional RF heating system has been used mostly at laboratory scale and only a few studies have been used for industrial applications (Jiao et al. 2012; Wang et al. 2007a, b).

All of these reasons suggest that comprehensive research using a 50-ohm RF heating system for disinfestation is important. There have been a limited number of resources available for the use of this technology, especially for industrial application. The use of this technology requires sufficient knowledge of RF energy to achieve a successful application. Therefore, the objective of this study was to provide a guideline for the installation of the 50-ohm RF heating system for disinfestation of insect pests in stored agricultural materials. This involved comprehensive discussions of the understanding the parts of the system, applicator design and fabrication, importance of impedance matching in relation to tuning the matching network with its electrical parameters (voltage standing wave ratio, inductance, capacitance, impedance, and frequency) for maximum power transfer to the load, and the problems encountered during operation such as RF arcing and fire. Furthermore, suggestions are given for a successful installation and application of a 50-ohm RF heating system for disinfestation.

2.3 Materials and methods

2.3.1 Parts of 50-ohm RF heating system

There are four parts to the 50-ohm RF heating system: RF generator, 50-ohm coaxial cable, an automatic matching network (AMN), and an RF applicator (Figure 2.1). Any RF heating related company can supply the first three parts. In the case of this study, Coaxial Power Systems Ltd. (Eastbourne, E. Sussex, United Kingdom) as our partner industry supplied the first three parts. The last part (applicator) was designed by the author and fabricated at the Engineering Shop at the University of Saskatchewan. The RF generator (Figure 2.2) is the source of RF energy that generates alternating charges in the electrodes. The 50-ohm coaxial cable (Figure 2.3) links the automatic matching network and the RF generator. This is where the name of the modern type of RF heating system comes from- the impedance of the load and the cable (50-ohms), which are commonly used by the communications industry and were later applied by the RF industry. Fifty ohms was set as standard because it is a good compromise impedance in handling high voltage and power (Microwaves101 2017; Lampen 2012; Breed 2007). While the AMN (Figure 2.4) is a special part of this system that helps the generator to have maximum power applied to the load. Lastly, the applicator is the heart of the system. It is where the materials are heated. The applicator is composed of two electrodes (hot and ground) with the gap to admit materials. The configuration of the electrode is dependent on the desired application. It can be separated from the generator, and users can design and build according to their applications.

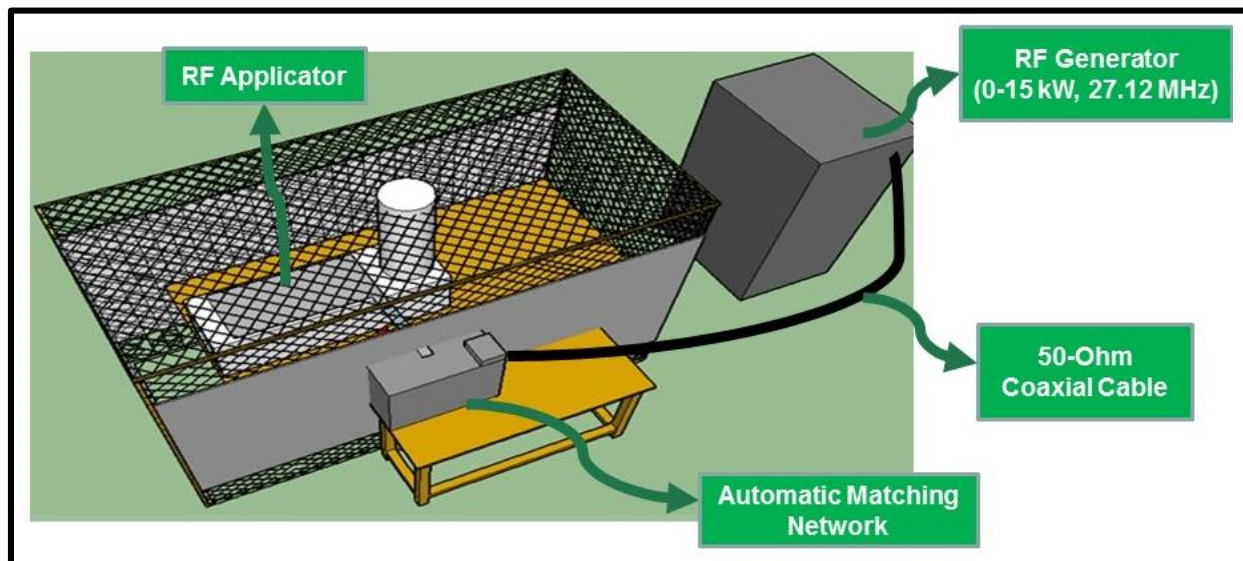


Figure 2.1. 50-ohm technology based radio frequency (RF) heating system (Macana et al. 2018e).



Figure 2.2. Photographs of the RF generator (27.12 MHz, 15 kW).



Figure 2.3. The 50-ohm coaxial cable used for connecting the AMN and RF generator.



Figure 2.4. Photograph of the automatic matching network (AMN).

2.3.2 Applicator design and fabrication

The applicator designed for this study can be used in both batch and continuous processing. However, continuous disinfestation is the main purpose of this design to economically utilize the advantages of the 50-ohm RF heating system and to improve on the non-uniform heating of existing conventional RF heating systems. It also is important to include the batch type of disinfestation in this study because it is the first time to use a 50-ohm RF heating system for disinfestation and a better test can be conducted under a controlled environment. Continuous disinfestation can be done by installing an auger system inside a tubular channel (Figure 2.5).

The auger (Figure 2.5) is driven by a motor (1-200 rpm) that stirs and conveys the grain continuously until it passes between the two electrodes (hot and ground) attached to both sides of the tubular channel. The dimensions of the auger are the following: overall length of auger = 1.62 m, overall length of flight = 1 m, shaft diameter = 0.05 m, shaft length = 0.43 m, pitch = 0.08 m, screw diameter = 0.29 m, and gap between auger and tubular channel = 0.01 m. Both the auger and tubular channel are made of polypropylene, which is an RF transparent material. Three RF transparent materials were considered in this study for the auger and tubular channel: acrylonitrile butadiene styrene (ABS), polypropylene (PP), and polyvinylchloride (PVC). All of them have a low dielectric loss factor: ABS (0-0.0665), PP (0-0.0066), and PVC (0-0.0561) (Lapointe 2018; RF Cafe 2018). However, ABS (77.2°C) and PVC (60°C) are not recommendable as they have low melting points, whereas PP (121.1°C) has the highest melting point and the lowest

dielectric loss factor (RF Cafe 2018). Still, PVC and ABS could work as RF transparent materials in lower temperature applications. For batch type disinfestation, the auger system is removed as shown in Figure 2.6. The diameter of the tubular channel is 30 cm; the tube is capable of holding approximately 45 kg (wheat) or 40 kg (canola). The electrodes on the sides of the channel are made of aluminum; their dimensions are 0.7 m length and 0.3 m width. In addition, a piece of aluminum is used with a bolt to connect the AMN and the applicator both the ground and the hot electrode. During inline disinfestation, a mixture of grain and insect pests is loaded into the funnel and the auger conveys and stirs them while it is subjected to the RF field. Macana and Baik (2017) and Pan et al. (2012) stated that moving the material by an auger while being subjected to RF heating improves heating uniformity. Thus, the advantage of this design is not only moving the materials but also mixing the non-uniformly heated materials.

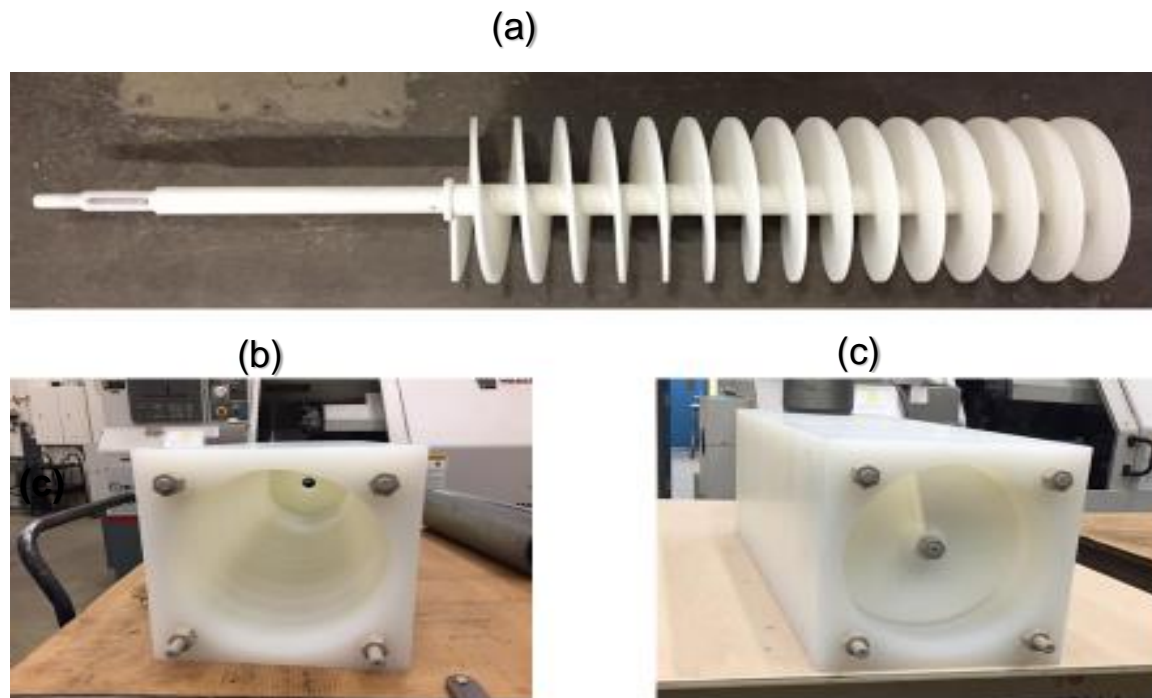


Figure 2.5. Auger system (made of polypropylene): (a) Auger (b) Tubular channel (c) Auger inside the tubular channel.

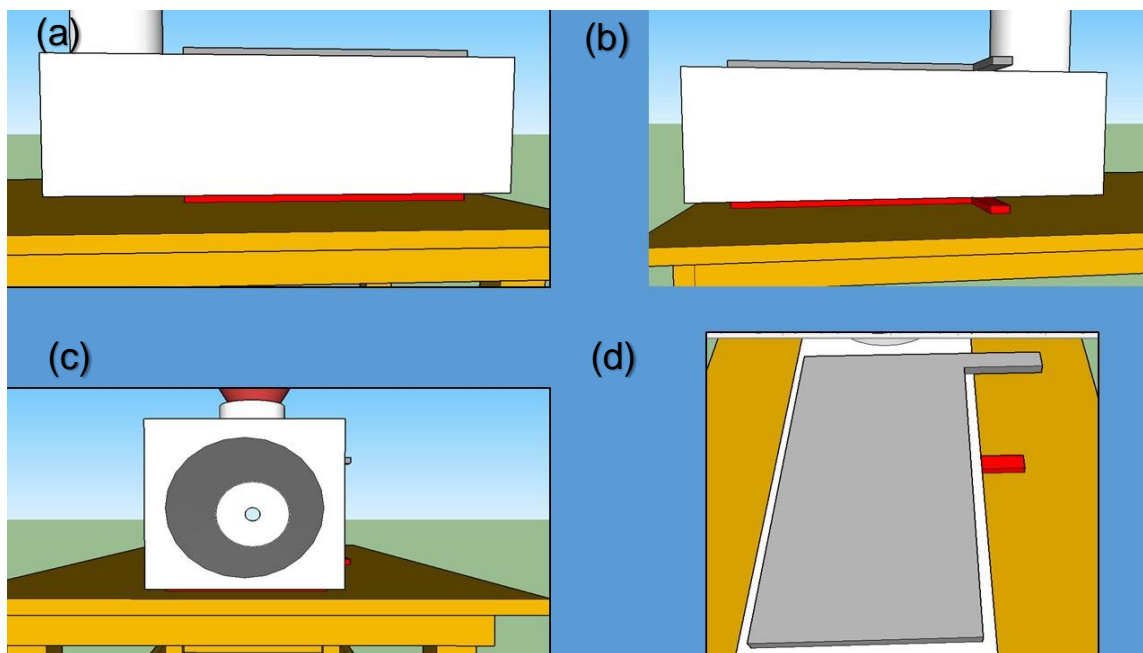


Figure 2.6. Designed applicator with the auger system: (a) left view (b) right view (c) front view (d) top view.

2.3.3 Impedance matching

For all applications of RF heating, matching the impedance of the load and that of the generator at 50 ohms is essential (Figure 2.7). The RF generator is designed to transfer maximum power when the impedance of the load is similar to that of the generator. The impedance of the load keeps changing during processing. However, with the help of the matching network, the 50-ohm impedance of the load can be maintained. This is one of the advantages of the 50-ohm RF heating system, as the matching network converts the impedance of the load into 50-ohms so that the generator sees a similar impedance. When this is ensured, maximum power applied to the load, with no power reflected to the generator. However, this is possible only when the matching network is properly tuned.

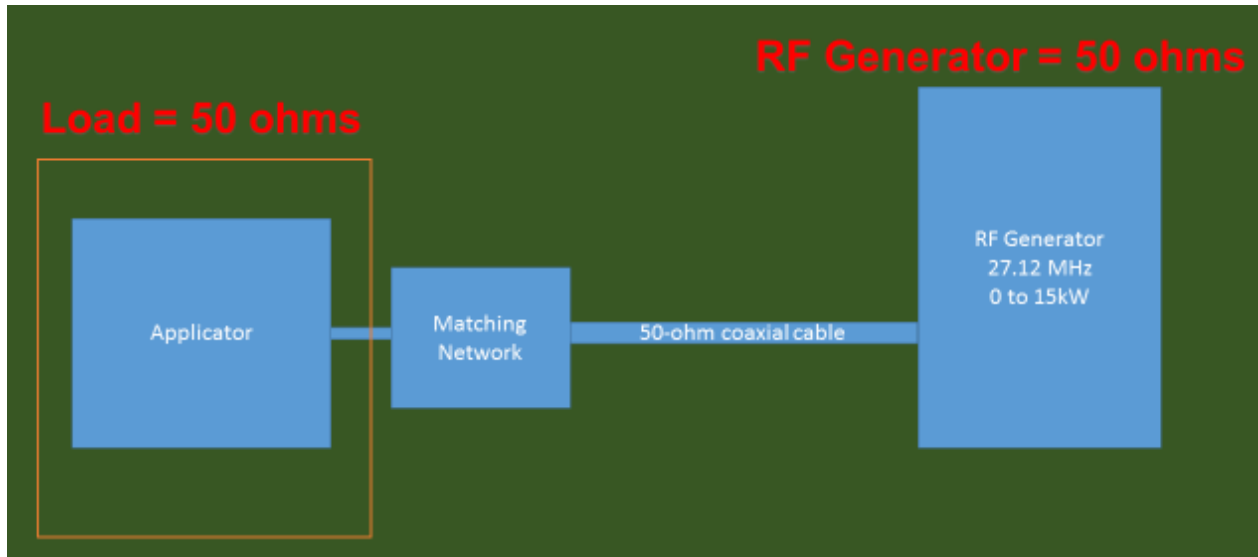


Figure 2.7. Impedance matching between generator and load.

2.3.3.1 Automatic matching network

The matching network (AMN) used in the 50-ohm RF heating system adjusts the impedance of the load automatically during the process. The AMN has an L configuration (Figure 2.8); the name comes from the L arrangement of the three impedances (C1, C2, and L1). It is composed of two tuning elements, C1 (tune capacitor) and L1 (inductor). The network is able to match the load impedances below 50 ohms. Inside the AMN (Figure 2.9), C1 and C2 are consist of vacuum capacitors adjusted by the AMN controller in the generator. The AMN controller controls the servomotors that drive the two capacitors (load and tune). Therefore, during the process, the positions of the capacitors are adjusted by the servomotors to the positions that give result in maximum power applied to the load.

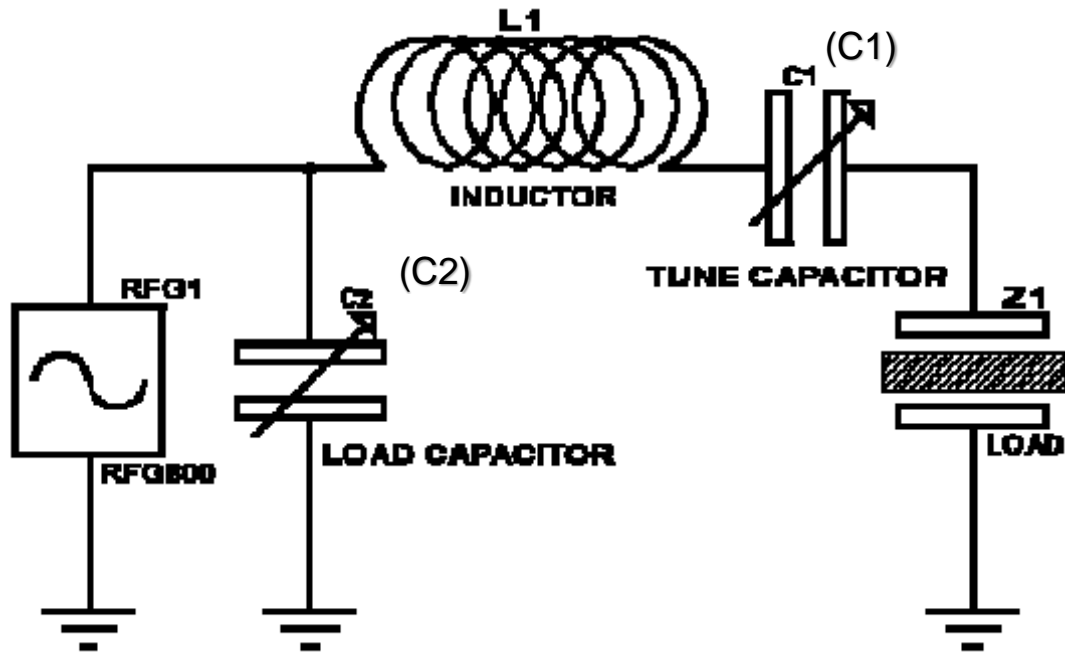


Figure 2.8. The L configuration of the automatic matching network (Coaxial Power Systems Ltd. 2001).

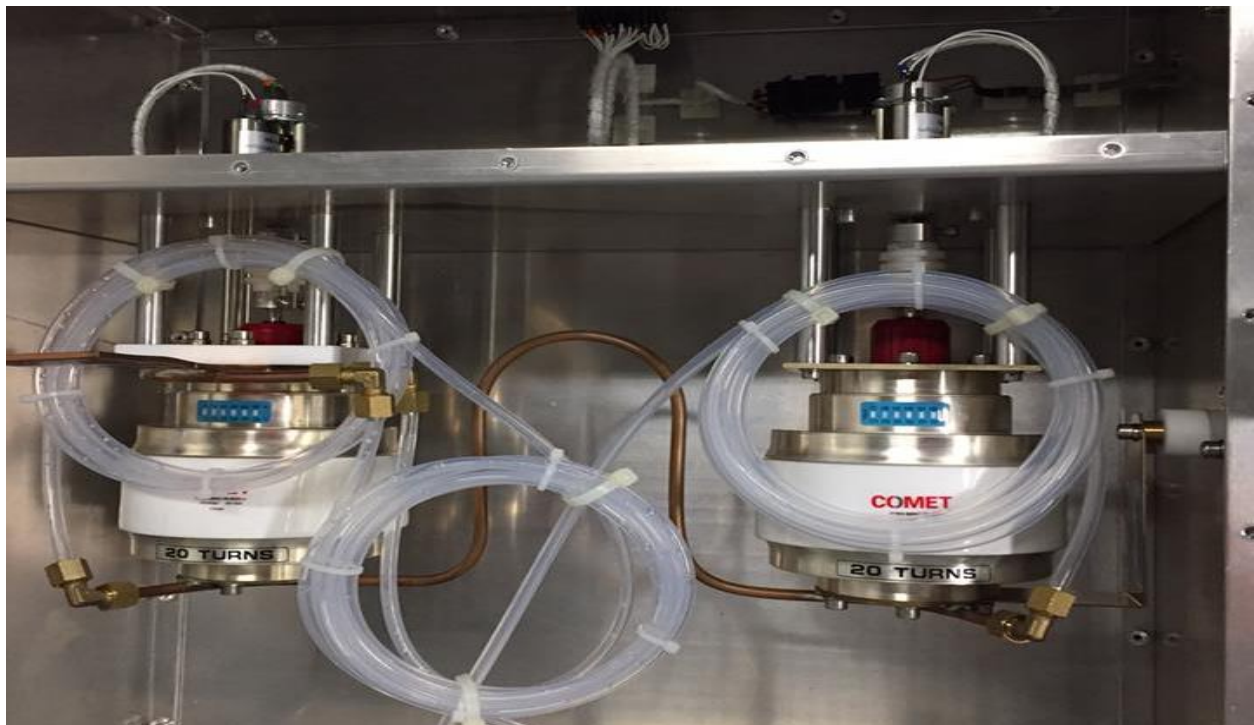


Figure 2.9. Actual photograph inside the matching network with L configuration.

2.3.3.2 Basic electrical parameters

For tuning the AMN, the tuning elements are the tune capacitor and the fixed inductor inside the network. For the first application of the 50-ohm RF heating system, for example in disinfestation, tuning the system is critical. Thus, understanding the basic electrical parameter (impedance, capacitance, inductance, and frequency) relationships is essential to tuning the matching network successfully. To do this, an RF impedance-measuring instrument is required for monitoring matching between the load and the generator. This section shows the relationship between the impedance of the capacitance (capacitive reactance) and inductance (inductive reactance) to obtain 50-ohm impedance in the load. Furthermore, equations 2.1 to 2.4 present the relationships of all electrical parameters needed for tuning the matching network (EEWeb 2018; Ferdous 2015; Orsat 1999; ILO/ICNIRP 1998), and the network analyzer (MFJ SWR) shown in Figure 2.10 helps in investigating the relationships between the electrical parameters.

$$C = A \frac{\epsilon}{d} \quad (2.1)$$

$$L = N^2 \mu_0 \mu_r \left(\frac{D}{2} \right) \left(\ln\left(\frac{8D}{d}\right) - 2 \right) \quad (2.2)$$

$$X_C = \frac{1}{2} \pi f C \quad (2.3)$$

$$X_L = 2\pi f L \quad (2.4)$$

Where: A is the total area of one plate (m^2), ϵ is the relative dielectric constant of the material between the plates with respect to vacuum, d is the spacing between the two

plates (m), X_C is the capacitive reactance (Ω), f is the frequency (MHz), N is the number of turns, D is the loop diameter (m), d is the wire diameter (m), μ_r is the relative permeability, X_L is the inductive reactance (Ω), μ_0 is the relative permeability of free space, and C is the capacitance (F).

2.3.3.3 Voltage standing wave ratio (VSWR)

Voltage standing wave ratio is one of the parameters for an indication of power reflected back to the generator. The perfect value of VSWR is 1 (Patel and Negi 2012) - this means that there is no reflected power going to the generator and load absorbs all the power. When the value of the VSWR is greater than 1, there is a return of power. The network analyzer (MFJ Enterprises Inc., Starkville, MS USA) is capable of measuring the VSWR of the system (Figure 2.10). To conduct the tuning, the network analyzer is



Figure 2.10. The network analyzer used for measuring the basic electrical parameters and tuning the system.

connected to the end of the coaxial cable, which is connected to the RF generator, and observes the value of VSWR in the analyzer while adjusting the (tune and load capacitor) value of the capacitor in the RF generator.

2.3.4 The arcing and fire problem

Arcing is common to MW and RF heating system applications. It occurs when the air molecules or atoms get ionized and become conductive between the hot and ground electrodes (Moongilan 2009). Oftentimes, arcing leads to arcing discharge (plasma discharge) resulting in extreme heat ranging from 3000°C to 10,000 °C (Hines 2018). Therefore, arcing can cause fire, from mild to severe, inside and outside of the heating system. According to Macana et al. (2018d), there are three components needed to start a fire: fuel, heat, and oxygen. Removing one of them can stop the fire. However, fuel and oxygen are already present in the heating system. Fuel can be any combustible material (solid, liquid, and gas) in the system and oxygen is everywhere because air is made up of 20% oxygen. Thus, when arcing occurs, it causes a very high temperature that can lead to a fire. The fire can damage the materials being processed, equipment, and even the building. Therefore, this paper investigated the causes of arcing with the designed applicator for the 50-ohm RF heating system. The following are the parameters to be investigated: (a) unrounded edges and corners of the electrodes (Unrounded), (b) rounded edges and corners of the electrodes (Rounded), (c) no gap between the hot electrode and the table (No gap), (d) 8- cm gap between the table and the hot electrode (8-cm gap), and (e) the presence of burn marks on the applicator (Burn marks).

2.4 Results and discussions

2.4.1 VSWR of the original configuration of the matching network

The designed applicator shown earlier in this chapter produces a higher value for capacitance because the dimensions and distance between the plates are larger than for the existing applications. Therefore, the load presents a higher impedance compared to other applications matched by this network. Thus, the VSWR was measured to determine whether the current configuration of the network could still match the load into 50-ohm impedance at 27.12 MHz. The results showed that the matching network could not convert the impedance of the load into 50-ohms at 27.12 MHz for all adjustments of the load and tune capacitors in the generator. Initially, the value of the VSWR was greater than 25. This means that most of the power was reflected back to the generator and little power was absorbed by the load. Hence, since the network could not match the load in its current configuration, changes to the network were needed. This was expected because this was the first time application of this system for disinfestation at the pilot-scale applicator. To tune the network, modifications of the network can be done by adding capacitance, inductance, or a combination of both (Koral 2014; Orsat 1999).

2.4.2 Capacitance and inductance inside the matching network

Inside the matching network, there are two tuning elements (capacitance and inductance). Balancing of these two is essential to obtain the 50-ohm impedance of the load. When a match is achieved at a higher frequency, this means that the addition of capacitance is needed, whereas, when the match occurs at a lower frequency, more inductance is required. The relationship of capacitance, inductance, and frequency is

presented in equations 2.3 and 2.4 earlier in this chapter. This relationship is significant with respect to understanding the tuning of the matching network. The matching network can establish the impedance of the load at 50-ohms by balancing the values of inductance and capacitance in the network. It is an auto-tuning but this rough tuning or adjusting tuning boundaries is needed for optimum performance. Table 2.1 shows the results of the effect of inductance and capacitance in tuning the matching network to establish the impedance of the load at 50-ohm at 27.12 MHz. The capacitance and inductance values were based on the lowest VSWR after adding copper coil (loop diameter= 40 mm, wire outside diameter= 6mm) to the system to tune the matching network. Increasing the inductance by increasing the number of turns decreases the value of the capacitance in the system. In contrast, decreasing the value of the capacitance in the system by decreasing the number of turns increases the value of inductance.

Table 2.1. VSWR, capacitance, and inductance of copper coil (loop diameter= 40 mm, wire diameter= 6mm) at 27.12 MHz and 50-ohm impedance at different number of turns.

Number of Turns	Voltage Standing Wave Ratio (VSWR)	Capacitance (pF)	Inductance (μ H)
1	1.3	533	0.060
2	2.2	393	0.086
3	7.2	143	0.240
4	14.9	131	0.262
5	11.1	133	0.258
6	>25	127	0.270
7	>25	132	0.260
8	>25	131	0.264

2.4.3 Addition of inductance to tune the matching network

The higher impedance of the load due to its higher capacitance signifies that the solution to tuning the matching network is to add inductance (inductive reactance) to cancel the high capacitive reactance. The common source of inductance is a coil. Previous applications of RF heating systems with lower impedance used a copper coil with a wire diameter of 4 mm and 50 mm loop diameter. Increasing the wire diameter and the number of turns of the coil increases the value of inductance. Therefore, a 6 mm wire diameter with a 50 mm loop diameter was investigated to tune the matching network at various numbers of turns (Figure 2.11). Table 2.2 shows the results of adding the copper coil in tuning the matching network. Two turns of the copper tube wound at 50 mm and then stretched to 70 mm perfectly tuned the system with a VSWR of 1. This means that at the present impedance of the load, the matching network can convert it into 50-ohms so that the generator can forward maximum power to the load. It also has a desirable magnitude of tune of 53%, which means more room for further adjustment if needed during the process (0% to 100%). When the load changes its impedance (increases or decreases), the matching network can still adjust the position of the Load and Tune capacitors, either increasing or decreasing to make the impedance of the load into 50 ohms with Tune capacitor value of 53% and a Load capacitor value of 56%. In contrast with three and four turns of copper tubing with the loop diameter and length of the coil, the values of the Tune capacitor have less room for adjustment going down, 25% and 12%, respectively. Thus, the addition of 2 turns of the copper tube coil tunes the matching network. With this result, for future application of 50-ohm RF heating system for disinfestation, it is suggested to design and build a matching network that fits the

disinfestation application at pilot-scale. An alternative for this suggestion is the modification of the L configuration of the matching network by putting more inductance on it.

Table 2.2. Results of the addition of a copper coil to tune the matching network.

Number of Turns	Length of the coil (mm)	Frequency (MHz)	Impedance (Ohms)	Tune Value (%)	Load Value (%)	VSWR
1	----	27.12	Cannot get 50 ohms	83	67	4.2
2	70	27.12	50	53	56	1.0
3	90	27.12	50	25	52	1.0
4	120	27.12	50	12	47	1.0
5	120	27.12	50	50	50	>25

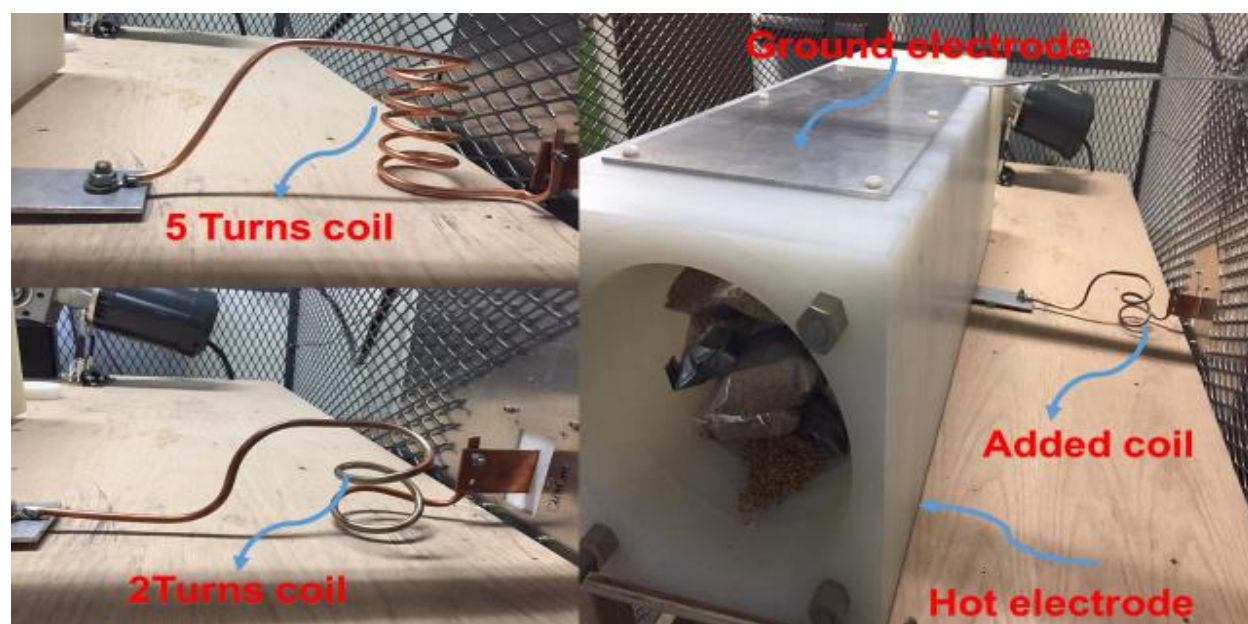


Figure 2.11. Coil added between the applicator and matching network.

2.4.4 Causes of arcing in the 50-ohm RF applicator

Table 2.3 shows the results of causes of arcing in the designed applicator for 50-ohm RF heating system at different power levels of the RF generator. It was found that at 9 kW forwarded power of the RF generator, the unrounded edges and corners of the electrodes and no gap between the wood table and hot electrode caused arcing. Figure 2.12 is a photograph of the incident. It shows that the burn marks from arcing on the tubular channel (polypropylene) and the table (wood) are on the corners and edges of the hot electrodes. This was caused by the high electric field strength on those portions of the electrodes. The electric field intensity in the heating system was above the air ionization and breakdown threshold (Sun et al. 2016; Moonngilan 2009), and was concentrated at the edges and corners of the metal, which caused the electrode to arc. When the edges and corners of the electrodes were rounded and an 8-cm gap between the tubular channel and wood table was provided (Figure 2.13), no arcing was observed at 9 kW of power. This was because of the reduction of the concentration of the electric field of the rounded corners and edges of the electrodes. In addition, the 8-cm gap provided acted as an insulator preventing the table from being heated repeatedly, which causes the arcing. On the other hand, when burn marks (carbon soot) were present in the applicator it caused arcing at even lower power levels. The burn marks were over-dried and arc-producing materials. Thus, when arcing has occurred already, it is likely to come back again unless proper cleaning has been implemented. For example, the burn marks in any part of the RF applicator should be thoroughly removed. Shiffman (2001) reported that a common source of arcing in previous applications of RF heating system

(batch and continuous was over dehydrated materials remained in the heating system, which led to charring and carbonization. Examples here include product caught in the conveyor belt (inline process) and a piece of meat or bacon in the applicator (batch process), which repeatedly heated causing over drying of materials (Shiffmann 2001).

Table 2.3 Causes of arcing at different situations of the applicator and power levels of the RF generator: Unrounded, rounded, no gap, 8-cm gap, and burn marks.

Power (kW)	Unrounded	Rounded	No gap	8-cm gap	Burn marks
1	No Arcing	No Arcing	No Arcing	No Arcing	No arcing
3	No Arcing	No Arcing	No Arcing	No Arcing	Arcing
5	No arcing	No arcing	No arcing	No arcing	Arcing (Expected)
7	No arcing	No arcing	No arcing	No arcing	Arcing (Expected)
9	Arcing	No arcing	Arcing	No arcing	Arcing (Expected)
11	Arcing	_____	Arcing	_____	Arcing (Expected)
13	Arcing (Expected)	_____	Arcing (Expected)	_____	Arcing (Expected)
15	Arcing (Expected)	_____	Arcing (Expected)	_____	Arcing (Expected)

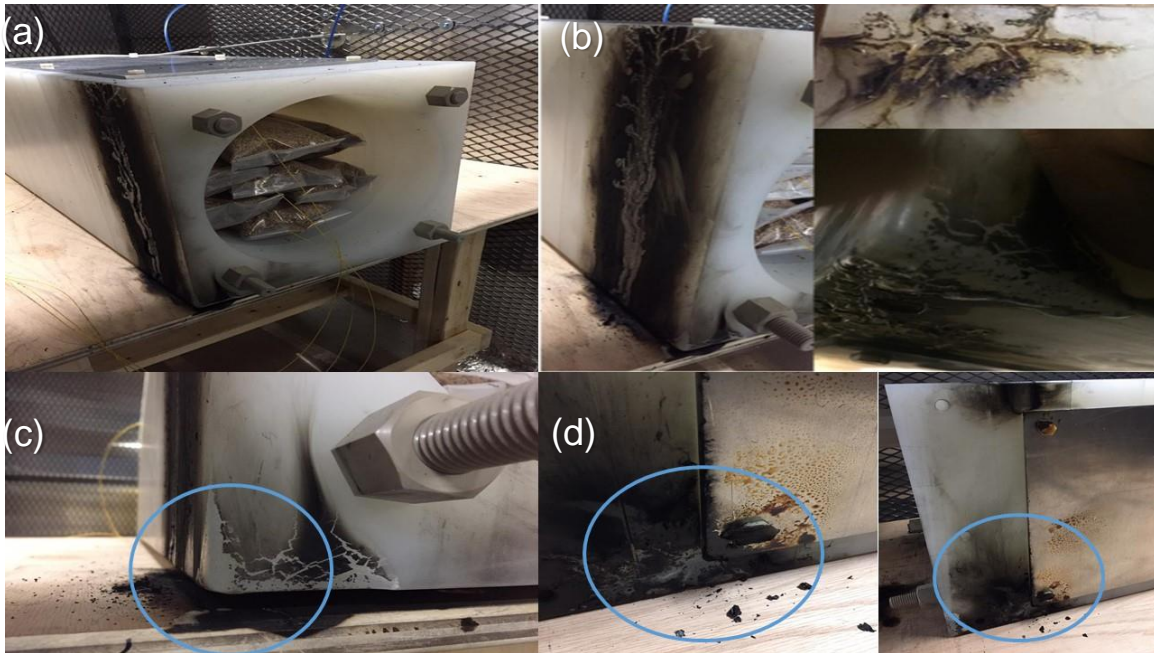


Figure 2.12. Photographs of the applicator after arcing and fire occurred at 11 kW and 27.12 MHz: (a) Applicator (b) Arcing and fire marks (c) Burnt marks between table and hot electrode (d) Showing arcing occurred on the edges and corner of the electrodes.

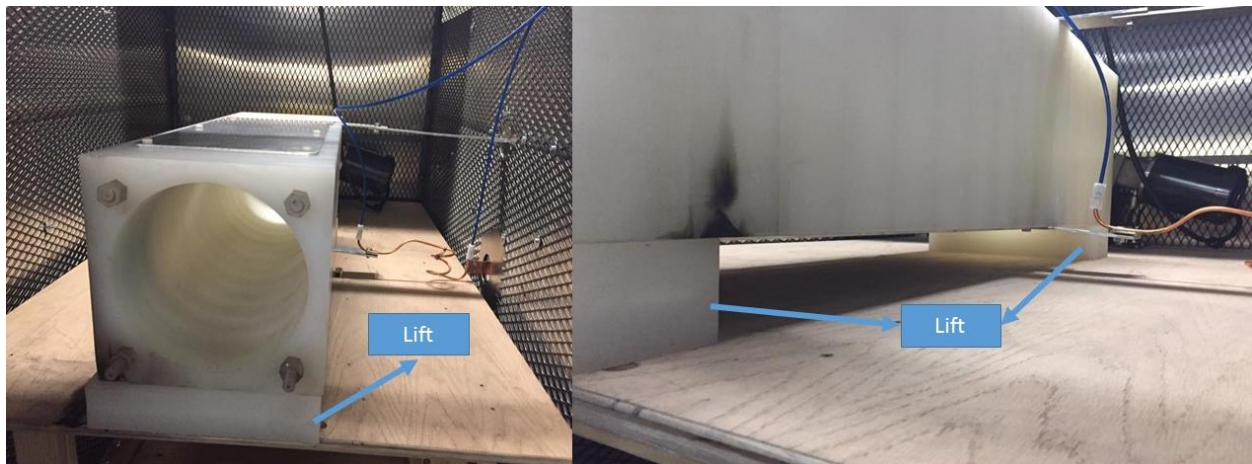


Figure 2.13. Photograph of the applicator with 8-cm lift placed between the tubular channel and table.

2.5 Problems encountered and solutions were provided during the installation of the 50-ohm RF heating system

2.5.1 Tuning the system

One of the problems encountered during the installation of the 50-ohm RF heating system was the maximum power was not applied to the load. The reflected power going to the generator was higher than the forward power. This problem resulted to not heating the grains and killing the insect pests. The solution provided for this problem was tuning the system and it was discussed earlier in this chapter on how to tune the system. Tuning the system by adding inductance outside the matching network (Figure 2.14) resulted in having maximum forwarded power applied to the load and zero reflected power. However, the coil was overheated. The color of the copper tube turned to silver. This signifies that the copper tube was melted due to RF heating. The solution provided in this problem was using a water cooling system. Figure 2.15 shows the set-up of a water cooling system in the coil. The water flows from the faucet to the coil inside the matching network, to the coil added, and going back to the sink.



Figure 2.14. Coil added with maximum power transfer to the load



Figure 2.15. Water cooling system connection

2.5.2 RF leakage

Another problem encountered during installation was RF leakage. RF leakage is a critical problem for the health of workers. High exposure to RF energy results to thermal effects in our body especially to parts which are heat sensitive. In addition, RF energy leakage can interfere with the function of the matching network and other surrounding digital devices. This resulted in a wrong reading of the AMN controller that balanced the impedance of the system because the matching network circuits and tuning elements (capacitors and inductor) were very sensitive to the RF signal. Moreover, RF leakage could damage any unshielded cable and digital devices. This was what happened to the cable which connected the matching network and AMN controller. The cable (Figure 2.16) exposed to the RF leakage was melted resulted in damage to the cable.

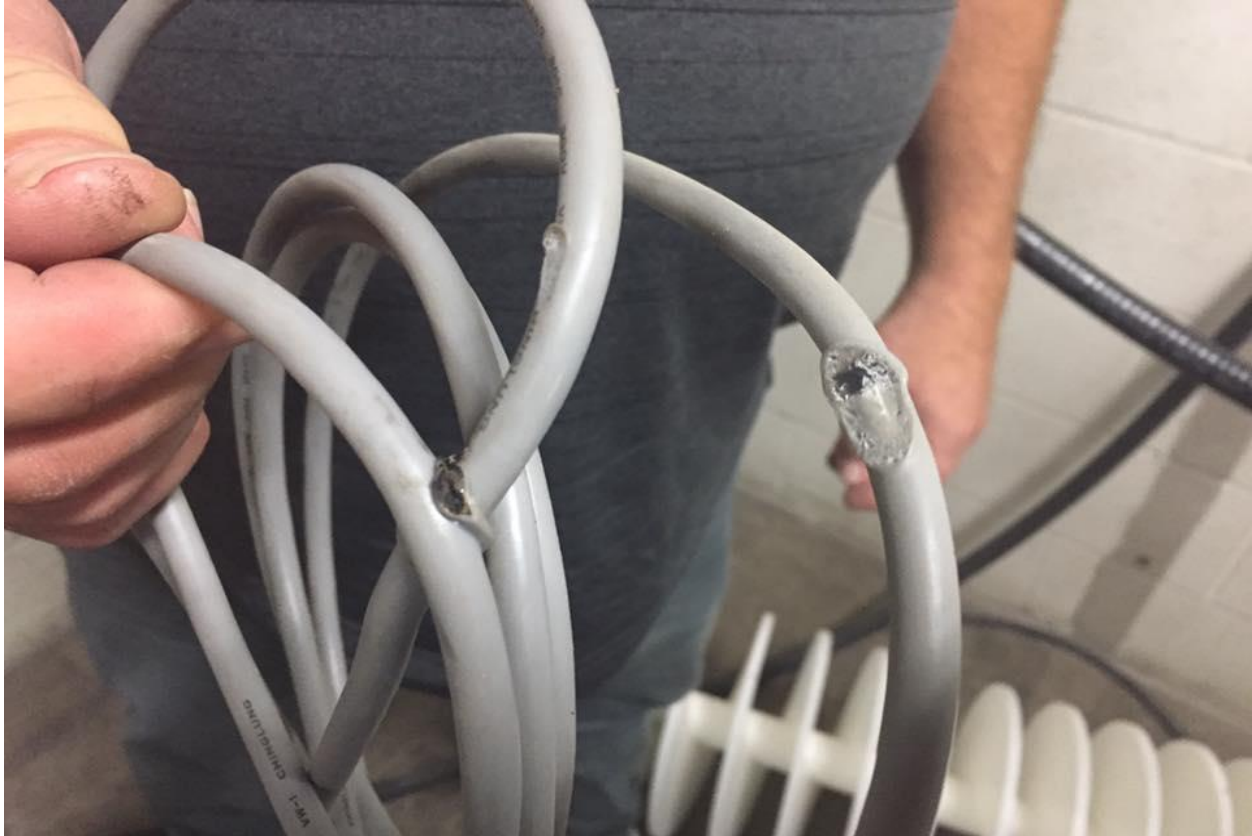


Figure 2.16. Cable melted because of RF leakage

The solutions provided for this problem were good shielding which had a proper connection between the metals of the RF shielding cage (Figures 2.17 and 2.18) and proper connection of the shield to the ground. However, RF leakage was still present and it was going to the matching network resulted in negative values of the AMN controller. This signifies that expanded steel metal is not the best shield for RF energy. Steel has a lower conductivity compared to aluminum and copper. Copper is the best for shielding for RF radiation but it is very expensive. So, aluminum sheets were added on both sides of the shielding cage and the matching network has good contact with the cage and the ground as shown in Figure 2.19. The results showed that adding aluminum sheet between the matching network and the aluminum meshed metal cage improved the reading the

AMN controller and maximum power was applied to the load. Nevertheless, there was still RF energy leakage in the surroundings. This would be resolved by adding aluminum metal on all sides of the cage.

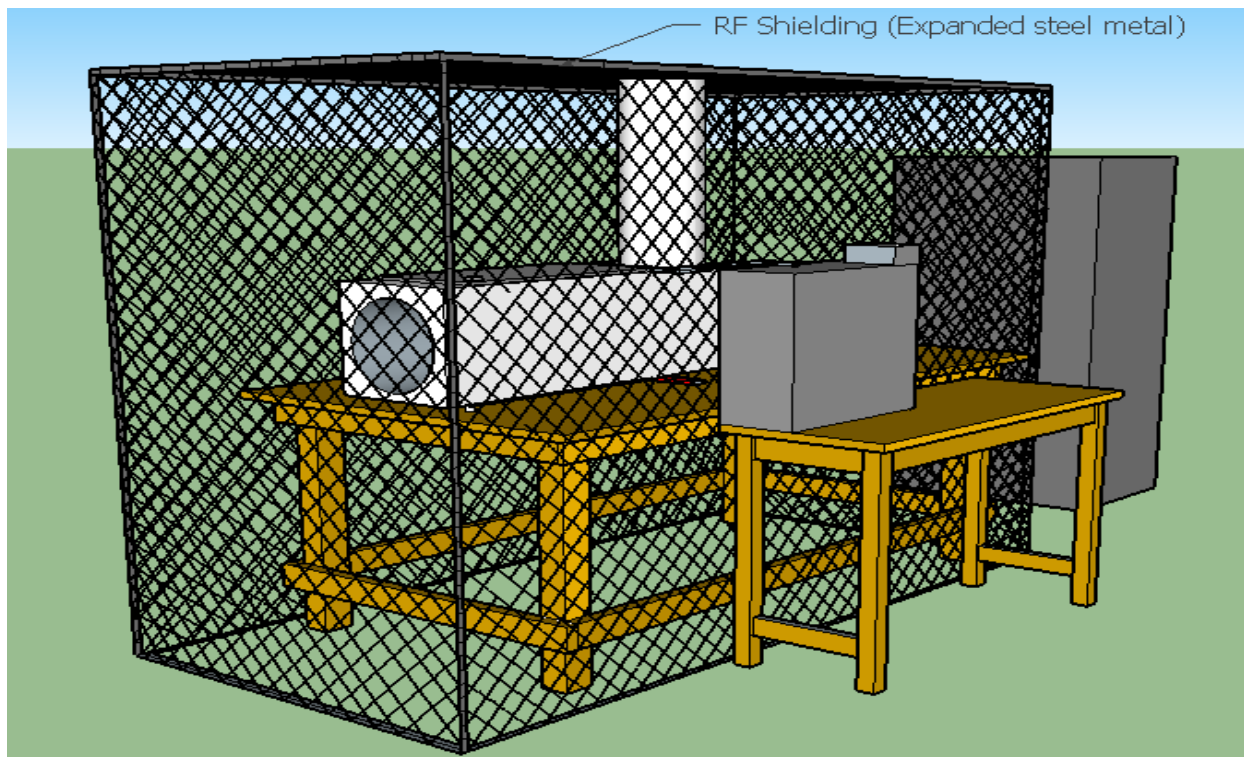


Figure 2.17. RF shielding (Expanded steel metal)



Figure 2.18. RF shielding photograph (expanded steel metal)



Figure 2.19. RF shielding: (a) Addition of aluminum metal sheet in both sides, and (b) Matching network has a good contact to the shielding and the ground

2.5 Concluding remarks and suggestions

Fifty-ohm radio frequency heating is proposed as an alternative method for disinfestation of insect pests in stored grains. Successful installation and application of this technology requires understanding of the important modules (RF generator, 50-ohm coaxial cable, automatic matching network, and RF applicator), impedance matching relating to basic electrical parameters (voltage standing wave ratio, impedance, capacitance, inductance, and frequency), and solving problems encountered such as arcing and fire, tuning the system, and RF leakage. Lack of knowledge about the use of a 50-ohm RF heating system causes a biased judgment of this technology. Therefore, collaboration with the RF manufacturer and RF experts is needed for a successful application.

During the installation, it was found out that inductance was needed to tune the system. Thus, two turns of copper tubing (loop diameter = 50 mm, wire diameter = 6mm) was added and connected to the hot electrode outside AMN. With this result, it is suggested to design and build a matching network intended for disinfestation, with modification of the L configuration by putting more inductance in the matching network. In addition, the arcing in an RF heating system is dangerous because it can cause a fire that can damage the components of the system, materials to be processed, and even the building. Hence, the following are suggestions for arcing and fire prevention for the system. First, make sure all parts are clean with no arc producing materials (carbon soot, sharp metals, over dehydrated materials) in the RF applicator. Second, in running the RF generator, an empty applicator should be avoided because the components of the applicator might melt and arc because of overheating. Lastly, avoid direct contact

between the hot electrode and dielectric materials, as it might result in overheating of the product and cause the arcing.

2.6 References

Ark, P. and W. Parry. 1940. Application of high-frequency electrostatic fields in agriculture. *The Quarterly Review of Biology* 15: 172–191.

Azab, M., A. Darwish, R. Mohamed and M. Sanad. 2013. Comparative efficacy of controlled atmospheres against two stored product insects. *Journal of Crop Protection* 2: 343–353.

[Breed, G. 2007. There's nothingmagic about 50 ohms. High Frequency Electronics in 2007 Summit Technical Media, LLC Editorial. Accessed on June 2007 at http://www.summittechmedia.com/highfregelec/Jun07/HFE0607_Editorial.pdf](http://www.summittechmedia.com/highfregelec/Jun07/HFE0607_Editorial.pdf)

Coaxial Power Systems Ltd. 2001. Automatic matching network with separate remote controller installations and operating instructions. Spectrum House, Finmere Road, Eastbourne, E.Sussex BN22 8QL UK Web: www.coaxialpower.com

[EEWeb. 2018. Coil inductance. Accessed on January 7, 2018 at https://www.eeweb.com/tools/coil-inductance](https://www.eeweb.com/tools/coil-inductance)

Ferdous, M.S. 2015. Design of a radio frequency heating system for electrolytic liquid and sludges. A Thesis Submitted to Electrical Engineering of the College of Graduates Studies, University of British Columbia. Master of Applied Science. January 2015.

Govindasamy, R., J. Italia and C. Liptak. 1997. Quality of agricultural produce: consumer preferences and perceptions. New Jersey Agricultural Experiment Station, P-02137-1-97, http://www.cook.rutgers.edu/~agecon/pub/qual_ag.pdf.

Guo, W., S. Wang, G. Tiwari, J. Johnson and J. Tang. 2010. Temperature and moisture dependent dielectric properties of legume flour associated with dielectric heating. *LWT Food Sci. Technol.* 43: 193–201.

Hines, D. 2018. Electrical fire causation. SAMAC Engineering Ltd. Accessed on July 1, 2018 at <https://www.samaceng.com/articles/electrical-fire-causation/>

Hou, L., J. Johnson and S. Wang. 2016. Radio frequency heating for postharvest control of pests in agricultural products: a review. *Postharvest Biology and Technology* 113: 106–118

Huang, Z., H. Zhu, R. Yan and S. Wang. 2015b. Simulation and prediction of radiofrequency heating in dry soybeans. *Biosystems Engineering* 129: 34-47.

ILO/ICNIRP. 1998. Safety in the use of radiofrequency dielectric heaters and sealers. ILO Occupational Health and safety series 69. International Labour Office, Geneva.

Jiao, S., J.A. Johnson, J. Tang and S. Wang. 2012. Industrial-scale radio frequency treatments for insect control in lentils. *J. Stored Prod. Res.* 48: 143–148.

Koral, T. 2014. Industrial radio-frequency heater. In *radio-frequency heating in food processing principles and applications*, Awuah, G.B.; Ramaswamy, H.S.; Tang, J., Ed.; CRC: New York, 93–118.

Lagunas-Solar, M., Z. Pan, N. Zeng, T. Truong, R. Khir and K. Amaratunga. 2007. Application of radio frequency power for non-chemical disinfestation of rough rice with full retention of quality attributes. *Asabe* 23: 647–654.

[Lampen, S. 2012. 50-ohms: the forgotten impedance. BELDEN Accessed on August 27, 2017. at <http://www.belden.com/blog/broadcastav/50-Ohms-The-Forgotten-Impedance.cfm>](http://www.belden.com/blog/broadcastav/50-Ohms-The-Forgotten-Impedance.cfm)

LaPointe, R.E. 2018. Electrical properties of plastics. Accessed on September 6, 2018 at <http://members.tm.net/lapointe/Plastics.htm>

Macana, R.J. and O.D. Baik. 2017. Disinfestation of insect pests in stored agricultural materials using microwave and radio frequency heating: A review, Food Reviews International 34(5): 483-510.

Macana, R.J., T.T. Moirangthem, and O.D. Baik. 2018d. Causes and prevention of arcing in 50-ohm pilot scale radio frequency heating system. CSBE/SCGAB 2018 Annual Conference, Guelph, Ontario, July 22-25, 2018.

Macana, R.J., T.T. Moirangthem, and O.D. Baik. 2018e. Mortality of insect pests in stored grains using 50-ohm radio frequency heating system at pilot-scale. CSBE/SCGAB 2018 Annual Conference, Guelph, Ontario, July 22-25, 2018.

Marra, F., L. Zhang, and J. Lyng. 2009. Radio frequency treatment of foods: review of recent advances. Journal of Food Engineering 91: 497–508.

[Microwave101. 2017. Why fifty ohms? Accessed on September 6, 2017 at https://www.microwaves101.com/encyclopedias/why-fifty-ohms](https://www.microwaves101.com/encyclopedias/why-fifty-ohms)

Moongilan, D. 2009. Corona and arcing in power and RF devices. 2009 IEEE Symposium on Product Compliance Engineering. 26-28 October 2009.

Nelson, S. 1966. Electromagnetic and sonic energy for insect control. Transaction of the ASAE 9: 398– 403.

Nelson, S. 1996. Review and assessment of radio-frequency and microwave energy for stored grain control. Transaction of the ASAE 39: 1475–1484.

Orsat, V. 1999. Radio frequency thermal treatments for agri-food products. A Thesis Submitted to the Faculty of Graduates Studies and Research, McGill University. Doctors of Philosophy.

Pan, L., S. Jiao, S. Wang, L. Gautz and T. Kang. 2012. Developing radio frequency postharvest treatment protocol for disinfesting coffee beans. *Transaction of the ASABE* 55: 2293–2300.

Patel, K. and P.S. Negi. 2012. Importance and estimation of mismatch uncertainty for RF parameters in calibration laboratories. *International Journal of Metrology and Quality Engineering* 3: 29-37.

RF Café. 2018. Dielectric constant, strength, & loss tangent. Accessed on September 6, 2018 at <http://www.rfcafe.com/references/electrical/dielectric-constants-strengths.htm>

Schiffmann, R.F. 2001. Fires in microwave and RF heating systems: causes and prevention. *Microwaves: Theory and Applications in Materials Processing V*, Ceramic Transactions, American Ceramic Society 111: 255-362.

Shrestha, B., O.D. Baik. 2013. Radio frequency selective heating of stored-grain insects at 27.12 mhz: a feasibility study. *Biosystems Engineering* 114: 195–204.

Shrestha, B., D. Yu and O.D. Baik. 2013. Elimination of *crystolestes ferrungineus* in wheat by radio frequency dielectric heating at different moisture contents. *Progress in Electromagnetics Research* 139: 517–538.

Sun, J., W. Wang, and Q. Yue. 2016. Review on microwave-matter interaction fundamentals and efficient microwave-associated heating strategies. *MPDI Materials* 9(4): 231.

UNEP. 2006. Handbook for the montreal protocol on substances that deplete the ozone layer. 7th ed. Nairobi, Kenya: United Nations Environmental Program, Ozone Secretariate.

Wang, Y., Y. Li, S. Wang, L. Zhang, M. Gao and J. Tang. 2011. Review of dielectric drying of foods and agricultural products. *International Journal of Agricultural and Biological Engineering* 4: 1 –19.

Wang, S., M. Monzon, J.A. Johnson, E.J. Mitcham and J. Tang. 2007a. Industrial-scale radio frequency treatments for insect control in walnuts I: heating uniformity and energy efficiency. *Postharvest Biology and Technol.* 45: 240–246.

Wang, S., M. Monzon, J.A. Johnson, E.J. Mitcham and J. Tang. 2007b. Industrial-scale radio frequency treatments for insect control in walnuts II: insect mortality and product quality. *Postharvest Biology and Technology* 45: 247–253.

Wang, S., J. Tang, R. Cavalieri and D. Davis. 2003. Differential heating of insects in dried nuts and fruits associated with radio frequency and microwave treatments. *Transaction of the ASAE* 46(4): 1175–1182.

Wang, S. and J. Tang. 2001. Radio frequency and microwave alternative treatments for insect control in nuts: a review. *Agricultural Engineering Journal* 10: 105–120.

CHAPTER 3

Mortality and thermal death kinetics of rusty grain beetle in stored wheat using a pilot-scale 50-ohm RF heating system

To be submitted for journal publication.

Contribution of this paper to the overall study

This chapter determined mortality of rusty grain beetles in stored wheat grain (specific objective 4) and determined parameters of thermal death kinetics during RF heating of insects in stored grain based on experimental mortality (specific objective 5). All experiments in this chapter were conducted and the journal paper manuscript was drafted by myself.

3.1 Abstract

Fifty-ohm technology based RF heating system is more advantageous than the conventional RF heating for disinfestation because of its installation flexibility and maximum power transfer to the load. Therefore, this chapter dealt with the assessment of the mortality of insect pests at all life stages and studied the thermal death kinetics of the insects under a pilot-scale, 50-ohm RF heating treatment. The results showed that

disinfestation of insect pests in stored agricultural materials using the 50-ohm RF technology was promising. One hundred percent mortality rates of adult rusty grain beetles were found at all moisture contents of bulk wheat grain at 343K and 353K. It also was observed that as the target temperature and moisture content were increased, the mortality rate of the insect pests increased significantly. For all life stages of rusty grain beetle, the target temperatures with a 100% mortality rate were used for their mortality assessment. The complete mortalities at all life stages were achieved at a 353K target temperature at three moisture contents of the bulk wheat samples, whereas, at the 343K target temperature, the 100% mortality rates of the insect pests were found at 15% and 18% moisture content of the bulk wheat samples. For the thermal death kinetics of the rusty grain beetle under the 50-ohm RF heating system, E_a , K_0 , and n were 97,490 J/mol, $6.74 \times 10^{13} \text{ 1/s}$, and 1. There was good agreement between the simulated mortalities based on the thermal kinetic model and the experimental mortalities.

3.2 Introduction

Non-chemical methods for disinfestation have been studied for many years to replace the chemical methods. One of them is conventional heating, which was tried but did not successfully work because it was not efficient in killing insect pests and required a large amount of energy. Another nonchemical method is using electromagnetic waves [microwave (MW) and radio frequency (RF)]. Electromagnetic disinfestation offers many advantages over conventional heating: non-contact, volumetric and fast heating. However, an RF heating system is preferred over an MW heating system for disinfestation due to its higher penetration depth and greater selective heating effect (Macana and Baik

2017; Shrestha et al. 2013; Wang et al. 2011, 2003; Guo et al. 2010; Nelson 1996). Thus, in recent years, a conventional RF heating system has been used for disinfestation of wheat, rice, apple, black-eyed peas, mung beans, chickpeas, lentils, cherry, orange, persimmon, walnut, almond, coffee beans, pistachios, rapeseeds, corn, macadamia, soybeans, and chestnut (Macana and Baik 2017; Shrestha et al. 2013; Wang et al. 2010, 2008, 2007a, 2007b, 2003, 2002a, 2002c, 2001; Tiwari et al. 2008; Lagunas-Solar et al. 2007; Birla et al. 2005). Nevertheless, nothing has been done using a 50-ohm RF heating system. The 50-ohm RF heating is the advanced type of RF heating system. It is advantageous compared to the conventional RF heating system because of its matching network that ensures that maximum power is applied to the load. In addition, the applicator can be separated from the generator, hence the system is flexible in terms of installation and application. The applicator can be separated from the RF generator by the use of a coaxial cable and the applicator can be designed and built to fit the type of application.

The thermal death kinetic model has been used to study the disinfestation of insects, and has been helpful for predicting the mortalities of the insects under proper heating conditions. Numerous studies have been undertaken on kinetic models for the mortalities of insect pests during thermal processing. In most of the studies, the thermal death kinetics were determined based on experiments at constant temperature (Johnson et al. 2003, 2004; Wang et al. 2002a; Tang et al. 2000). For example, Wang et al. (2002a) reported the thermal death parameters for *Cydia pomonella* using a heating block system at constant temperatures of 46°C, 48°C, 50°C, and 52°C. The current study used a new

method of thermal heating and the temperature of the samples was continuously increased. Therefore, the reported kinetic models could not be applied.

For all of these reasons, this paper used a 50-ohm RF heating system for disinfestation of insects. This involved the investigation of the immediate and delayed mortality of rusty grain beetle at all life stages (egg, pupa, larva, and adult) in stored wheat at different moisture contents and temperatures of the host grains at 7 kW, 27.12 MHz. In addition, the thermal death kinetics model of the insects was estimated from the dynamic experimental mortalities using the Runge-Kutta method. The determined kinetic model can predict the mortalities without knowing the temperature of the insect body. Moreover, suggestions were given for a successful disinfestation using a 50-ohm RF heating system.

3.3 Materials and methods

3.3.1 The 50-ohm RF heating system

The 50-ohm RF heating system used for this study (Figures 3.1) is composed of four main parts: RF generator (15 kW and 27.12 MHz); an automatic matching network (AMN); 50-ohm coaxial cable; and the RF applicator. The first three parts were supplied by our partnered industry, Coaxial Power Systems Company and the applicator was designed by the author. The RF generator produced the RF signal between the two electrodes and thus was transferred to the load, which killed the insects. A 50-ohm coaxial cable linked the RF generator and the AMN. The AMN was the controller of the system, which ensured that the load received the maximum signal to kill the insects. The applicator was the receiver of the signal.

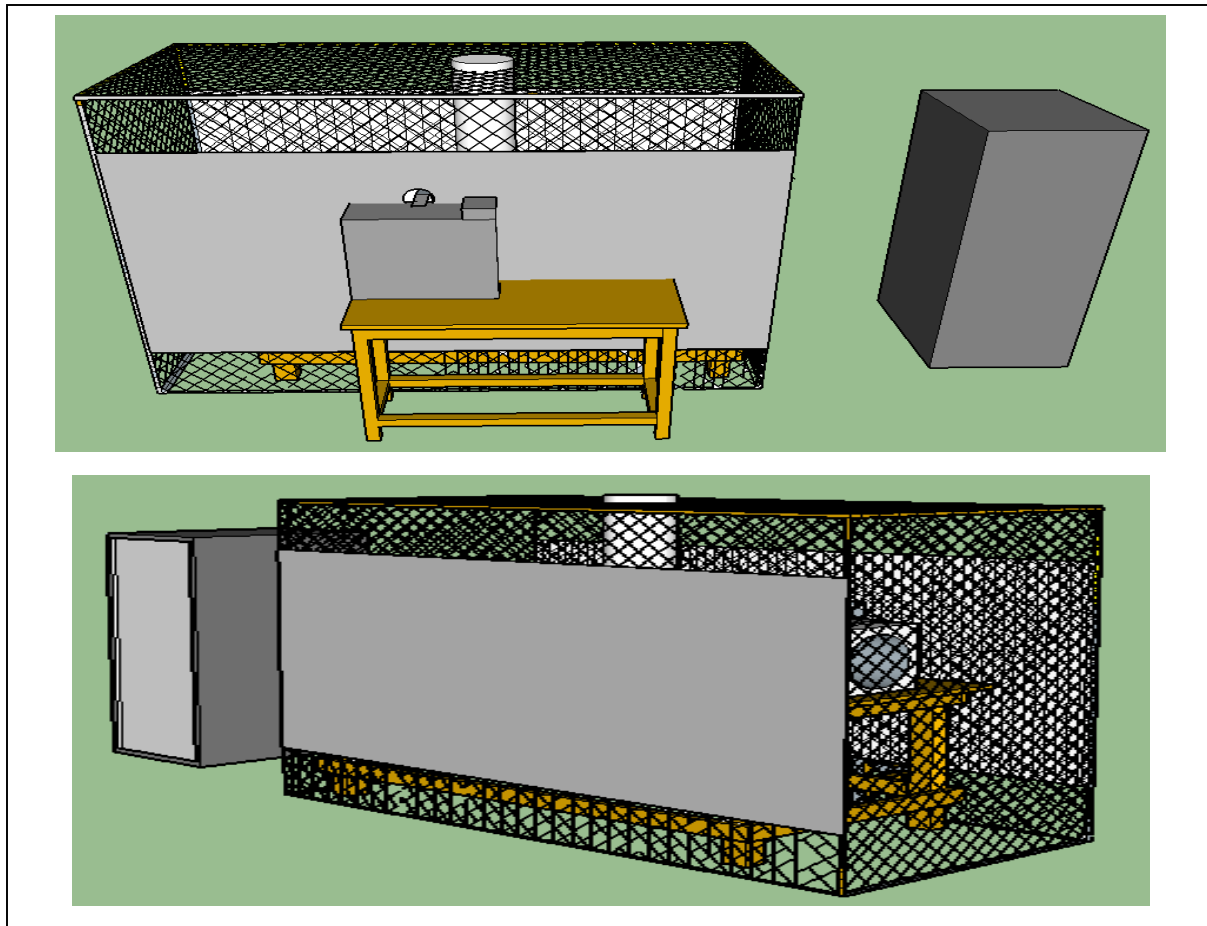


Figure 3.1. The 50-ohm RF heating system (27.12 MHz, 15 kW): (a) Left view (b) Right view.

3.3.2 The RF applicator and its hottest spot location

The applicator had two electrodes (hot and ground) as shown in Figure 3.2. In between the two electrodes was the tubular channel, which was made of polypropylene and had a diameter of 30 cm. The length of the electrode was 70 cm and the gap size between the two electrodes was 36 cm. The materials (insects and grains) were in the channel and acted as an insulator during the RF heating. This was where the insects were killed and the wheat samples were heated. The hottest spot location was on the

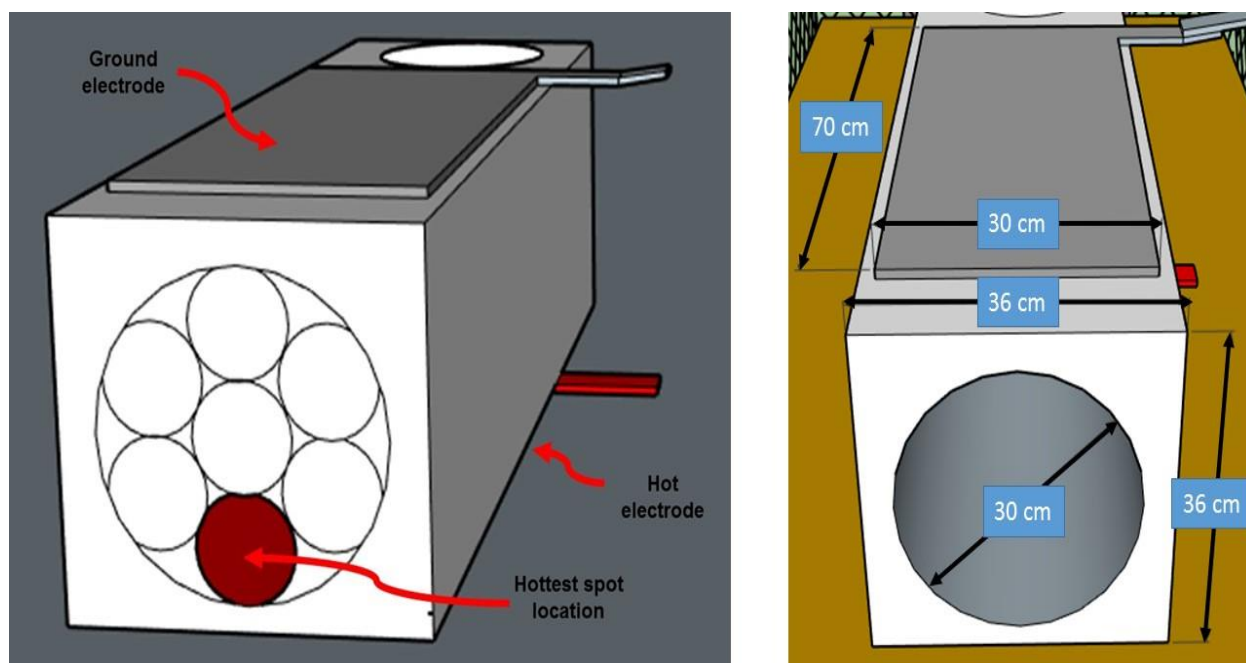


Figure 3.2. The technical details of applicator for 50-ohm RF heating system with its hottest spot location.

front bottom side of the applicator. The hottest spot was determined based on preliminary tests of heating uniformity in the applicator. The heating uniformity was also discussed in chapter five in this thesis.

3.3.3 Wheat preparation

Top quality CWRS wheat grain, cv. Lillian (11% MC w.b.) was provided by our industrial partner, Viterra Inc. (Regina City, Saskatchewan, Canada) for this study and stored in a refrigerator at 4°C. Wheat with moisture contents of 12%, 15%, and 18% (w.b.) was prepared for the experiments. A pre-calculated amount of distilled water was sprayed to reach the target moisture content of the samples with known initial moisture content and mass. The samples with adjusted moisture content were placed in the air-tight bins and stored at room temperature (24°C) for 3 days with regular mixing to achieve an

equilibrium moisture content. Moisture content measurements were done by drying 10 g of wheat grains for 19 h at 130°C using standard hot air oven.

3.3.4 Rusty grain beetle preparation

Four hundred adults of rusty grain beetle (*Cryptolestes ferrugineus*) were provided by our collaborator from Agriculture and Agri-food Canada. The insects were cultured using the procedure reported by Shrestha et al. (2013). The insects were cultured for 10 weeks in a 2-litre glass jar containing 1.5 kg of a mixture of wheat kernels (15% MC w.b.), wheat germ, and wheat cracks in a proportion of 90-5-5 (%) by weight, respectively, and stored in a temperature and humidity chamber (30°C and 70% RH). The insects were separated from the mixture of wheat kernels by using a # 40 Canadian standard sieve; counting them to determine mortality was done following the method adopted by Shrestha et al. (2013) using the suction assembly shown in Figure 3.3.

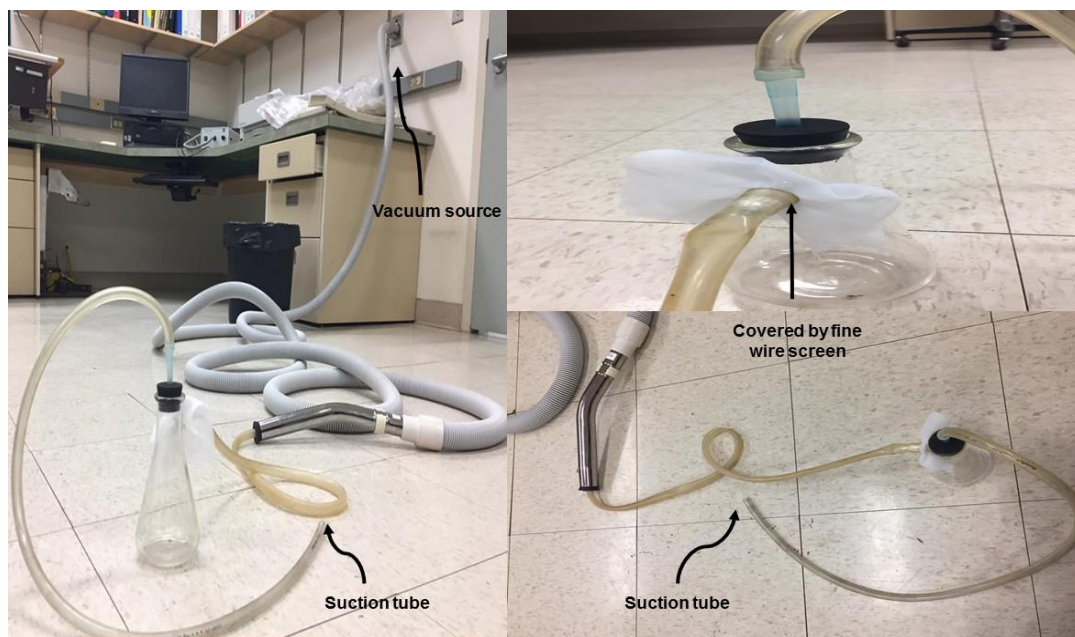


Figure 3.3. The suction assembly for collecting and counting the insects.

3.3.4 Temperature histories

The temperature histories of the wheat samples at different moisture content levels (12%, 15%, and 18%) were measured using fibre optic temperature sensors with an accuracy of ± 0.8 K (Neoptix, Quebec City, Canada). The temperature readings were transferred automatically through the I/O device (NI USB 6008, TX) to the data acquisition program (oven.vi) developed on Labview (2010v.10) platform. The temperatures of the sample were displayed and recorded every 2 s to reach 353 K (target temperature) from 297 K (initial temperature). Regression models were developed for the temperature (K) of the wheat samples as a function of RF heating time (s). The RF heating times of the wheat samples were determined when each target temperature (303 K, 313 K, 323 K, 333 K, 343 K, and 353 K) was reached. The regression models based on the dynamic temperatures of the wheat samples served as input data in the kinetic model used in this study for mortality simulation.

3.3.5 Mortality at all life stages of the insects

The 10-week cultured, 400 adult insects, which became approximately 3000 adult insects (confirmed and counted) and numerous eggs, larvae, and pupae (confirmed under a microscope but not counted), were used in determining the mortality rate of all life stages of the insects in mixture with wheat grain (with 12%, 15%, and 18% MC wet basis). Thirty active (strong and healthy) adult insects were used for the immediate mortality experiments by mixing them with 1 kg of wheat kernels. The mixture of adult insects and wheat kernels was then placed in a polypropylene bag (10 cm diameter and 15 cm length) and placed in the hottest spot during RF heating (7 kW, 27.12 MHz) to different

temperature levels (303K, 313K, 323K, 333K, 343K, and 353K). The immediate mortality was counted, followed by putting the dead insects in culture in the growth chamber to determine delayed mortality. The delayed mortality culture was checked after 1 day, 1 week, 2 weeks, 3 weeks, 4 weeks, and 5 weeks, which was enough time to determine the effect of RF heating. For mortality assessment of all life stages of the insects, two 10-week cultures with thousands of adults insects and numerous larva, egg, and pupa (confirmed by microscope) were mixed well and divided into 18 samples for experiments at all moisture contents (12%, 15%, 18%) and temperatures producing 100% mortality of the adult (343K and 353K). The samples of all life stages of insects were then mixed with 1 kg wheat kernels in a polypropylene bag (10 cm diameter and 15 cm length) and placed in the hottest spot during RF heating (7 kW, 27.12 MHz). After RF heating, the treated samples, which contained dead insects and other life stages were cultured in the growth chamber (30°C and 70% RH). Live insects were counted as they emerged after 5 and 8 weeks, because the normal growing period from egg to adult is about 4 - 5 weeks (Shrestha et al., 2013). That would be enough time to determine the effect of RF energy at all life stages of insects. The mortality rates were calculated using equation (3.1).

$$Mortality\ rate = \left(1 - \frac{Number\ of\ treated\ live\ insects}{Number\ of\ non-treated\ live\ insects}\right) \times 100 \quad (3.1)$$

3.3.6 Thermal death kinetic modeling of rusty grain beetle

The thermal death kinetic model for the adult rusty grain beetle is presented in Equation (3.2), which was similar for the model used by Yu et al. (2017). The model was derived from the kinetic model in Equation (3.3) and the temperature-dependent reaction rate constant using the Arrhenius relationship in Equation (3.4).

$$\frac{d(N/N_0)}{dt} = -k_0 \cdot \exp\left(-\frac{E_a}{RT}\right) (N/N_0)^1 \quad (3.2)$$

$$\frac{d(N/N_0)}{dt} = -k (N/N_0)^1 \quad (3.3)$$

$$k = k_0 \cdot \exp\left(-\frac{E_a}{RT}\right) \quad (3.4)$$

Where k_0 is the frequency factor, E_a is the activation energy (J/mol), R is the universal gas constant (8.314 J/mol·K), T is the temperature of the bulk wheat samples, t is the heating time (s), N and N_0 are the number of live insects at time and the initial number of insects, respectively, k is the reaction rate constant (1/s), and n is the order of the reaction.

The values of the constants (n , E_a and k_0) were based on inverse simulation of mortality of the insects with the different sets of mortality vs heating time (end temperature) at different moisture contents (heating rates). The first order differential equation (3.3) with temperature dependent coefficient (3.4) were solved together as (3.2) using ODE 45 solver in MATLAB. The solver was based on the fourth-order Runge-Kutta method. The simulated values were compared to the experimental values. Then the optimum set of the constant parameters, k_0 and E_a was then found based on the lowest total RMSE value after numerous trials and errors.

3.3.7 Data analysis

All experiments were done in triplicate. Excel (MSO 2016) was used to process and analyze data. Analysis of variance (ANOVA) was used to determine statistical differences in temperature, moisture content, immediate mortality, and delayed mortality at a 95% confidence interval (p -value < 0.05).

3.4 Results and discussions

3.4.1 Temperature histories of wheat grain samples

Figure 3.4 shows the temperature histories of wheat samples at different moisture contents. The heating time to reach the target temperature (353K) in bulk wheat was 354 s at 12% MC, 326 s at 15% MC, and 276 s at 18% MC. The heating rate increased when the moisture content of the grain was higher resulting in a lower heating time to reach the target temperature. The heating rate was dominantly dependent on the dielectric loss factor (Shrestha and Baik, 2013), which is also dependent on the moisture content. Increasing the moisture content increased the dielectric loss factor (Macana and Baik, 2017). This was because of the enhanced movement of dipoles and ions at higher moistures resulting in a higher dielectric loss factor and a faster temperature increase (Shrestha et al. 2013).

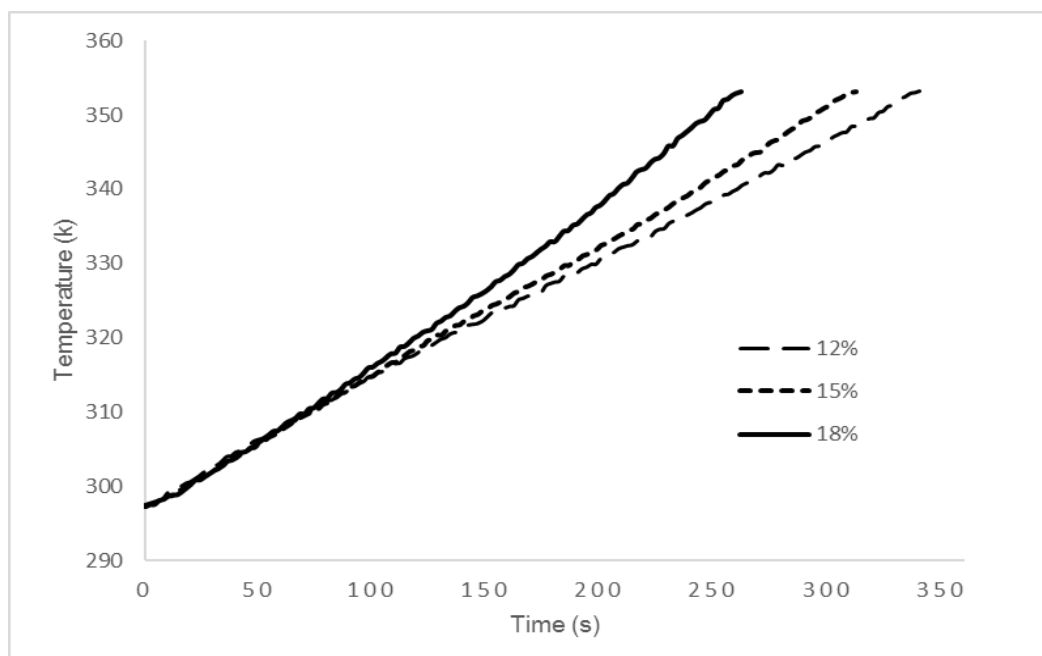


Figure 3.4. The temperature histories of wheat grain at three moisture contents.

Regression models for the temperature of the wheat grain as a function of RF heating time were determined at different moisture content levels: 12% MC in equation (3.5), 15% MC in equation (3.6), and 18% MC in equation (3.7). At all moisture contents, the lines in Figure 3.4 are experimental data, which shows a linear increase in temperature. This is an advantage for predicting the heating rate of the sample easily. The regression models developed from dynamic temperature histories of the wheat samples served as input data for equation (3.2) for the thermal death kinetic model.

$$T = -1E-05t^2 + 0.1667t + 295.28 \quad (3.5)$$

$$T = 3E-05t^2 + 0.1685t + 294.81 \quad (3.6)$$

$$T = 0.0002t^2 + 0.1591t + 294.82 \quad (3.7)$$

3.4.2 Mortality of rusty grain beetles at different temperature levels

Figure 3.5 shows the results of immediate mortalities of rusty grain beetle as a function of wheat grain temperature (303-353 K) at three moisture contents (12%, 15%, and 18%). It was determined that the mortality rate of insect pests was very significantly affected by the temperature at higher MCs, p-value ≤ 0.01 (12%MC), p-value ≤ 0.01 (15%MC) and p-value ≤ 0.01 (18%MC). The optimum mortality rate (100%) were found at 343 K and 353 K target temperatures at all moisture contents. The effect of moisture content on the mortality rate was significant at 323 K and 333 K with p-values of 0.02 and 0.02, respectively, but very significantly affected at lower temperatures (303 K and 313 K), p-values ≤ 0.01 and ≤ 0.01 , respectively. As the moisture content was increased, the dielectric loss factor of the insect pests increased, resulting in a higher rate of temperature increase and power dissipation from the insect bodies (Macana and Baik 2017, Shrestha

et al. 2013). The temperature of the insect pests was expectedly higher than the target temperature (wheat sample temperature), which can be confirmed from the mortality

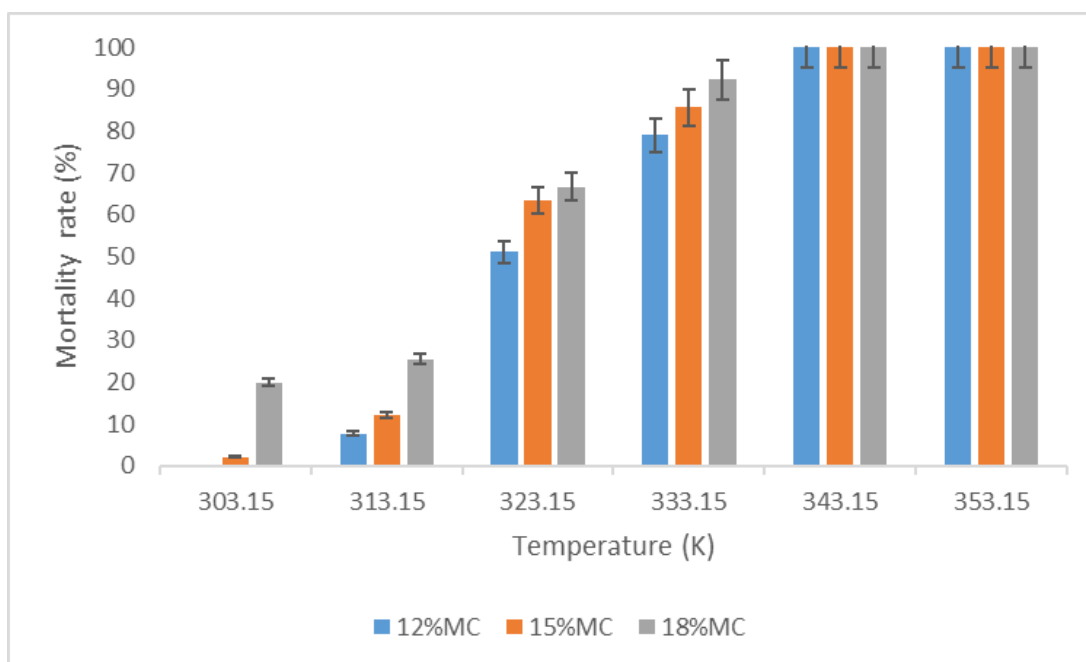


Figure 3.5. Immediate mortality of rusty grain beetle at different temperature levels.

results at lower temperatures, especially at a higher moisture content of the samples. At 18% MC, the mortality rates of insect pests at lower temperatures (303 K, 313 K, 323 K, and 333 K) were 20%, 25.6%, 66.7%, and 92.2%, accordingly, whereas, the mortality rate at the same temperatures at lower MCs were 2.2%, 12.2%, 63.3%, and 85.6% (15% MC) and 0%, 7.8%, 51.1%, and 79% (12% MC), respectively. In summary, increasing the target temperature and the moisture content of the samples increased the mortality rate of insect pests rusty grain beetle. The results were attributed to the effect of selective heating of RF energy to the insect pests.

Figure 3.6 shows the results of delayed mortalities of rusty grain beetle at three MCs (12%, 15%, and 18%) and six heating temperatures (303 K, 313 K, 323 K, 333 K,

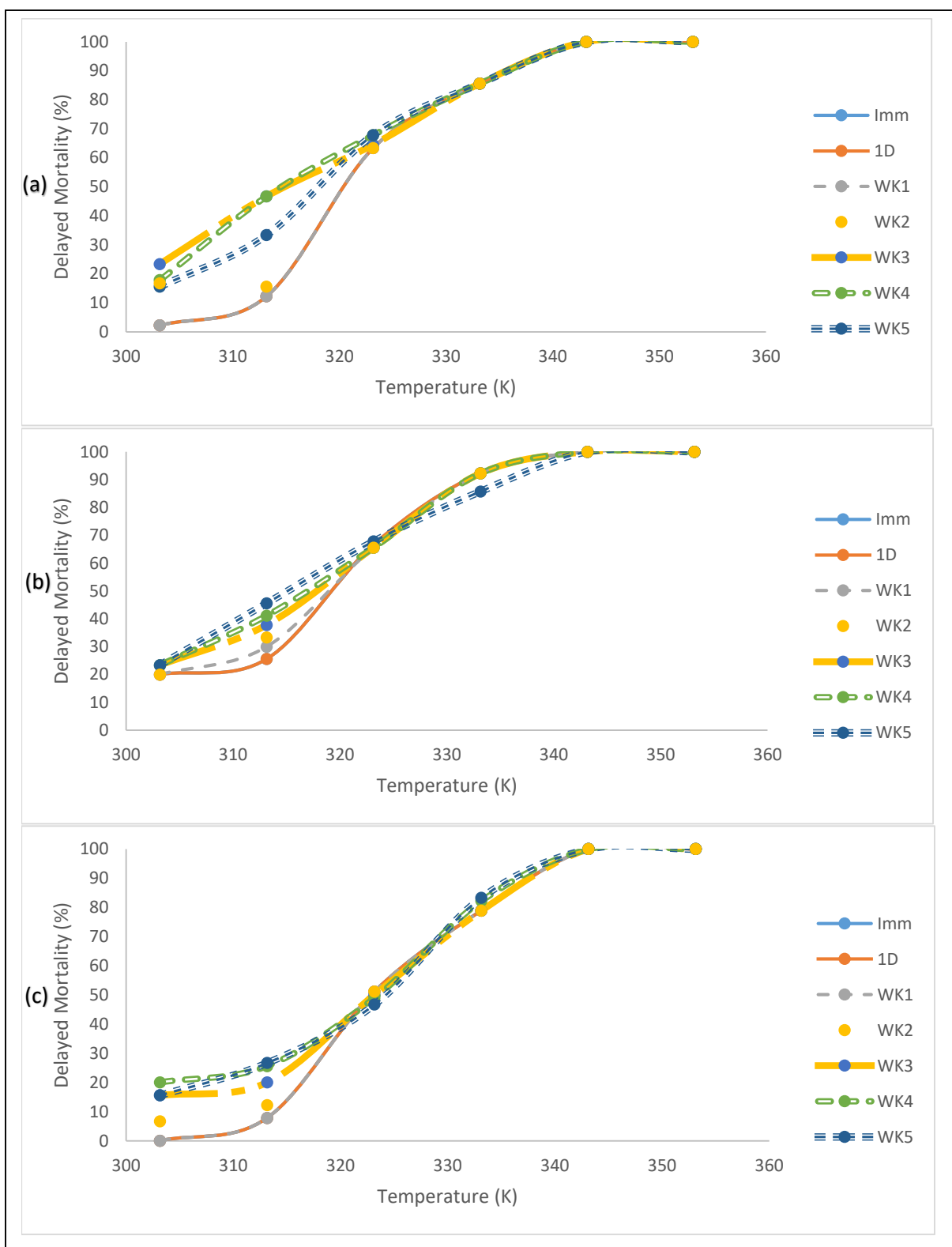


Figure 3.6. Delayed mortalities of rusty grain beetle at different temperature levels: (a) 12% MC (b) 15% MC (c) 18% MC. (Note: The experimental data points are connected with a cubic spline curve for visual presentation).

343 K, and 353 K). Most of the results for delayed mortality at all moisture contents of the samples were higher than the immediate mortalities. Increasing the mortality rate was found from day 1 to five weeks of observation. This was attributed with the effect of RF energy on the bodies of the insect pests. At 12% MC of the wheat sample, there was no significant difference in the delayed mortality at target temperatures of 333 K and 323 K, p -values = 0.74 and 0.98, respectively. However, at lower temperatures, there was a significant effect on delayed mortality, p -values ≤ 0.01 (313 K) and p -values ≤ 0.05 (303 K). The differences between the immediate mortality rate and the delayed mortality rate at 303 K and 313 K heating temperatures were 15.57% and 18.87%, respectively. At 15% MC, there was no significant difference in delayed mortality at temperatures of 303 K, 323 K, and 333 K, (p -values = 0.12, 0.96, and 0.99, respectively), but there was a slight difference at a 303K target temperature (p -value = 0.03). At 18% MC, there was a significant difference in the delayed mortalities of the insect pests at heating temperatures of 313 K (p -value ≤ 0.01) and 333 K (p -value ≤ 0.01). Nonetheless, there was no significant change between the immediate and delayed mortalities at heating temperatures of 303 K (p -value = 0.55) and 323 K (p -value = 0.99). At 313 K heating temperature, the mortality rate increased from 25.6% (immediate mortality) to 45.6% (delayed mortality at 5-week). In summary, there was no emergence of new insects after five weeks of observation. In general, changes in the mortality rate were due to an increase in the number of dead insects as time passed by. The 100% mortality rate at heating temperatures of 343 K and 353 K at all MCs of the sample remained unchanged. This implies that the adult rusty grain beetle was completely killed by RF energy with these temperatures at all MCs.

For all life stages of the insect pests in stored agricultural materials (egg, pupa, larva, and adult), the larva was more resistant to heat than were adults (Shrestha et al. 2013). Nonetheless, their resistance to heat or susceptibility to RF energy varies with the species (Nelson 1996). It was found that when a mixture of wheat and rusty grain beetles at all life stages were treated with RF energy at 353 K at all MCs (12%, 15%, and 18%), there was no emergence of new insect pests after 8 weeks. Similar results were reported by Shrestha et al. (2013); when all life stages of insects were heated at the same temperature, no live insects were found after 8 weeks, confirming 100% mortality rate at all life stages. Earlier in this paper, it was reported that a 100% mortality rate of adult rusty grain beetles was observed also at 343 K. However, when all life stages of rusty grain beetle were treated at this temperature, there was an emergence of new insects after eight weeks at 12% moisture. At 15% and 18% MC of the wheat samples, no insect pests were found after 8 weeks (343 K treatment). This implies that all life stages of the insects were not dead when treated at this temperature at 12% MC. However, at higher MCs, all life stages of the insects were destroyed completely. The selective heating effect of insect pests at 12% was lower than at higher MCs. Therefore, the insects had time to move around and find a more comfortable place (colder spot). This is the problem in disinfestation, insect pests are smart, and they can migrate to the colder spot. The migration of insect pest could be overcome by designing an applicator that can provide uniform heating, and by using a high power RF system to lessen the time for insect pests to move and survive.

3.4.3 Thermal death kinetics

3.4.3.1 Best fit kinetic model and its performance

The model was made for the estimation of thermal death kinetics of the insect pests as shown in equation 3.9. The model was a first-order reaction. Similar to the model of Yu et al. (2017) of an adult *T. castaneum*, Ben-lalli et al. (2009) reported that the first-order model was the most appropriate to describe the thermal death kinetics of eggs of *Ephesia kuehniella* (Zeller). When comparing to the 0.5th order of reaction of the thermal death kinetics of the insect pests used by Wang et al. (2002a) and Johnson et al. (2003, 2004), the first-order kinetic model was more suitable (Yu et al. 2017). The determined activation energy for the thermal death kinetics of rusty grain beetle was 97.490 kJ/mol. It is slightly lower than the adult *T. castaneum*, 100 kJ/mol (Yu et al. 2017). This implies that rusty grain beetle was more susceptible to RF energy than the above insect pest. However, the difference was insignificant, similarly to the study of Ben-lalli et al. (2009) on survival kinetics of *Ephesia kuehniella* during a 46-75°C heat treatment, where the activation energy was 102 kJ/mol. In contrast with insect pests with higher activation energies such as the *Amyelois transitella* (Walker) (510 kJ/mol to 520 kJ/mol) by Wang et al. (2002b); *P. interpunctella* (506.3 KJ/mol) by Johnson et al. (2003); and *C. pomonella* (472 kJ/mol) by Wang et al. (2002).

$$\frac{d(N/N_0)}{dt} = -6.74 \times 10^{13} \cdot \exp\left(\frac{-9.749 \times 10^4}{RT}\right) (N/N_0)^1 \quad (3.9)$$

Table 3.1 shows the performance of the best fitted kinetic model in predicting the mortalities of adult rusty grain beetles in stored wheat grain at different moisture contents using a 50-ohm RF heating system. However, it should be noted that the kinetic parameters were estimated based on temperature histories of insects not on wheat

sample temperatures. When comparing the mortalities of the adult rusty grain beetle using the kinetic model and the experimental values, the results agreed reasonably well at three MC levels (12%, 15%, and 18%). At 12% MC, the RMSE value was 1.461 and the R^2 value was 0.979. The values for mortality at 12% using the model were in good agreement with the experimental values, resulting in low RMSE and high R^2 . At 15% MC, the RMSE was a somewhat higher and the R^2 was slightly lower than at 12% MC. Similarly, at 18% MC, the RMSE and R^2 values were higher and lower than at the lower MC. The RMSE was 4.602 and the R^2 was 0.941. However, their values were still acceptable and the model agreed well with the experimental results. When increasing the moisture content of the sample, the R^2 decreased and the RMSE increased. Thus, the highest RMSE and the lowest R^2 were found at the highest MC of the samples. The same happened with Yu et al. (2017) in their study on thermal death kinetics of red flour beetle at four MC levels (5%, 7%, 9%, and 11%), in that the highest RMSE and the lowest R^2 were found at 11% MC. This was because of the steam effect at the higher MC, resulting in a sudden dropped in mortality of insect pests (Yu et al. 2017). Nonetheless, the simulated and experimental data fit reasonably well as shown in Figure 3.7. The continuous line is the simulated values of the mortality of rusty grain beetle, whereas the scattered points are the experimental values.

Table 3.1. The performance of the kinetic model in predicting the mortalities of the adult rusty grain beetle at different moisture content levels

E_a (kJ/mol)	k_0 (1/s)	n	MC (%,w.b)	R^2	$RMSE^a$	$d.f.$
97.490	6.74×10^{13}	1	12	0.979	1.461	6
			15	0.968	3.166	6
			18	0.941	4.602	6

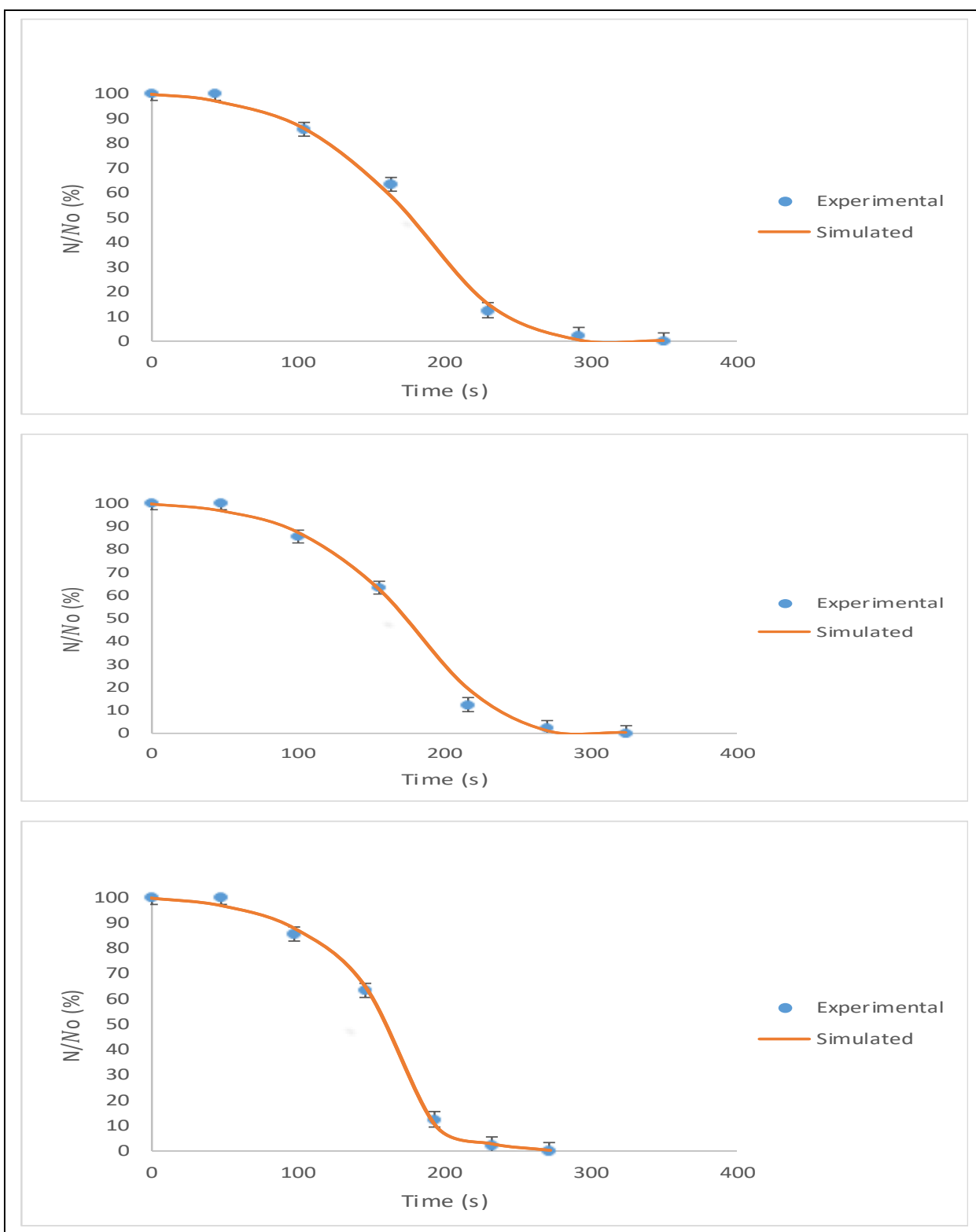


Figure 3.7. The survival rate of insect pests rusty grain beetle at different temperature levels: (a) 12% MC (b) 15% MC (c) 18% MC.

3.4.3.2 Numerically simulated lethal RF exposure time

The thermal death kinetics model was used to predict the RF exposure lethal time for the insect pests. Table 3.2 shows the numerically simulated heating times for the insect pests to achieve 100%, 99%, 95%, and 90% mortality at three moisture contents (12%, 15%, and 18%). The predicted lethal time for 100% mortality rate overall MCs ranged from 248 s to 328 s. At a 99% and 95% mortality rate, the lethal time overall MCs ranged from 242 s to 280 s and 226 s to 256 s, respectively. At a 90% mortality rate, the lethal time was ranged from 214 s to 242 s overall moisture contents. The simulated RF exposure times agreed reasonably well with those from the experiments. Complete mortality of the insects in wheat grain from experiments was achieved with RF exposure time ranged from 272 s to 350 s. The determined exposure time was in the range of RF lethal time ranging 140 s to 1080 s reported by Yu et al. (2017) for the complete destruction of the adult insect in the canola seeds.

Table 3.2. Numerically simulated RF exposure time with 100%, 99%, 95%, and 90% mortality rate at three moisture content levels (12%, 15%, and 18%).

MC (% <i>w.b.</i>)	RF Lethal Time (s)			
	100%	99%	95%	90%
12	328	280	256	242
15	276	270	248	234
18	248	242	226	214

A shorter RF exposure time was achieved at higher moisture contents at all mortality rate of the insect pests. Similar observation was reported by Yu et al. (2017) and Shrestha et al. (2013) on the effect of moisture content to RF exposure lethal time for the insects. This was attributed to the slow heating rate of lower MC. Thus, RF disinfestation can be done before drying for better efficiency and potential drying after RF treatment for longer storage.

3.5 Conclusions

Disinfestation of rusty grain beetles in stored wheat grain is possible with a 100% mortality rate using a 50-ohm RF heating system. Complete mortality of adult insect pests was achieved at 343 K and 353 K at all MCs of the wheat samples. Complete mortalities at all life stages of the rusty grain beetle were obtained at 353 K (12%, 15%, and 18% MC) and at 343 K (15% and 18% MC). Increasing the temperature from 303 K to 353 K and the moisture content of the wheat sample from 12% to 18%, the mortality rate of the insect pests increased. The thermal death kinetic parameters of the adult rusty grain beetle were numerically calculated using an inverse simulation. The mortality results derived from the developed kinetic model were in good agreement with the experimental values. Therefore, the experimental and the thermal kinetic model mortality results would be useful for designing RF applicators for disinfestation of rusty grain beetle and other insect pests in stored agricultural materials.

3.6 References

Ben-lalli, A., J.M. Méot, P. Bohuon and A. Collignan. 2009. Survival kinetics of *Ephesia kuehniella* eggs during 46–75 °C heat treatment. *Journal of Stored Products Research* 45(3): 206–211.

Birla, S.L., S. Wang, J. Tang, J.K. Fellman, D.S. Mattinson and S. Lurie. 2005. Quality of oranges as influenced by potential radio frequency heat treatments against Mediterranean fruit flies. *Postharvest Biology and Technology* 38: 66-79.

Guo, W., S. Wang, G. Tiwari, J. Johnson and J. Tang. 2010. Temperature and moisture dependent dielectric properties of legume flour Associated with dielectric heating. *LWT Food Science and Technology* 43: 193–201.

Johnson, J.A., K. A. Valero, S. Wang and J. Tang. 2004. Thermal death kinetics of red flour beetle (*Coleoptera: tenebrionidae*). *Journal of Economic Entomology* 97 (6): 1868–1873.

Johnson, J.A., S. Wang and J. Tang. 2003. Thermal death kinetics of fifth-instar plodia interpunctella (Lepidoptera: pyralidae). *Journal of Economic Entomology* 96 (2): 519–524.

Lagunas-Solar, M.C., Z. Pan, N.X. Zeng, T.D. Truong, E. Khir and K.S.P. Amaratunga. 2007. Application of radio frequency power for non-chemical disinfestations of rough rice with full retention of quality attributes. *Applied Engineering in Agriculture* 23: 647–654.

Macana, R.J., O.D. Baik. 2017. Disinfestation of insect pests in stored agricultural materials using microwave and radio frequency heating: A review, *Food Reviews International* 34(5):483-510.

Macana, R.J., T.T. Moirangthem, and O.D. Baik. 2018e. Mortality of insect pests in stored grains using 50-ohm radio frequency heating system at pilot-scale. CSBE/SCGAB 2018 Annual Conference, Guelph, Ontario, July 22-25, 2018.

Nelson, S. 1996. Review and assessment of radio-frequency and microwave energy for stored-grain control. Transaction of the ASAE 39: 1475–1484.

Shrestha, B.; Baik, O.D. 2013. Radio frequency selective heating of stored-grain insects at 27.12 MHz: A feasibility study. Biosystems Engineering 114: 195-204.

Shrestha, B., D. Yu, O.D. Baik. 2013. Elimination of *Cryolestes ferrugineus* in wheat by radio frequency dielectric heating at different moisture contents. Progress in Electromagnetics Research 139: 517-538.

Tang, J., J.N. Ikediala, S. Wang, J.D. Hansen and R.P. Cavalieri. 2000. High-temperature-short-time thermal quarantine methods. Postharvest Biology and Technology 21 (1): 129-145.

Tiwari, G., S. Wang, S.L. Birla and J. Tang. 2008. Effect of water-assisted radio frequency heat treatment on the quality of 'Fuyu' persimmons. Biosystems Engineering 100: 227-234.

Wang, Y., Y. Li, S. Wang, L. Zhang, M. Gao and J. Tang. 2011. Review of dielectric drying of foods and agricultural products. International Journal of Agricultural and Biological Engineering 4: 1–19.

Wang, S., G. Tiwari, S. Jiao, J.A. Johnson and J. Tang. 2010. Developing postharvest disinfestation treatments for legumes using radio frequency energy. Biosystems Engineering 105: 341-349.

Wang, S., J. Yue, B. Chen and J. Tang. 2008. Treatment design of radio frequency heating based on insect control and product quality. *Postharvest Biology and Technology* 49: 417-423.

Wang, S., A. Monzon, J.A. Johnson, E.J. Mitcham and J. Tang. 2007a. Industrial-scale radio frequency treatments for insect control in walnuts I: Heating uniformity and energy efficiency. *Postharvest Biology and Technology* 45: 240-246.

Wang, S., M. Monzon, J.A. Johnson, E.J. Mitcham and J. Tang. 2007b. Industrial-scale radio frequency treatments for insect control in walnuts II: Insect mortality and product quality. *Postharvest Biology and Technology* 45: 247-253.

Wang, S., J. Tang, J. Johnson, E. Mitcham, J. Hansen, G. Hallman, S. Drake and Y. Wang. 2003. Dielectric properties of fruits and insect pests as related to radio frequency and microwave treatments. *Biosystems Engineering* 85: 201–212.

Wang, S., J.N. Ikediala, J. Tang and J.D. Hansen. 2002a. Thermal death kinetics and heating rate effects for Fifth-instar *Cydia pomonella* (L.) (Lepidoptera: Tortricidae). *Journal of Stored Products Research* 38 (5): 441–453.

Wang, S., J. Tang, J.A. Johnson and J.D. Hansen. 2002b. Thermal death kinetics of fifth-instar *Amyelois transitella* (Walker) (Lepidoptera: Pyralidae). *Journal of Stored Products Research* 38(5): 427-440.

Wang, S., J. Tang, J.A. Johnson, E. Mitcham, J.D. Hansen, R.P. Cavalieri, J. Bower and B. Biasi. 2002c. Process protocols based on radio frequency energy to control field and storage pests in in-shell walnuts. *Postharvest Biology and Technology* 26: 265-273.

Wang, S., J.N. Ikediala, J. Tang, J.D. Hansen, E. Mitcham, R. Mao and B. Swanson. 2001. Radio frequency treatments to control codling moth in in-shell walnuts. *Postharvest Biology and Technology* 22: 29-38.

Yu, D., B. Shrestha and O.D. Baik. 2017. Thermal death kinetics of adult red flour beetle *Tribolium castaneum* (Herbst) in canola seeds during radio frequency heating. *Journal International Journal of Food Properties* 20: 3064-3075.

CHAPTER 4

Effect of 50-ohm RF energy on the quality of stored wheat after disinfestation

To be submitted for journal publication.

Contribution of this paper to the overall study

This chapter compared the physicochemical, germination, baking, and milling qualities of wheat before and after 50-ohm RF disinfestation (specific objective 6). All the experiments in this chapter were conducted and the journal paper manuscript was drafted by myself.

4.1 Abstract

The germination of wheat kernels was not affected when treated by 50-ohm RF energy up to 60°C to 80°C at 12% MC of the samples. However, it was slightly affected at 15% MC and significantly affected at 18% MC. The indicators for baking qualities (falling number (FN), mixing development time (MDT), peak to height (PKH), and peak-bandwidth (PBW)) were not degraded. The FN was not significantly affected by RF energy at all MCs and temperatures. The MDT, PKH, PBH were significantly affected but their values are still in the top quality range for baking. The milling qualities were not significantly affected by RF energy at all MCs and temperatures. Furthermore, the

physicochemical qualities of the host wheat grains were significantly affected by RF energy after disinfestation for moisture content, bulk and particle density, and porosity. These changes were not negative for disinfestation of stored grains at higher MCs. The changes were advantageous for drying the grains at the same time. This is “hitting two birds (disinfestation and drying) with one stone (RF energy)”. The colour of the wheat kernels was not changed significantly after RF treatment.

Therefore, it was possible to disinfest stored grains without damaging the important qualities of the host wheat grain using 50-ohm RF heating. However, non-uniform heating was an urgent challenge for maintaining the quality of the host materials. Thus, it is suggested to design an applicator to reduce the temperature difference between the hottest spot and the coldest spot in the applicator.

Keywords: Radio frequency (RF) waves; 50-ohm RF heating; Disinfestation; Dielectric heating; Stored grains quality

4.2 Introduction

Disinfestation of insect pests in host materials using electromagnetic energy has been studied for many years. Radio frequency (RF) and microwave (MW) heating are electromagnetic radiation based disinfestation. The US Federal Communications Commission (FCC), which is the regulatory agency for out-of-band emissions from domestic, medical, and scientific applications in the United States, has allocated the following frequencies for industrial applications: 13.56 MHz, 27.12 MHz, 40.68 MHz for RF and 915 MHz, 2450 MHz, 5800 MHz and 24125 MHz for MW (Macana and Baik 2017; Wang et al. 2011). However, the frequencies at 27.12 MHz (RF) and 2450 MHz

(MW) are commonly used for all applications (Macana and Baik 2017). Both RF and MW have been investigated as alternatives for chemical disinfestation. The main advantages of these methods over conventional heating methods are volumetric and fast heating. The electromagnetic energy heats all parts of the material (surface and inside) at the same time, whereas with the conventional heating, the heating process starts at the surface of the material slowly going inside. Several studies demonstrated the applications of electromagnetic energy in disinfestation. For example, MW electromagnetic energy has been used for the disinfestation of barley, chickpea, corn, date fruit, green gram, mung beans, pigeon pea, rye, soil, walnut, and wheat (Das et al. 2014; Jian et al. 2014; Purohit et al. 2013; El-Naggar and Mikhael 2011; Singh et al. 2011; Vadivambal et al. 2011, 2008; Mavrogianopoulos et al. 2000), and RF electromagnetic energy for the disinfestation of almond, apple, black-eyed peas, cherry, chickpeas, coffee, lentils, mung beans, orange, persimmon, rice, walnut, and wheat (Shrestha et al. 2013; Pan et al. 2012; Jiao et al. 2011; Wang et al. 2010, 2008, 2007a, 2007b, 2006a, 2006b, 2005, 2003, 2002, 2001; Tiwari et al. 2008; Monzon et al. 2007; Birla et al. 2005, 2004; Mitcham et al. 2004; Ikediala et al. 2002). The reported studies for disinfestation using electromagnetic energy also investigated the quality of the host materials after electromagnetic treatment. For instance, using MW energy, Das et al. (2014) studied the effects on the moisture content, water activity, colour, peroxide value (PV) and free fatty acids (FFA) of the walnut kernel.; El-Naggar et al. (2011) assessed the effects on the quality of wheat grain and flour (protein, fibre, fat, carbohydrates, ash, and germination); and Manickavasagan et al. (2013) investigated the effects on the instrumental texture (hardness, adhesiveness, springiness, cohesiveness, and chewiness), sensory attributes, and surface colour of

date fruits. Several studies also have been done to investigate the effects of RF energy on host materials after disinfestation. Shrestha et al. (2013) evaluated the effects of conventional RF heating (class C oscillator) on the physicochemical, baking, milling, and germination qualities of wheat after treatment. Other studies on different materials were done also by Birla et al. (2005) (orange), Monzon et al. (2007) and Tiwari et al. (2008) (persimmon), Wang et al. (2002, 2007) (walnuts), Lagunas-Solar et al. (2007) (rice), Wang et al. (2010) (legumes), and Gao et al. (2010) (almond) to determine the effect of RF energy on quality. Macana and Baik (2017) reported that disinfestation using electromagnetic waves (MW and RF) is possible without affecting the important qualities of the host materials. Nonetheless, the disinfestation using radio frequency energy is preferred because of its greater penetration depth and more highly selective heating effect over microwave heating. There are two types of RF heating systems: conventional (class C oscillator) and 50-ohm RF. Fifty-ohm RF is a modern type of RF heating and more advantageous than the conventional RF heating system (Macana et al. 2018a, 2018b, 2018c; Macana and Baik 2017; Shrestha et al., 2013; Jones and Rowley, 1996). Based on the review of literature, no studies have been done for disinfestation of rusty grain beetle in stored wheat grains using the modern type of RF heating system. Therefore, this paper deals with the assessment of physicochemical, germination, indicators for baking, and milling qualities of the host materials (wheat grain) before and after 50-ohm RF disinfestation.

4.3 Materials and methods

4.3.1 Wheat samples preparation

The wheat samples (cv. Lillian) at approximately 11% MC (wet basis) was provided by our industrial partner, Viterro Inc. Prior to the experiments, the samples were stored in a refrigerator at 4°C. The wheat samples were then conditioned to the desired moisture contents (12%, 15%, and 18%) for the experiments. This was done by placing the wheat samples in an airtight bin and spraying a pre-calculated amount of distilled water on them. The samples with adjusted moisture content were kept at room temperature (24°C) for 3 days with regular mixing and shaking to achieve an equilibrium moisture content. The moisture content was determined following ASABE standards (ASABE R2008) by drying 10 g of wheat grains for 19 h at 130°C using a standard hot air oven. When the target moisture content was reached, the samples were then put in polypropylene bags (10 cm diameter) with a length similarly that of the electrode (70 cm) before treatment with 50-ohm RF energy. Figure 4.1 shows the photograph of bulk wheat samples in polypropylene bags before RF treatment.



Figure 4.1. Bags of polypropylene with wheat samples.

4.3.2 The 50-ohm RF heating system

The 50-ohm RF heating system (Figure 4.2) was used in this study for heating the bulk wheat samples at different moisture contents (12%, 15%, and 18%) and temperatures (60°C, 70°C, and 80°C). One of the important parts of the 50-ohm RF heating system is the applicator, where the material is heated. The design of the applicator and its temperature distribution are important for the quality of the material. Figure 4.3 shows the configuration of the applicator. The applicator was made of parallel plate electrodes (70 cm length and 30 cm width). The hot electrode was at the bottom and the ground was at the top. Between the electrodes was a tubular polypropylene channel (30 cm diameter and 36 cm electrode gap). The seven wheat samples were subjected to RF heating. The samples at the hottest spot were collected and placed in a Ziplock® bag for storage in a cold room at 4°C.

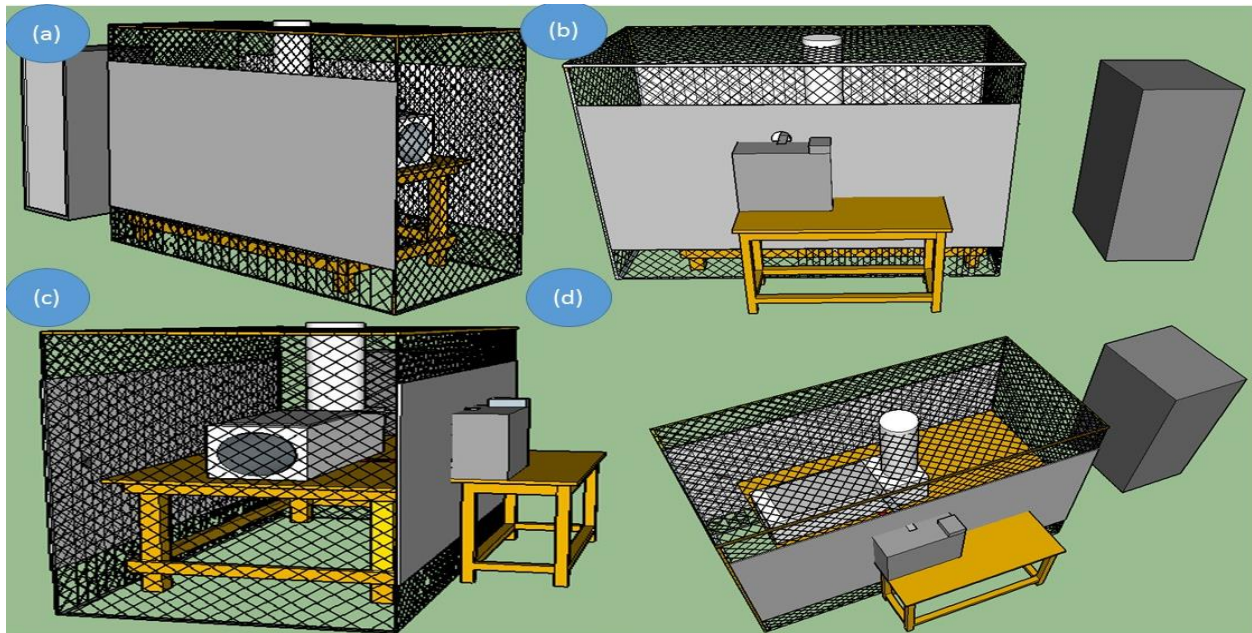


Figure 4.2. The 50-ohm RF heating system: (a) Left view (b) Right view (c) Front view (d) Top view.

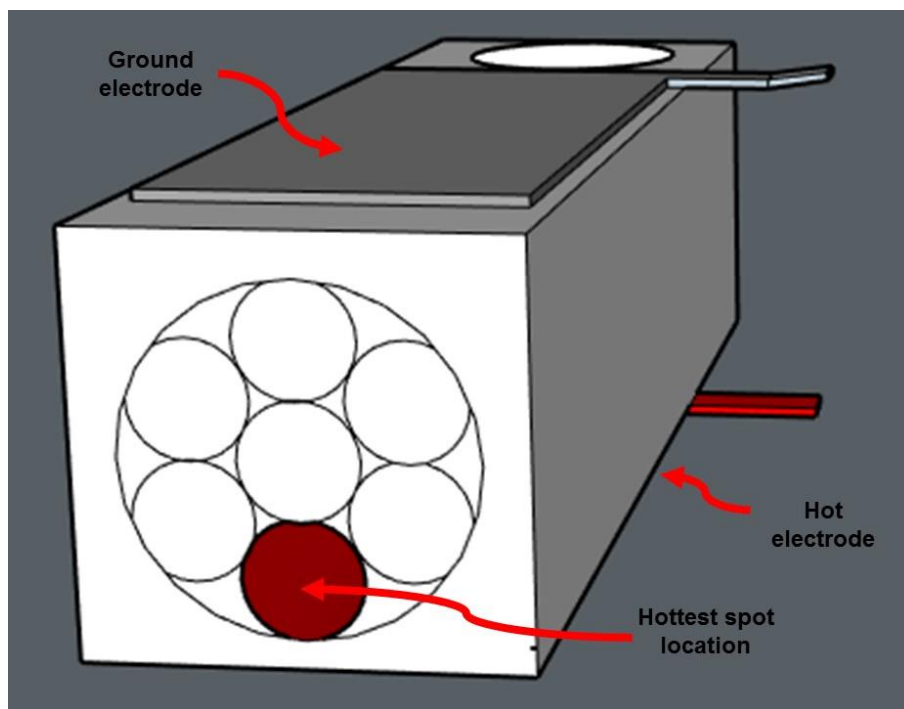


Figure 4.3. Temperature distribution of the applicator.

4.3.3 Measurement of the physicochemical properties of wheat grains

4.3.3.1 Moisture content

The moisture content of the wheat grain was measured before and after RF heating. It was done by drying 10 g of wheat kernels using a standard hot-air oven for 19 h at 130°C. The dried samples were placed in a desiccator for 45 min and then weighed with an analytical scale. Measurements were made in triplicate.

4.3.3.2 Bulk density

The bulk density of wheat kernels was measured using a scaled cylinder (SWA951, Superior Scale Co. Ltd., Winnipeg, MB) with 0.5 L capacity, steel rod, and funnel (Figure 4.4). The wheat kernels were loaded to the funnel and dropped into the scaled cylinder. The cylinder was filled and the steel rod was used to level the wheat kernels. The cylinder was then weighed and recorded. The measurement was repeated three times.

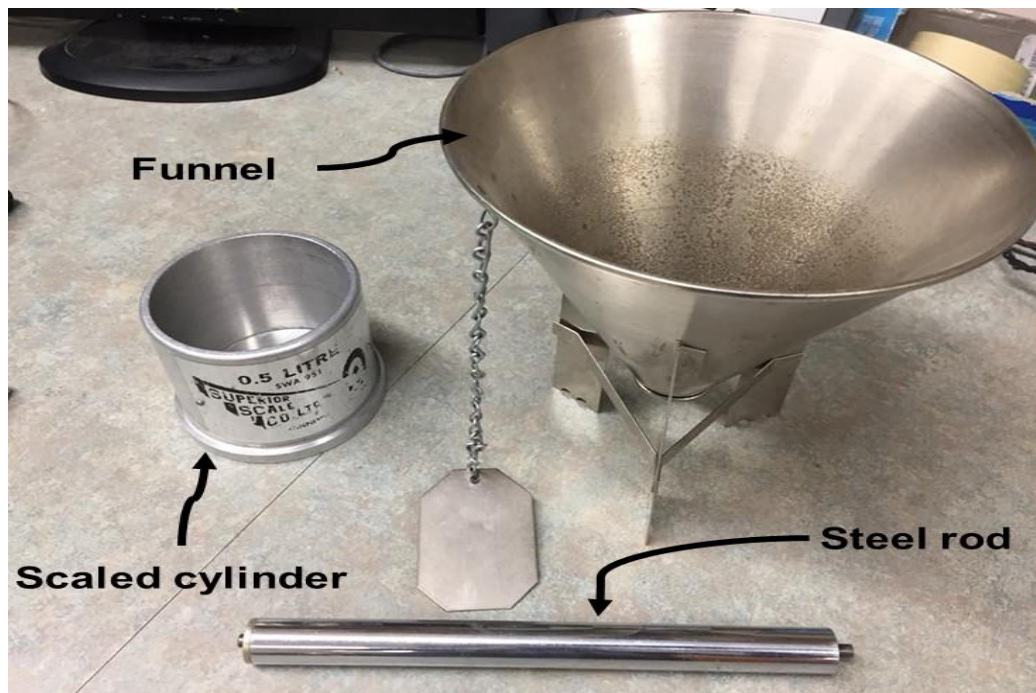


Figure 4.4. Bulk density measurement materials.

4.3.3.3 Particle density

The particle density of the bulk wheat samples was determined using a gas multi-pycnometer (QuantaChrome, Boynton Beach, FL) as shown in Figure 4.5. The measured volume of a known mass of wheat was used for calculating its particle density.

Approximately 12 g of wheat kernels was poured into a small cell after calibrating. The reference cell was filled with nitrogen gas at approximately 117 kPa (17 psig), and the reference cell was connected to the small cell which contained the sample. Following Archimedes' principle, the gas pressure in the reference cell decreased depending on the particle volume until a new lower equilibrium pressure was reached. The known sample and reference volumes, and the final and initial pressures were used in the gas equation for calculating the particle volume.



Figure 4.5. Measurement of particle density using a multi pycnometer.

4.3.3.4 Porosity

The porosity of the wheat samples is a measure of the void spaces in the bulk samples. The porosity of the bulk wheat samples was calculated using Equation 4.1. The equation is based on the bulk density - particle density relationship. Thus, porosity was determined using the values for the bulk density and the particle density of the bulk wheat samples.

$$Porosity (\%) = \left(1 - \frac{Bulk\ density}{Particle\ density}\right) \times 100 \quad (4.1)$$

4.3.3.5 Colour

The colour of the wheat kernels was measured using a spectrophotometer (CM-700d, Konica Minolta Inc., Tokyo City, Japan). A thin glass petri dish (50 mm diameter and 15 mm in height) was filled with the wheat kernels and placed on the aperture of the equipment for colour measurement (Figure 4.6). The equipment was connected to the



Figure 4.6. Measurement of the colour of wheat kernels using the spectrophotometer.

computer and the software was set to take the measurement. The sample was measured in different orientations on the aperture and the average value was recorded.

4.3.4 Germination of wheat kernels

The germination test was done by following the method adopted by Shrestha et al. (2013). A photograph of the method is presented in Figure 4.7. Thirty wheat kernels were plated on Whatman #3 filter paper moistened with 6 mL of distilled water in a petri dish (90 mm diameter). The samples were then placed in a Ziploc® bag to keep the kernels moist and the bags were kept in the temperature-humidity chamber at 25°C for 7 days.

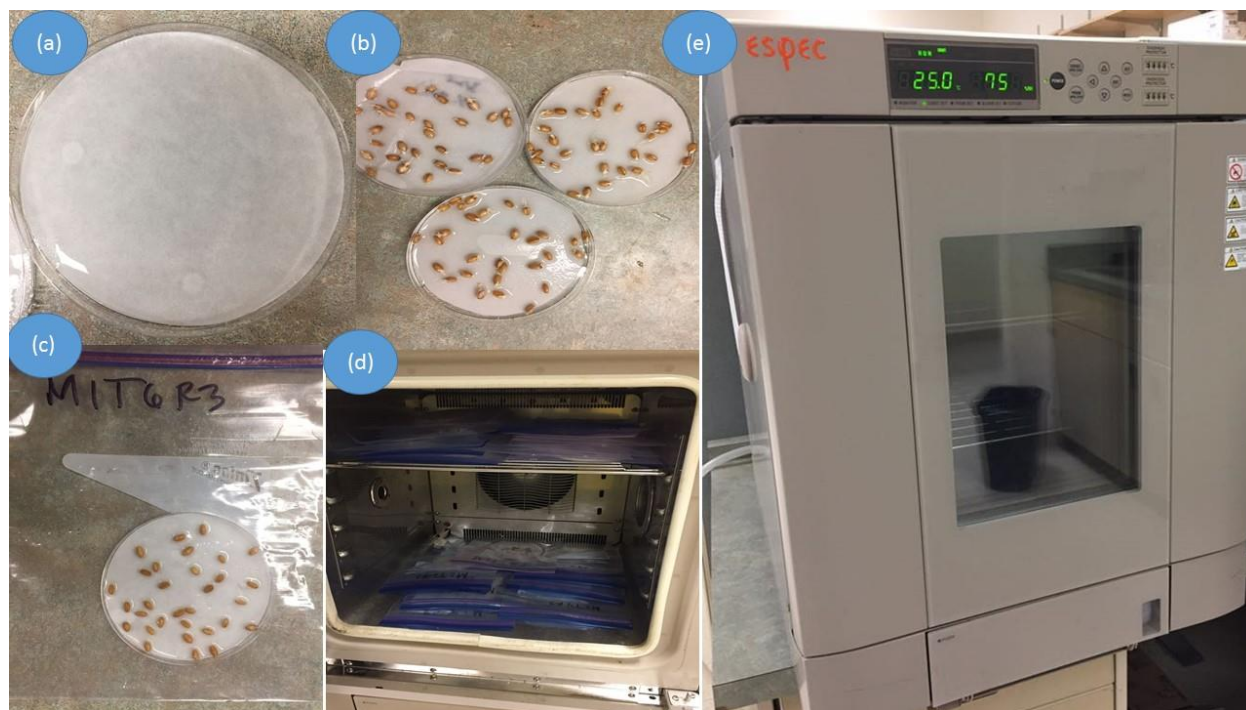


Figure 4.7. Germination of wheat kernels procedure (a) Moistened Whatman filter paper in the petri dish (b) Wheat kernels were added (c) Ziploc bag with the samples (d) Inside the chamber (e) Outside the chamber.

4.3.4 Measurement of baking quality predictors of the wheat samples

The measurement of baking quality predictors was done at Grains Innovation Laboratory in the Crop Development Centre at the University of Saskatchewan. The procedure followed the standard of the American Association of Cereal Chemist (AACC). Baking quality predictors determined in this chapter were the following: falling number (FN), mixing development time (MDT), peak to height (PKH), and peak-bandwidth (PBW).

4.3.4.1 Falling number

The FN was measured using the Perten FN apparatus following the procedure (AACC Method 56-81B). The procedure provides an estimation of the activity of alpha-amylase in the wheat samples. Alpha-amylase activity will reduce the viscosity of a starch paste. The FN was the time (s) required for the stirrer to fall down by its own weight in the Perten FN apparatus. The longer the time, the lower the apparent alpha-amylase activity in the samples.

To start the FN measurement, water bath of the apparatus was brought to a boil. A visual presentation of the test is presented in Figure 4.8. Wheat samples were ground using a UDY Cyclone grinder. After the grinding, the following procedure was performed. First, 25 ml of distilled was added to the viscometer tube. Six point six grams (14% w.b.) of the ground sample then was added to the viscometer tube. The sample was mixed using a Perten Shakermatic automatic sample mixer. The stirrer then was inserted into the viscometer tube, which then was placed into the cassette. The cassette was inserted into the water bath of the apparatus and the process was started. After 55 seconds of

stirring, the stirrer was released and allowed to fall. The FN value was the required time for the stirrer to reach the bottom of the tube.

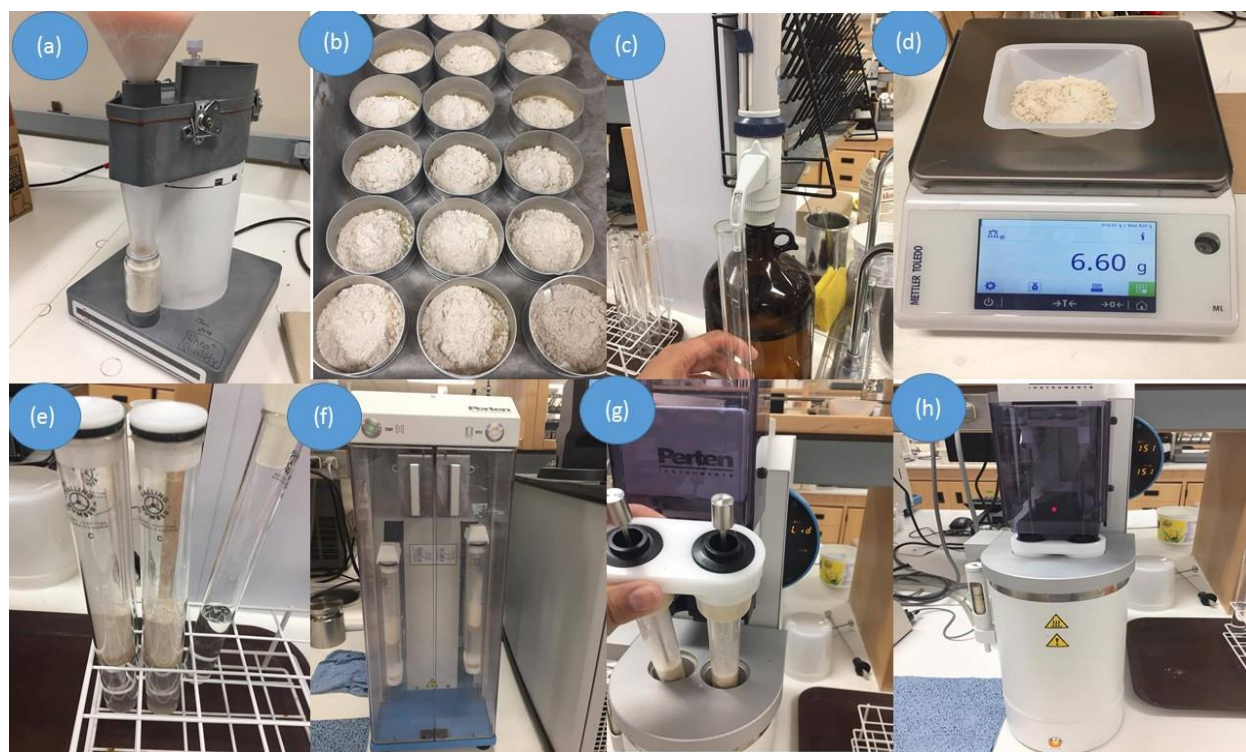


Figure 4.8. Falling number determination procedure: (a) UDY Cyclone grinder (b) Moisture content dishes with the ground sample (c) 25 ml distilled water in viscometer tube (d) Weighing samples (e) Samples added into the viscometer tube with distilled water (f) Sample and water are mixed well using Perten Shakermatic automatic sample mixer (g) Stirrer in the viscometer tube placed into the cassette and the cassette was inserted into the boiling water bath of the Perten FN apparatus (h) The stirrer inside the apparatus started to fall down by its own weight.

4.3.4.2 Mixing development time, PKH, and PBW

A mixograph was used to measure the predictors of baking quality of the wheat samples. The quality can be assessed by the following parameters provided by the mixograph: MDT, PKH, and PBW. Method (AACC 54-50A) using a constant amount of water was used to do the measurements, as shown in Figure 4.9. Nine point nine grams (14% w.b.) of wheat flour was placed in the mixing bowl and 63.3 ml of reverse osmosis

(RO) water was added. The mixing bowl was connected to the computer and the mixogram was displayed on the screen when the mixing started until 7 minutes.

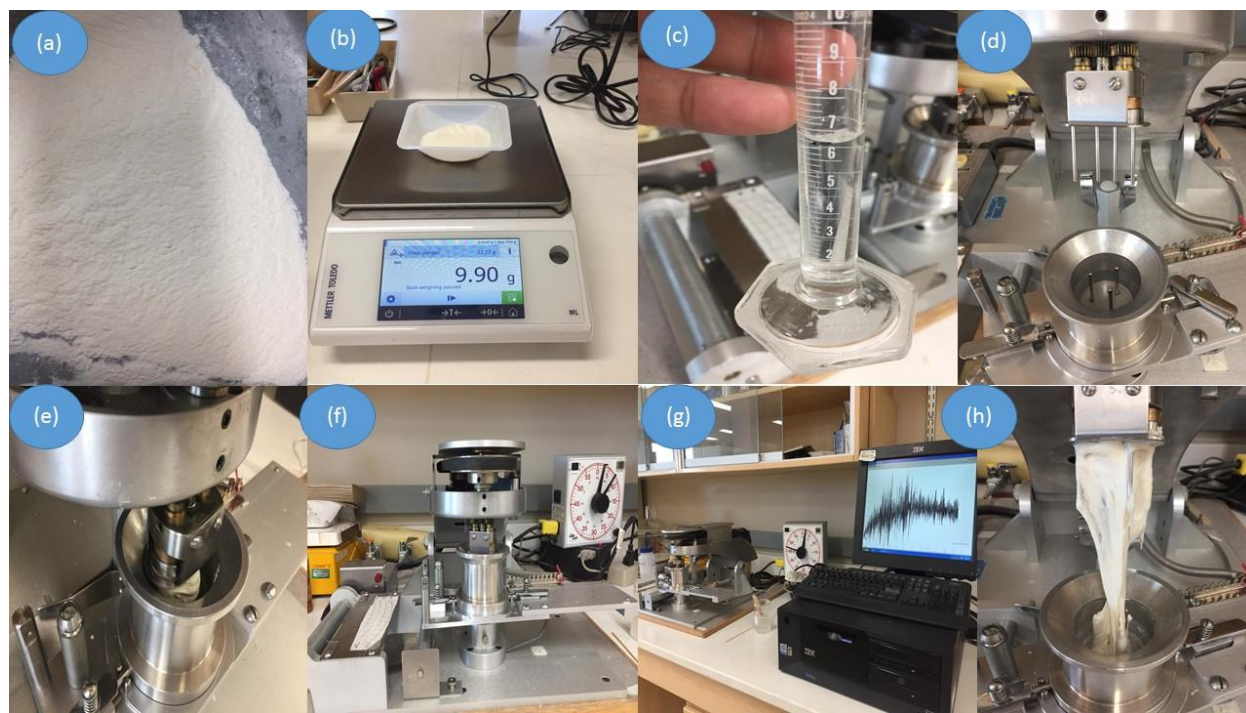


Figure 4.9. Measurement baking qualities using a mixograph procedure: (a) Wheat flour (b) Weighing (c) RO water (d) Mixing bowl (e) mixing the dough (f) Mixing bowl and the clock (g) Curve on the screen (h) Dough when the run completed.

4.3.5 Measurements of the milling quality of the wheat samples

The measurement of milling quality was done at Grains Innovation Laboratory in the Crop Development Centre at the University of Saskatchewan. A day before milling the wheat samples, the moisture content was determined using the AACC procedure. Three grams of ground wheat was dried for 1 h at 130°C using a standard hot-air oven. The samples were then tempered to 14.5% MC w.b. (Figure 4.10) by adding a pre-calculated amount of water. The milling was done using the bread flour milling method by Brabender Quadrumat Sr (Grains Innovation Laboratory, Saskatoon City, Canada). In this method, two mills and two shakers were used (break side and reduction side) (Figure

4.11). The weights of the milling products were recorded, and photographs are presented in Figure 4.12.



Figure 4.10. Preparation of samples a day before milling: (a) Grinding the wheat using Wiley (b) Moisture content measurement (c) Tempering the wheat grains.



Figure 4.11. The mills and the shakers: (a) Quadrumat Sr. Flour mill consisting two milling heads, the break side at the right and the reduction side at the left (b) Wheat samples at break side mill (c) Break sieve (d) Reduction sieve.



Figure 4.12. Milling products: (a) Results after the break side mill (b) Bran (c) Break flour (d) Middlings (e) Reduction flour (f) Shorts (g) Weighing scale for weight measurement.

4.3.6 Data Analysis

All experiments were performed in triplicate. Excel (MSO 2016) was used to process and analyze the data. Analysis of variance (ANOVA) was used to determine statistical differences for all experiments at a 95% confidence interval (p -value < 0.05).

4.4 Results and discussions

4.4.1 Physicochemical properties

4.4.1.1 Moisture content, bulk and particle density, and porosity

Physicochemical properties are important information in the different processes applied to wheat such as milling, baking, pasta making, drying, and other food applications. The moisture content, density, and porosity are important properties that affect the hardness, susceptibility to breakage, milling, drying rate, and resistance to fungal development (Chang 1987). These properties also are important during packaging, storage, and marketing. Changes in these properties are important information to be considered in designing processing equipment, including for RF processing. Table 4.1 shows the moisture content, bulk and particle densities, and porosity after processing at different end temperatures (60°C, 70°C, and 80°C) using 50-ohm RF equipment. At higher moisture contents (15% and 18%) of the wheat grains heated by RF energy up to the end temperatures of 60°C to 80°C, there was a significant loss of moisture from 0.16% to 1.07% (15% MC) and 1.25% to 2.1% (18% MC), $p < 0.01$ and $p < 0.01$, respectively. With treatment at a lower moisture content (12%), the difference was just 0% to 0.12%, which was much lower than at the higher moistures. For bulk and particle density, there was a significant effect of RF energy at 18% MC of wheat grains, $p \leq 0.01$ and $p \leq 0.01$, respectively. At 12% MC, the bulk and particle densities of wheat samples after RF treatment up to 60°C to 80°C increased from 800.95 Kg/m³ to 805.09 Kg/m³ and 1433.50 Kg/m³ to 1440.75 Kg/m³, respectively. However, at 12% and 15% MC, only the bulk density was affected by RF heating ($p < 0.01$ and $p < 0.01$), respectively.

Table 4.1. Physicochemical properties of the 50-ohm RF treated and untreated wheat samples at three levels of MC and temperature.

Moisture Content (%, w.b.)	Temperature	Moisture Content (%, w.b.)	Bulk Density (kg/m ³)	Particle Density (kg/m ³)	Porosity (%)
12	Control	12.00	800.56	1435.82	44.24
	60°C	11.88	802.16	1435.76	44.13
	70°C	12.03	800.95	1433.50	44.13
	80°C	11.51	805.09	1440.75	44.12
	<i>p-value</i>	<i>< 0.01</i>	<i>< 0.01</i>	<i>< 0.05</i>	<i>0.11</i>
15	Control	15.00	784.60	1423.69	44.89
	60°C	14.84	785.20	1425.17	44.90
	70°C	14.29	787.73	1426.24	44.77
	80°C	13.93	792.40	1430.24	44.60
	<i>p-value</i>	<i>< 0.01</i>	<i>< 0.01</i>	<i>< 0.01</i>	<i>< 0.01</i>
18	Control	18.00	740.88	1403.89	47.23
	60°C	16.75	761.51	1423.29	46.50
	70°C	16.11	768.24	1432.18	46.36
	80°C	15.90	775.59	1338.54	42.06
	<i>p-value</i>	<i>< 0.01</i>	<i>< 0.01</i>	<i>< 0.01</i>	<i>< 0.01</i>

For porosity, there was no significant effect of RF heating treated up to 60°C to 80°C at 12% MC of the wheat grain ($p = 0.11$). In contrast, the porosity of the wheat grain at 15% and 18% MC was greatly affected by RF heating. Increasing the moisture content of the wheat grains, increased its porosity after heating. However, when the target temperature was increased, the porosity decreased. A similar trend was observed for bulk density and particle density, where increasing the moisture content and decreasing the target temperature, increased the porosity. The results agreed with the observations of Shrestha et al. (2013). There was a significant change in the moisture content, density, and porosity after RF heating. Still, the changes would be beneficial for drying purposes. This

confirmed the report of Macana and Baik (2017) that the RF disinfestation method is “hitting two birds (killing the insect pests and drying the stored grains) with one stone”.

4.4.1.2 Colour

Colour changes are sometimes undesirable in food processing, especially when the quality of the product is degraded. Not all changes in colour can be seen by the human eye but can be measured using a colour measurement device such as a spectrophotometer. The spectrophotometer instrument gives three different coordinates: L^* , a^* , and b^* . The L^* denotes the lightness of the material, the a^* indicates the red/green coordinates, and the b^* represents the yellow or blue coordinate. To identify the colour differences, the following rules are followed: ΔL^* is the difference in lightness and darkness (+ = lighter, - = darker); Δa^* is the difference in red and green (+ = redder, - = greener); and Δb^* is the difference in yellow and blue (+ = yellower, - = bluer). Table 4.2 shows the results of the colour measurement of wheat grain after RF heating at a different temperatures and moisture contents. ΔL^* at 12% MC treated up to 60°C and 70°C, and at 18% MC with heating up to 60°C has negative values (-1.30, -0.92, and -1.21, respectively), which means the samples were darker than the control. Whereas, the remaining treatments, L^* increased, which means the samples were lighter than the control. Δa^* for the wheat samples with heating up to 60°C at all MCs and 80°C at 12% and 15% MC has negative values (greener than the control), whereas treatments exhibited positive values, which means they were redder than the control. The negative values of Δb^* (bluer than the control) were seen in the wheat samples heated up to 60°C at all MCs and 70°C at 12% MC. While the positive values of the Δb^* signify that the

colour of the treatment is yellower than the control. The positive and negative values of the colour coordinates signify changes in colour when treated by RF heating. However, for treatments, the colour was not significantly affected at all moisture content levels ($p \geq 0.05$). In fact, when comparing the values of the total colour difference (ΔE^*), there was no significant differences among RF-treated wheat samples at all temperatures (60°C, 70°C, and 80°C): $p = 0.36$ (12% MC), $p = 0.76$ (15% MC), and $p = 0.40$ (18% MC).

Table 4.2. Assessment of the colour of wheat grains after RF heating at different temperature and moisture content levels.

Moisture Content (%, w.b.)	Temperature	L*	a*	b*	ΔL^*	Δa^*	Δb^*	ΔE^*
12	Control	50.66	8.20	18.97				
	60°C	49.36	7.95	17.76	-1.30	-0.25	-1.21	1.96
	70°C	49.75	8.36	18.82	-0.92	0.16	-0.15	1.22
	80°C	50.94	7.98	19.63	0.28	-0.22	0.66	0.96
	<i>p-value</i>	<i>0.17</i>	<i>0.22</i>	<i>< 0.05</i>				<i>0.36</i>
15	Control	49.04	7.87	19.49				
	60°C	51.27	7.48	19.01	2.23	-0.39	-0.48	2.52
	70°C	51.38	7.96	20.00	2.34	0.09	0.52	2.52
	80°C	52.92	7.02	20.46	3.88	-0.85	0.98	4.30
	<i>p-value</i>	<i>0.49</i>	<i>0.41</i>	<i>0.11</i>				<i>0.76</i>
18	Control	50.25	7.58	18.58				
	60°C	49.04	7.31	18.49	-1.21	-0.27	-0.08	1.80
	70°C	51.97	8.52	20.51	1.71	0.95	1.93	2.92
	80°C	51.40	8.91	21.09	1.14	1.33	2.51	3.08
	<i>p-value</i>	<i>0.08</i>	<i>< 0.01</i>	<i>< 0.01</i>				<i>0.40</i>

4.4.2 Germination

Figure 4.13 shows the germination rates of the wheat kernels (12%, 15%, and 18% MC) heated with 50-ohm RF energy up to three end temperatures (60°C, 70°C, and 80°C.) At 12% moisture content, the effect of the RF heating on germination at any temperatures was not statistically significant ($p = 0.92$). Whereas at the higher moisture contents (15% and 18% MC), germination of the wheat kernels was affected significantly at 95% confidence level ($p \leq 0.01$ and 0.01 , respectively). In Figure 4.13, the germination rate of the wheat kernels at 12% MC at different temperatures was slightly higher than that of control. The wheat kernel heated up to 60°C had the highest germination rate (91.1%), followed by heating up to 70°C (90%), 80°C (88.9%), and the control (88.9%). In contrast, with the treatment at 15% and 18% MC, the control is much higher than the treatment at all temperatures. It can be seen that the germination at 15% MC, after the control (90%), the treatment up to 60°C (84.4%) has the optimum germination rate, followed by the treatment up to 70°C (80%) and 80°C (68.9%). Similarly, for the wheat kernels at 18% MC, the treatment up to 60°C (72.2%) has the higher germination rate, next to the control (80%), and followed by the treatment up to 70°C (66.7%) and 80°C (53.3%). In general, increasing the end temperature of the treatment decreased the germination rate of the wheat kernels at all moisture contents. This was attributed to thermal effects on the physicochemical and other properties favorable for germination of the seeds (Shrestha et al. 2013; Nelson and Walker 1961). However, at 12% MC, treatment with RF energy was effective and the germination rate was higher than the control, which agreed with the results reported by Nelson (1976) on alfalfa seeds and Shrestha et al. (2013) on wheat. The improvement in germination of seeds with RF energy

at lower MC was due to the decreased number of hard seeds. The presence of hard seeds is a challenge for germination. Shrestha et al. (2013) reported that the seed-coats of hard seeds might be converted into water permeable seed-coats favorable for germination when treated by RF energy, resulting in a slightly improved germination rate.

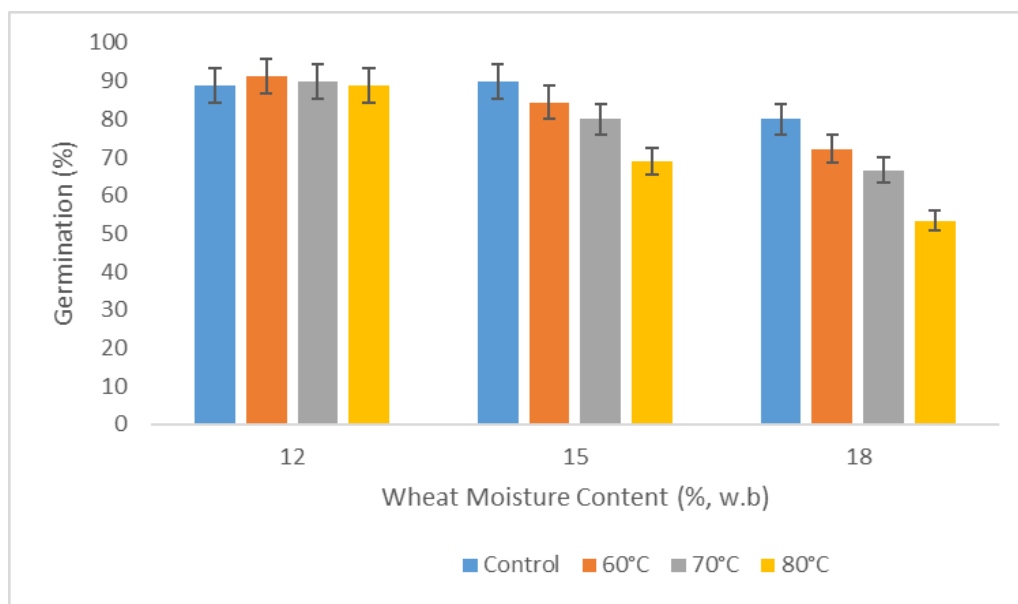


Figure 4.13. Germination rate of 50-ohm RF treated wheat kernels with three levels of MC at different temperature levels and the controls.

4.4.3 Baking quality predictors

4.4.3.1 Falling number

The most common way in predicting the baking quality of the samples is by using the Falling Number (FN) test. The FN test is used for estimating alpha-amylase activity in wheat. It is the time required in seconds for the stirring rod to fall through the starch paste. A low FN signifies a high activity of alpha-amylase in the samples. Alpha-amylase breaks down the gelatinized starch, resulting in lower viscosity and a lower FN. On the other

hand, a high FN indicates less alpha-amylase activity, which is desirable for the bread-making process. Tiley et al. (2012) reported that samples with FN of more than 300 seconds indicated the best baking quality. Figure 4.14 shows the comparison of FN of wheat samples (12%, 15%, and 18% MC) treated by 50-ohm RF energy up to three different temperatures (60°C, 70°C, and 80°C.) The results showed that there were no significant differences in FN between the treated samples at different temperatures and the controls at all MCs at a 95% confidence level: $p = 0.53$ (12%), $p = 0.23$ (15%), and $p = 0.39$ (18%). This means that the RF energy had no significant effect on the FN of the wheat samples, which confirms the results reported by Shrestha et al. (2013) on wheat treated using a conventional RF heating system. It can also be observed in the figure that the FN of the samples treated by RF energy were slightly greater than the controls at 12% and 18% MC. At 12% MC, for example, the FN of control was 343 seconds, which is lesser than the RF treated: 389 seconds (60°C), 372 seconds (70°C), and 381 seconds (80°C). In addition, the FN in both RF treated and the controls are greater than 300 seconds. The results agreed with the normal FN of 350 seconds or more for Canada Western Red Spring wheat (Canadian Grain Commission, 2016).

4.4.3.2 Mixograph

Mixing development time (MDT), peak to height (PKH), and peak-bandwidth (PBW) are important mixograph parameters estimating the baking quality of wheat samples. The parameters were used to predict the bread making potential of the wheat sample in terms of dough strength and loaf volume. MDT (min) was the time it took for the dough to reach peak consistency. The longer the time, the stronger the dough (Shrestha et al. 2013). However, higher dough strength does not always mean a larger

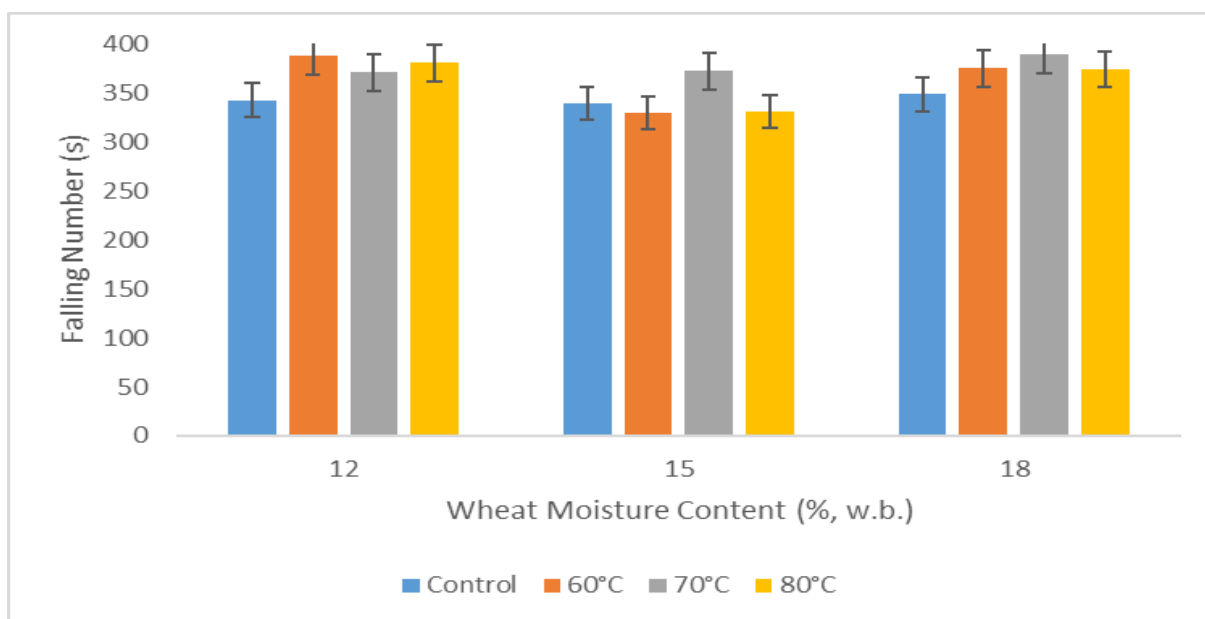


Figure 4.14. Comparison of falling number (FN) of wheat grain treated and untreated with RF energy at different temperature.

loaf volume. Peak to height and PBW can be used to estimate the loaf volume. The PKH is the actual energy measured and the PBW is the percent of the total energy within the curve envelope or span calculated from start to the end. The higher the volume, economically, it has a higher bread-making potential. Higher values for the PKH (N.m) and PBW (% N.m) can equate to larger loaf volume (Shrestha et al. 2013). Table 4.3 shows the effect of RF energy on the predictors of baking quality of the wheat samples at different temperatures and moisture contents. At 12% MC of the wheat sample, when increasing the end temperature from 60°C to 80°C, the MDT increased from 3 minutes to 4.97 minutes, whereas the PKH and PBW decreased from 55.40 to 48.13 and 26.15 to 21.09, respectively. At higher moisture contents (15% and 18%), a similar effect was observed.

Table 4.3. MDT, PKH, and BWP at different temperature and moisture content levels of wheat grain after RF heating.

Moisture Content (%, w.b.)	Temperature	MDT	PKH	BWP
12%	Control	2.94	53.14	24.87
	60°C	3.00	55.40	26.15
	70°C	3.15	52.91	25.29
	80°C	4.97	48.13	21.09
	<i>p-value</i>	<i>< 0.01</i>	<i>< 0.05</i>	<i>0.41</i>
15%	Control	3.70	50.92	20.84
	60°C	3.81	50.57	22.93
	70°C	5.32	47.98	23.09
	80°C	6.93	38.36	20.35
	<i>p-value</i>	<i>< 0.01</i>	<i>< 0.01</i>	<i>0.56</i>
18%	Control	2.82	58.10	35.84
	60°C	4.36	52.29	28.97
	70°C	5.83	44.63	19.26
	80°C	6.31	39.77	18.42
	<i>p-value</i>	<i>< 0.01</i>	<i>< 0.05</i>	<i>< 0.05</i>

When increasing the temperature from 60°C to 80°C, the MDT increased from 3.81 minutes to 6.93 minutes at 15% MC and 4.36 minutes to 6.31 minutes at 18% MC, whereas the PKH decreased from 50.57 to 38.36 at 15% MC and 52.29 to 39.77 at 18% MC. The PBW at 15% MC increased, then decreased, when the temperature was increased. Nevertheless, the PBW at 18% MC acted similarly to 12% MC, which decreased when increasing the temperature. When comparing the controls and the RF treated samples, the MDT and PKH were significantly affected at the three different MCs: $p < 0.01$ (12%), $p < 0.01$ (15%), $p < 0.01$ (18%) and $p < 0.05$ (12%), $p < 0.01$ (15%), $p < 0.05$, respectively. However, the PBW was not affected significantly by RF energy at 12%

MC and 15% MC, $p = 0.41$ and $p = 0.56$, respectively, but slightly affected at 18% MC with $p\text{-value} < 0.05$. The results for MDT and PKH (12% -18% MC) and PBW (12% -15% MC) confirmed a report on the baking quality of wheat using a conventional RF heating system by Shrestha et al. (2013). The effect of RF energy (50-ohm and conventional) was significant, but cannot be considered as negative because the MDT, PKH, and PBW values are still in the desirable ranges. The results of FN reported earlier in this paper also indicated that RF heating did not damage the baking properties of the wheat samples significantly.

4.4.4 Milling quality

For commercial purposes, the milling quality of wheat grain is important because most of the time it is sold as milled flour. The higher the total flour yield, the better the milling quality. The by-products such as bran, middlings, and shorts also are important for assessing milling quality. The total flour yield is the sum of break flour ($<150\text{ }\mu\text{m}$) and reduction flour ($<180\text{ }\mu\text{m}$). Bran is the material on the top of the break sieve shaker ($>500\text{ }\mu\text{m}$), whereas middlings ($>150\text{ }\mu\text{m}$) is a mixture of shorts and reduction flour, and shorts is the material on the top of the reduction sieve shaker ($>180\text{ }\mu\text{m}$). In milling quality, a lower yield of the bran and shorts is preferred. Table 4.4 shows the result for milling quality of wheat sample heated with RF energy at different temperatures and moisture contents. At 12% MC, the yield of bran and shorts at end temperatures of 60°C to 80°C was 21.16% to 23.78% and 5.33% to 6.06%, respectively. The total flour yield was approximately three times higher than the total yield of bran and shorts. The total flour yield at end temperatures of 60°C to 80°C was 69.62% to 71.53%; increasing temperature decreased the total flour yield. The results at different MCs were comparable to the results of the

study by Shrestha et al. (2013): shorts (9.2% to 9.6%), bran (18.1% to 19.0%), and total flour yield (71.3% to 72.1%). At 15% MC of the wheat samples, the total of the bran and shorts at 60°C to 80°C was 27.63% to 27.95%, whereas the total flour yield was 71.39% to 71.72%. The total flour yield was slightly higher than at 12% MC. At 18% MC, the total yield of the bran and shorts at 60°C to 80°C was 26.41% to 26.71%, which is slightly higher than at 15% MC. This means, as the moisture content of the wheat sample increased, the total flour yield increased and the total yield of bran and shorts decreased. Results for the milling quality of the wheat samples agreed with the report by Shrestha et al. (2013). There was no significant difference in total flour yield of the samples treated or not treated by RF energy at the three moisture content levels (12%, 15%, and 18%) ($p = 0.27$, $p = 0.77$, and $p = 0.79$, respectively).

Table 4.4. Milling quality of wheat grain at different temperature and moisture content levels treated by 50-ohm RF energy.

Moisture Content (% w.b.)	Temperature	Bran (%)	Midlings (%)	Break Flour (%)	Shorts (%)	Reduction Flour (%)	Total Flour Yield (%)
12	Control	22.16	52.16	25.67	5.96	45.65	71.32
	60°C	21.93	52.14	25.93	5.95	45.60	71.53
	70°C	22.39	51.81	25.80	5.33	45.44	71.24
	80°C	23.78	51.84	24.38	6.06	45.24	69.62
	<i>p-value</i>	0.38	0.96	0.14	0.35	0.93	0.27
15	Control	21.54	51.32	27.14	5.86	44.76	71.90
	60°C	21.95	50.69	27.36	5.68	44.36	71.72
	70°C	22.41	50.25	27.34	5.34	44.35	71.68
	80°C	22.50	50.12	27.38	5.45	44.01	71.39
	<i>p-value</i>	0.15	< 0.01	0.88	< 0.05	< 0.05	0.77
18	Control	20.60	53.30	26.10	6.37	46.18	72.28
	60°C	20.38	52.76	26.87	6.18	45.87	72.73
	70°C	20.36	50.13	27.13	6.05	45.76	72.89
	80°C	20.84	52.24	26.92	5.87	45.79	72.71
	<i>p-value</i>	0.84	0.38	0.09	< 0.05	0.83	0.79

4.5 Conclusions

The disinfestation of insect pests in stored wheat grains using a 50-ohm RF heating system is possible without degrading significantly the quality of the host material at certain moisture contents and end (target) temperatures. The quality properties (physicochemical, germination, baking, and milling) of the stored wheat grain were assessed after treatment with RF energy. The physicochemical properties (moisture content, bulk and particle densities, and porosity) were significantly affected by RF heating. However, the changes were advantageous for drying purposes. The colour of the wheat grain was not significantly altered when considering the total difference in colour. The germination of wheat kernels was not affected when treated up to 60°C to 80°C at 12% MC. However, it was moderately affected at 15% MC and significantly affected at 18% MC. The predictors for baking quality (Falling number (FN), mixing development time (MDT), peak to height (PKH), and peak-bandwidth (PBW)) were not degraded. The FN was not significantly affected by RF energy at all MCs and temperatures. The MDT, PKH, PBH were significantly affected but their values were still in the desirable range for baking. The milling quality (bran, shorts, and total yield of flour) were not significantly affected by RF energy at all MCs (bran and total flour yield) and at 12% MC (shorts). In terms of the total yield of flour, there were no significant changes in the milling quality after RF treatment. Thus, it can be concluded that disinfestation of insect pests using 50-ohm RF heating does not degrade wheat quality significantly.

4.6 References

Birla, S.L., S. Wang, J. Tang, J.K. Fellman, D.S. Mattinson and S. Lurie. 2005. Quality of oranges as influenced by potential radio frequency heat treatments against Mediterranean fruit flies. *Postharvest Biology and Technology* 38: 66-79.

Birla, S.L., S. Wang, J. Tang and G. Hallman. 2004. Improving heating uniformity of fresh fruit in radio frequency treatments for pest control. *Postharvest Biology and Technology* 33: 205-217.

Canadian Grain Commission. 2016. Procedures for the falling number test. Accessed on November 6, 2018 at <https://www.grainscanada.gc.ca/wheat-ble/method-methode/fnt-dic-eng.htm>

Chang, C.S. 1987. Measuring density and porosity of grain kernels using a gas pycnometer. *Cereal Chemistry* 65(1): 13-15.

Das, I., N.G. Shah and G. Kumar. 2014. Properties of walnut influenced by short time microwave treatment for disinfestation of insect infestation. *Journal of Stored Products Research* 59: 152-157.

El-Naggar, S. and A. Mikhael. 2011. Disinfestation of stored wheat grain and flour using gamma rays and microwave heating. *Journal of Stored Products Research* 47: 191-196.

Gao, M., J. Tang, Y. Wang, J. Powers and S. Wang. 2010. Almond quality as influenced by radio frequency heat treatments for disinfestation. *Postharvest Biology and Technology* 58: 225-231.

Ikediala, J.N., J.D. Hansen, J. Tang, S.R. Drake and S. Wang. 2002. Development of a saline water immersion technique with RF energy as a postharvest treatment against codling moth in cherries. *Postharvest Biology and Technology* 24: 209-211.

Jian, F., D.S. Jayas, N.D.G. White, P.G. Fields and N. Howe. 2014. An evaluation of insect expulsion from wheat samples by microwave treatment for disinfestation. *Biosystems Engineering* 130: 1-12.

Jiao, S., J. Tang, J.A. Johnson, G. Tiwari and S. Wang. 2011. Determining radio frequency heating uniformity of mixed beans for disinfestation treatments. *Transactions of the ASABE* 54: 1847- 1855.

Jones, P. and A. Rowley. 1996. Dielectric drying. *Drying Technology* 14: 1063-1098.

Lagunas-Solar, M.C., Z. Pan, N.X. Zeng, T.D. Truong, E. Khir and K.S.P. Amaratunga. 2007. Application of radio frequency power for non-chemical disinfestations of rough rice with full retention of quality attributes. *Applied Engineering in Agriculture* 23: 647–654.

Macana, R.J. and O.D. Baik. 2017. Disinfestation of insect pests in stored agricultural materials using microwave and radio frequency heating: A review, *Food Reviews International* 34(5): 483-510.

Macana, R.J., T.T. Moirangthem and O.D. Baik. 2018a. 50-ohm RF technology based applicator design and fabrication for disinfestation of insect pests in stored grains. *ASABE Annual International Conference*, Detroit, Michigan, July 29-August 1, 2018.

Macana, R.J., T.T. Moirangthem and O.D. Baik. 2018b. Principles and guidelines for installation of 50-ohm RF heating system for disinfestation of insect pests in stored grains. *ASABE Annual International Conference*, Detroit, Michigan, July 29-August 1, 2018.

Macana, R.J., T.T. Moirangthem and O.D. Baik. 2018c. Shielding effectiveness of electromagnetic energy from 50-ohm radio frequency heating system for disinfestation of

stored grains. . ASABE Annual International Conference, Detroit, Michigan, July 29-August 1, 2018.

Macana, R.J., T.T. Moirangthem, and O.D. Baik. 2018e. Mortality of insect pests in stored grains using 50-ohm radio frequency heating system at pilot-scale. CSBE/SCGAB 2018 Annual Conference, Guelph, Ontario, July 22-25, 2018.

Manickavasagan, A., P.M.K. Alahakoon, T.K. Al-Busaidi, S. Al-Adawi, A.K. Al-Wahaibi, A.A. Al-Reesi, R. Al-Yahyai and D.S. Jayas. 2013. Disinfestation of stored dates using microwave energy. *Journal of Stored Products Research* 55: 1-5.

Mavrogianopoulos G.N., A. Frangoudakis and J. Pandelakis. 2000. Energy Efficient Soil Disinfestation by Microwaves. *J. agric. Engng Res.* 75: 149 -153.

Mitcham, E.J., R.H. Veltman, X. Feng, E. De Castro, J.A. Johnson, T.L. Simpson, W.V. Biasi, S. Wang and J. Tang. 2004. Application of radio frequency treatments to control insects in in-shell walnuts. *Postharvest Biology and Technology* 33: 93-100.

Monzon, M.E., B. Biasi, E.J. Mitcham, S.J. Wang, J.M. Tang and G. Hallman. 2007. Effect of radio frequency heating on the quality of 'Fuyu' persimmon fruit as a treatment for control of the Mexican fruit fly. *Hortscience* 42: 125-129.

Nelson, S. O. and E.R. Walker. 1961. Effect of radio frequency electrical seed treatment. *Agr. Engr.* 42 (12): 688–691.

Nelson, S. O. 1976. Use of microwave and lower frequency RF energy for improving alfalfa seed germination. *Journal of Microwave Power* 11 (3): 271–277.

Pan, L., S. Jiao, S. Wang, L. Gautz and T. Kang. 2012. Developing radio frequency postharvest treatment protocol for disinfesting coffee beans. *Transactions of the ASABE* 55: 2293-2300.

Purohit, P., D.S. Jayas, B.K. Yadav, V. Chelladurai, P.G. Fields and N.D.G. White. 2013. Microwaves to control *Callosobruchus maculatus* in stored mung bean (*Vigna radiata*). Journal of Stored Products Research 53: 19-22.

Shrestha, B., D. Yu and O.D. Baik. 2013. Elimination of *Crystolestes ferrugineus* in wheat by radio frequency dielectric heating at different moisture contents. Progress in Electromagnetics Research 139: 517-538.

Singh, R., K.K. Singh and N. Kotwaliwale. 2011. Study on disinfestation of pulses using microwave technique. Journal of Food Science and Technology (July–August 2012) 49: 505–509.

Tilley, M., R.A. Miller and Y.R. Chen. 2012. Wheat breeding and quality evaluation in the U.S. In: Cauvain, S. P. editor. Bread Making: Improving Quality. 2nd edition. Cambridge, UK: Woodhead Publishing Limited. 216-236.

Tiwari, G., S. Wang, S.L. Birla and J. Tang. 2008. Effect of water-assisted radio frequency heat treatment on the quality of 'Fuyu' persimmons. Biosystems Engineering 100: 227-234.

Vadivambal R., D.S. Jayas and N.D.G. White. 2008. Mortality of stored-grain insects exposed to microwave energy. Transactions of the ASABE 51: 641-647.

Vadivambal, R., O.F. Deji, D.S. Jayas and N.D.G. White. 2010. Disinfestation of stored corn using microwave energy. Agriculture and Biology Journal of North America 1: 18-26.

Wang, S., S.L. Birla, J. Tang and J.D. Hansen. 2006b. Postharvest treatment to control codling moth in fresh apples using water assisted radio frequency heating. Postharvest Biology and Technology 40: 89-96.

Wang, S., J.N. Ikediala, J. Tang, J.D. Hansen, E. Mitcham, R. Mao and B. Swanson. 2001. Radio frequency treatments to control codling moth in in-shell walnuts. *Postharvest Biology and Technology* 22: 29-38.

Wang, S., A. Monzon, J.A. Johnson, E.J. Mitcham and J. Tang. 2007a. Industrial-scale radio frequency treatments for insect control in walnuts I: Heating uniformity and energy efficiency. *Postharvest Biology and Technology* 45: 240-246.

Wang, S., M. Monzon, J.A. Johnson, E.J. Mitcham and J. Tang. 2007b. Industrial-scale radio frequency treatments for insect control in walnuts II: Insect mortality and product quality. *Postharvest Biology and Technology* 45: 247-253.

Wang, S., J. Tang, J. Johnson, E. Mitcham, J. Hansen, G. Hallman, S. Drake and Y. Wang. 2003. Dielectric properties of fruits and insect pests as related to radio frequency and microwave treatments. *Biosystems Engineering* 85: 201–212.

Wang, S., J. Tang, J.A. Johnson, E. Mitcham, J.D. Hansen, R.P. Cavalieri, J. Bower and B. Biasi. 2002. Process protocols based on radio frequency energy to control field and storage pests in in-shell walnuts. *Postharvest Biology and Technology* 26: 265-273.

Wang, S., J. Tang, T. Sun, E.J. Mitcham, T. Koral and S.L. Birla. 2006a. Considerations in design of commercial radio frequency treatments for postharvest pest control in in-shell walnuts. *Journal of Food Engineering* 77: 304-312.

Wang, S., G. Tiwari, S. Jiao, J.A. Johnson and J. Tang. 2010. Developing postharvest disinfestation treatments for legumes using radio frequency energy. *Biosystems Engineering* 105: 341-349.

Wang, S., J. Yue, B. Chen and J. Tang. 2008. Treatment design of radio frequency heating based on insect control and product quality. *Postharvest Biology and Technology* 49: 417-423.

Wang, S., J. Yue, J. Tang and B. Chen. 2005. Mathematical modelling of heating uniformity for in-shell walnuts subjected to radio frequency treatments with intermittent stirrings. *Postharvest Biology and Technology* 35: 97-107.

Wang, Y., Y. Li, S. Wang, L. Zhang, M. Gao and J. Tang. 2011. Review of dielectric drying of foods and agricultural products. *International Journal of Agricultural and Biological Engineering* 4: 1 – 19.

CHAPTER 5

Heating rate and heating uniformity of bulk wheat grain with the designed parallel plate applicator for a pilot-scale 50-ohm RF heating system

To be submitted for journal publication.

Contribution of this chapter to the overall study

This chapter determined the heating rate and the temperature distribution of bulk wheat samples in the designed 50-ohm RF applicator at different RF power levels and wheat moisture contents (specific objective 7). All the experiments in this chapter were conducted and the journal paper manuscript was drafted by myself.

5.1 Abstract

Disinfestation of insects in host materials using a radio frequency (RF) heating system was proposed to be an alternative to traditional methods due to its fast, volumetric, and selective heating and being chemical free. However, non-uniform heating has been a challenge during conventional RF heating. Non-uniform heating

resulted in the migration of insects to the coldest spots and degrading the quality of the materials at the hottest spots. Therefore, this paper dealt with the assessment of heating uniformity of the bulk wheat grains at different moisture contents during 50-ohm RF heating at different RF power levels using a parallel plate applicator. The results showed that temperature distribution in the wheat grain in the applicator was not uniform at all moisture content and power levels. The coldest spot was found at the feed point where the matching network was connected, while the hottest spot was observed at the other end of the electrode. The temperature differences between the hottest and coldest spots at different MC and power levels (3 kW, 5 kW, and 7 kW) were 38.6°C, 38.7°C, and 39.1°C, respectively (12% MC) and 43°C, 43.6°C, and 41.9°C, respectively (18% MC). In addition, the temperature of the wheat grains decreased when increasing the distance from the hot electrodes due to the presence of air gaps in the samples. Thus, suggestions are given in this chapter to improve heating uniformity with the designed applicator for a successful disinfestation using a pilot-scale 50-ohm RF heating system, as a first step to industrialization.

5.2 Introduction

Radio frequency (RF) heating has been studied for years to replace the use of traditional chemical methods (fumigants and pesticides) for disinfestation. The use of chemicals has been banned and avoided because of its negative effect on the environment and the human body, whereas RF heating technology offers many advantages: fast and volumetric heating, and selective heating and its being chemical free. This technology has been applied in different applications such as post-baking of cookies and snack foods (Koral 2004), pasteurization of food and agricultural products

(Kim et al. 2012; Gao et al. 2011), thawing/tempering (Farag et al. 2011; 2010), drying (Wang et al. 2014; Lee et al. 2010), and disinfestation (Shrestha et al. 2013; Shrestha and Baik 2013; Lagunas-Solar et al. 2007; Wang et al. 2007a, 2007b; Wang et al. 2001). The principle of this method is similar to that of MW heating. However, RF heating is preferred in disinfestation over MW heating because of its higher penetration depth and stronger selective heating effect (Macana and Baik 2017; Shrestha et al. 2013; Wang et al. 2011, 2003; Guo et al. 2010; Nelson 1996). In general, RF heating has great potential in different applications due to its fast and non-chemical way of heating. Nevertheless, the potential of this technology has not yet been utilized in disinfestation for industrial applications due to its non-uniform heating properties. The non-uniform heating of the RF system creates hot spots and cold spots, resulting in greater chance of the insects surviving (Macana and Baik 2017). Two types of RF heating systems have been used in different applications: Conventional and 50-ohm RF. They offer many advantages over conventional heating and chemical methods. However, the 50-ohm RF heating system offers advantages than conventional RF heating (Macana and Baik 2017; Macana et al. 2018a, 2018b, 2018c; Jones and Rowley 1996) and no work on 50-ohm RF heating for disinfestation has been reported. The 50-ohm heating system is advantageous because of its locational flexibility. The applicator where the materials being heated can be separated from the RF generator. Thus, the applicator of the 50-ohm heating system can be designed and built to particular applications. In the conventional RF heating system, the applicator is attached to the generator, which makes it difficult to modify and relocate. The 50-ohm RF heating system has an automatic matching network (AMN), which gives maximum power transfer to the load.

The AMN balances the impedance of the load and ensures that the load receives maximum power from the RF generator. Lastly, the 50-ohm heating system has a stable frequency. This solved the problem with conventional RF heating, which has a lack of frequency stability causing the interference with other signals in communications and machines (Koral 2014). Therefore, the 50-ohm RF heating system has been studied to utilize its advantages and the potential of RF heating in different applications. Thus, this chapter deals with the assessment of heating uniformity of bulk samples using a designed parallel plate applicator in a pilot-scale 50-ohm RF heating system for the first time. This is the first step for industrialization of disinfestation using this technology. This includes the discussions of heating rate, heating time, temperature history, uniformity index, electric field strength, and temperature distribution at different locations in bulk grains in the applicator at different grain moisture contents and different power levels. In addition, suggestions are given to improve the heating uniformity of the applicator for successful disinfestation using the 50-ohm RF heating system.

5.3 Materials and methods

5.3.1 Wheat samples

Wheat samples, cv. Lillian at a moisture content of approximately 11% (w. b.) was provided by our partner industry, Viterra and stored in a cold room at 4°C. The initial and final moisture contents of the wheat were determined by drying 10 g of wheat grains for 19 h at 130°C using a standard hot air oven. The samples were weighed using an analytical scale. For adjusting the moisture content of the wheat samples to 12%, 15%, and 18% MC, the calculated amount of distilled water was added to achieve the desired

moisture content. The samples were contained in an airtight bin and placed at room temperature (24°C) for 3 days with regular mixing and tumbling. When the desired MC was achieved, the samples were then placed in polypropylene bags of 10 cm diameter and 70 cm length before RF heating. For every run of the experiment, seven bags of wheat were needed to conduct each temperature distribution measurement (Figure 5.1). Each bag weighed approximately 4.5 kg.



Figure 5.1. Wheat samples placed in the polypropylene bag before RF heating.

5.3.2 The 50-ohm RF heating system

The 50-ohm RF heating system is shown in Figure 5.2. The system has four main parts: RF generator, 50-ohm coaxial cable, automatic matching network, and applicator. The RF generator at 15 kW, 27.12 MHz was used in this study. It is the source of energy to heat the wheat samples. The applicator is the heart of the system, where the material

is heated. The AMN is the controller of the system, which ensures that the load received maximum power. The 50-ohm coaxial cable connects the AMN to the RF generator.

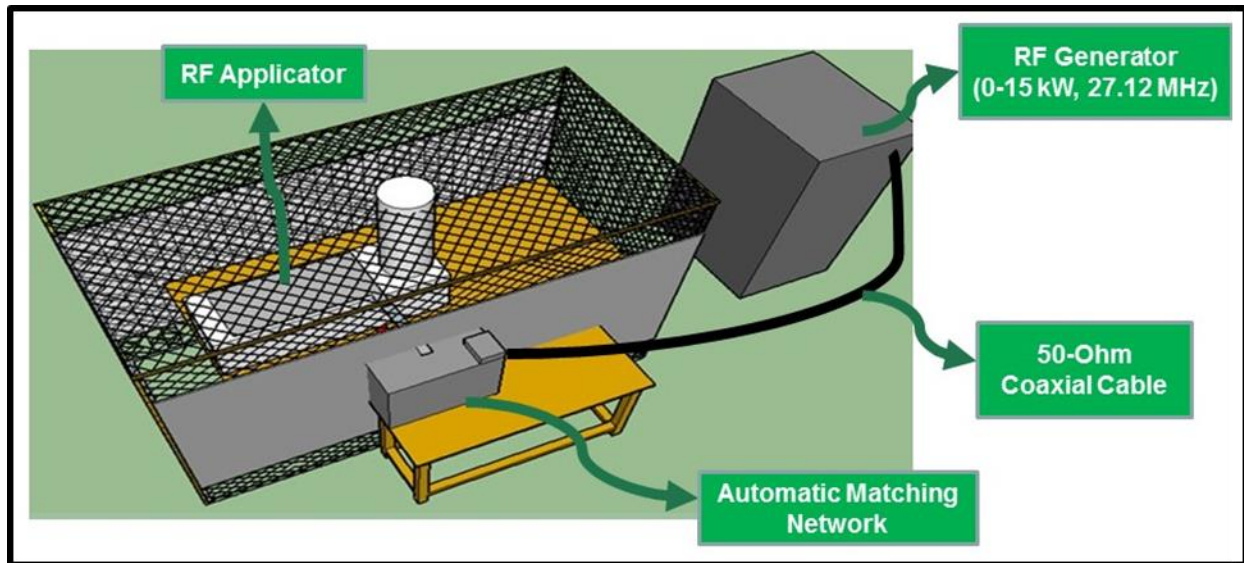


Figure 5.2. 50-ohm RF heating system (Macana et al. 2018e).

5.3.3 The RF applicator

The applicator (Figure 5.3) was made of two aluminum electrodes (length = 70 cm and width = 30 cm). The top electrode (grey colour) was the ground, while the bottom electrode (red colour) was the hot electrode. Between the electrodes was the polypropylene tubular channel where the seven bags of the wheat were heated. Polypropylene is considered an RF transparent material. The diameter of the channel was 30 cm, but the distance between the electrodes was 36 cm, which included the thickness (3 cm) of the channel for both the top and bottom electrode. The arrangement of the seven bags of wheat is shown inside the tubular channel.

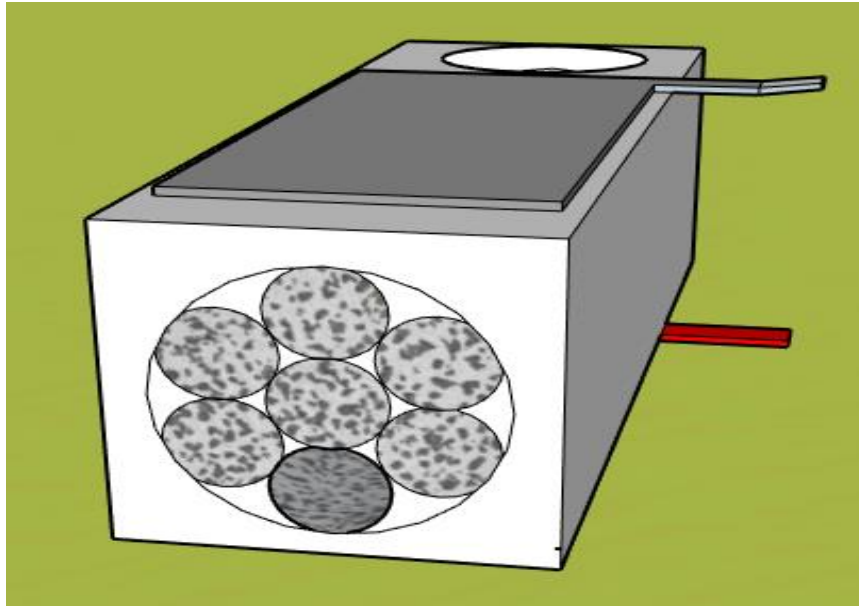


Figure 5.3. RF parallel plate applicator.

5.3.4 Temperature distribution measurement

For determination of temperature distribution, the applicator was divided into three sections (right, middle, and left). The right section is where the connector between the automatic matching network and the hot electrode (feed point) is located. The middle section was at the middle of the applicator, 35 cm away from the feed point. The left section was at the other end of the electrode as shown in Figure 5.4. To monitor the temperature, fiber optic temperature sensors with an accuracy of 0.8°C (Neoptix, Quebec City, QC, Canada) were used. Figure 5.5 shows the 21 points used for temperature monitoring. The total of 21 points was divided equally per section of the applicator. So, the seven points with their corresponding height from the hot electrode were: R1 (8 cm), R2 (13 cm), R3 (13 cm), R4 (18 cm), R5 (23 cm), R6 (23 cm), and R7

(28 cm) at the right section; M1 (8 cm), M2 (13 cm), M3 (13 cm), M4 (18 cm), M5 (23 cm), M6 (23 cm), and M7 (28 cm) at the middle section; and L1 (8 cm), L2 (13 cm), L3 (13 cm), L4 (18 cm), L5 (23 cm), L6 (23 cm), and L7 (28 cm) at the left section.

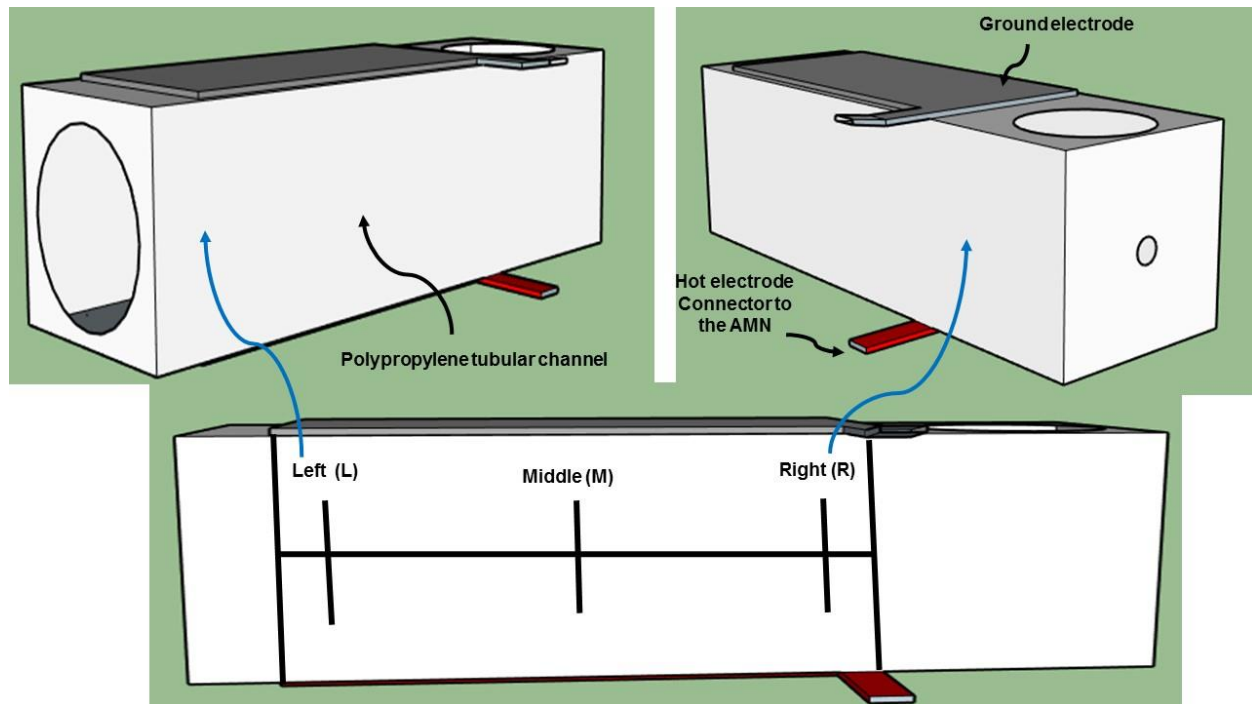


Figure 5.4. Three sections of the applicator for temperature distribution measurement.

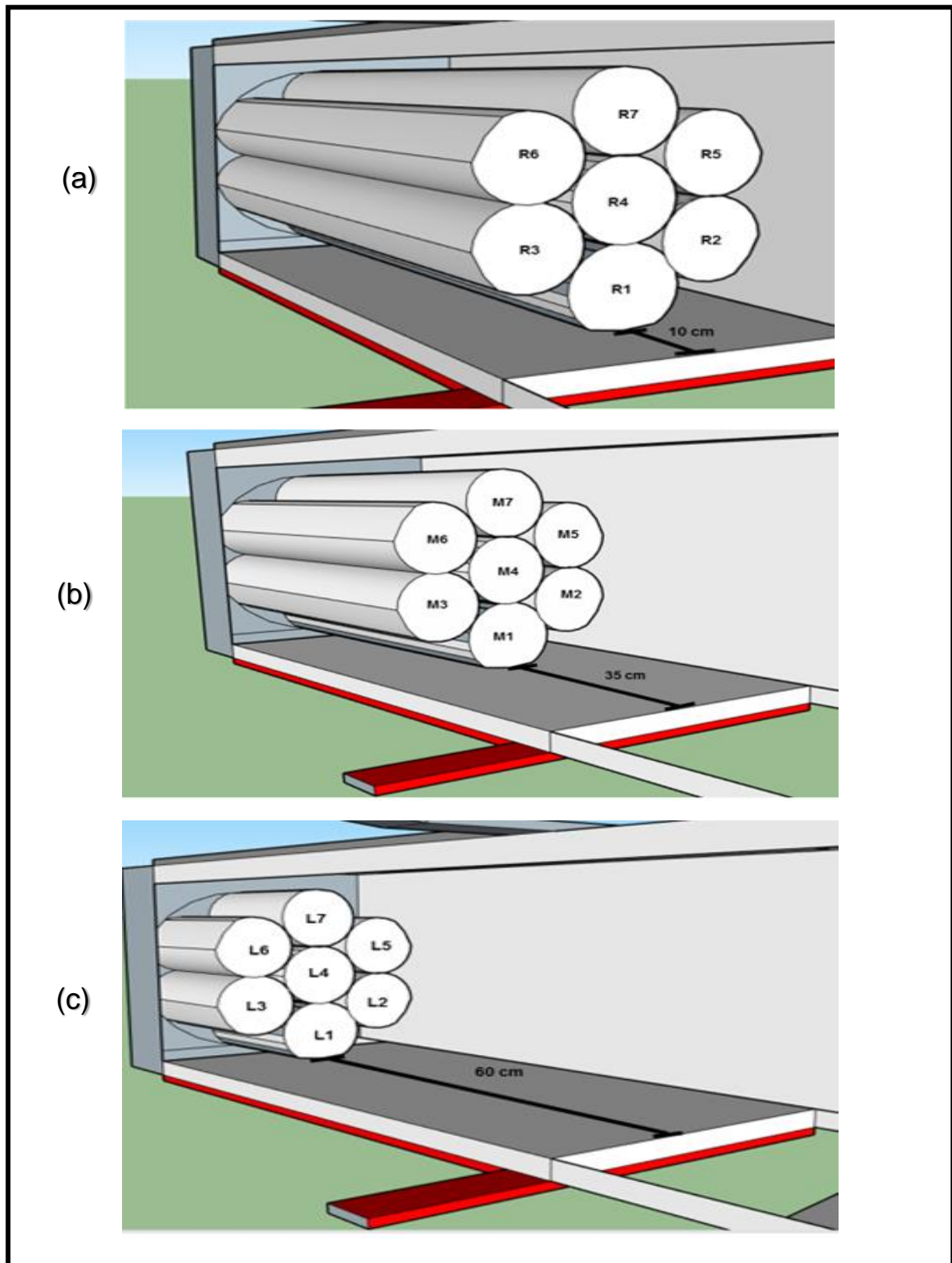


Figure 5.5. Three sections of the applicator with 21 points in total for temperature monitoring (a) Right (b) Middle (c) Left.

5.3.5 Heating uniformity index calculation

The heating uniformity index (λ) was calculated using the Equation (5.1). It is the ratio of the rise in the standard deviation of sample temperature to the rise in average sample temperature during RF heating. It is used for evaluating the uniformity of RF heating. The smaller the value of λ , the more uniform the RF heating of the sample. The equation was originally used by Wang et al. (2005) and later studies applied this for RF heating uniformity evaluation in a coffee bean (Pan et al. 2012), rice (Zhou and Wang 2016), and almond (Gao et al. 2010).

$$\lambda = \frac{\Delta\sigma}{\Delta\mu} = \frac{\sqrt{\sigma^2 \sigma_0^2}}{\mu^2 \mu_0^2} \quad (5.1)$$

Where μ_0 is the mean of the initial temperature distributions, μ is the mean of the final temperature distributions, σ_0 is the standard deviation of the initial temperature distribution, and σ is the standard deviations of the final temperature distributions.

5.3.6 Data Analysis

All experiments were done in triplicate. Excel (MSO 2016) was used to process and analyze data using analysis of variance (ANOVA) at a 95% confidence interval (p-value < 0.05), standard deviation, average, and linear regression.

5.4 Results and discussion

5.4.1 Heating time and the heating rate of wheat grains using a pilot-scale 50-ohm RF heating system

5.4.1.1 Under different moisture contents of the wheat sample

The effect of the moisture content of the wheat samples can be seen in Table 5.1. When the samples with 24°C initial temperature were treated at 7 kW to reach the target temperature of 80°C, the heating rate of the samples increased and RF heating time decreased when increasing the moisture content. At 12% to 18% MC, the heating rate increased from 9.49 °C/min to 12.17 °C/min, whereas the heating time decreased from 5.90 to 4.60 minutes. A similar trend was observed at 3 kW and 5 kW, when increasing the MC from 12% to 18%, the heating rate and RF heating time increased from 6.83 °C/min to 8.79 °C/min and decreased from 8.2 to 6.37 minutes, respectively for 5 kW, and increased from 6.83 °C/min to 8.79 °C/min and decreased from 8.2 to 6.37 minutes, respectively, for 5 kW.

Table 5.1. The heating rate and RF heating time at three MCs (12%, 15%, and 18%) at different power levels.

Power Level (kW)	Moisture Content (%, w.b.)	Heating rate (°C/min)	Heating Time (min)
7	12	9.49	5.90
	15	10.31	5.43
	18	12.17	4.60
5	12	6.83	8.2
	18	8.79	6.37
3	12	4.06	13.8
	18	4.83	11.6

Note: Heating time is the time (min) to reach the target temperature.

5.4.1.2 Under different power levels of the RF system

Table 5.2 shows a comparison of the heating rate and RF heating time of bulk wheat grain at three power levels (3 kW, 5 kW, and 7 kW) to achieve 85°C at the hottest spot of the applicator. At 12% MC, the values for the heating rate at the three power levels were 4.07 °C/min (3 kW), 6.91 °C/min (5 kW), and 9.64 °C/min (7 kW). The heating times to reach 85°C were 15 minutes (3 kW), 8.83 minutes (5 kW), and 6.33 minutes (7 kW). At 18% MC, the heating rate also increased and the RF heating decreased when the power level was increased. The heating rate (12.45 °C/min) at 7 kW was 2.53 times higher than at 3 kW, and the heating rate at 5 kW was 1.84 times higher than at the lower power. This means that at higher power, the samples heated faster due to its fast heating rate.

Table 5.2. Effect of power from the RF generator on the heating rate and heating time when the target temperature is 85°C and the sample initial temperature is 24 °C.

Moisture Content (%, w.b.)	Power Level (kW)	Heating rate (°C/min)	Heating Time (min)
12	3	4.07	15
	5	6.91	8.83
	7	9.64	6.33
18	3	4.92	12.4
	5	9.06	6.73
	7	12.45	4.9

5.4.2 Typical temperature histories of the bulk wheat samples at different MCs and power levels

The temperature history of the wheat samples is important for understanding the behaviour of the material during processing, depending on the type of equipment used. For example, using an RF heating system, the temperature profile is different compared

to conventional heating. RF heating is advantageous because of its volumetric heating. Radio frequency energy heats the inside and outside of the material at the same time, unlike with conventional heating where the surface of the material is heated first before the inside. Figure 5.6 shows the temperature histories of the wheat samples at three power levels and two MCs. The initial temperature of the bulk wheat samples was 24 °C. At 12% MC, the samples were heated for 380 seconds at 7 kW, 530 seconds at 5 kW, and 900 seconds at 3 kW to reach 85 °C. At 18% MC, the time required to reach the 85 °C was much lower. At different power levels (3 kW, 5 kW, and 7 kW), the heating times were 744 seconds, 404 seconds, and 296 seconds, respectively. In the figure, the temperature increased linearly at all moisture contents and power levels, with R^2 values ranging from 0.9916 to 0.9997. The linear model was in a good agreement with the polynomial model as shown in Table 5.3. The temperature profile was not at a constant temperature. Hence, Figure 5.7 shows the average temperature applied to the samples as functions of MC and power level. As the MC increased, the average temperature decreased at all power levels. The average temperatures ranged from 48.91-51.38 °C (7 kW), 48.25-51.41 °C (5 kW), and 49.2 – 51.74 °C (3 kW).

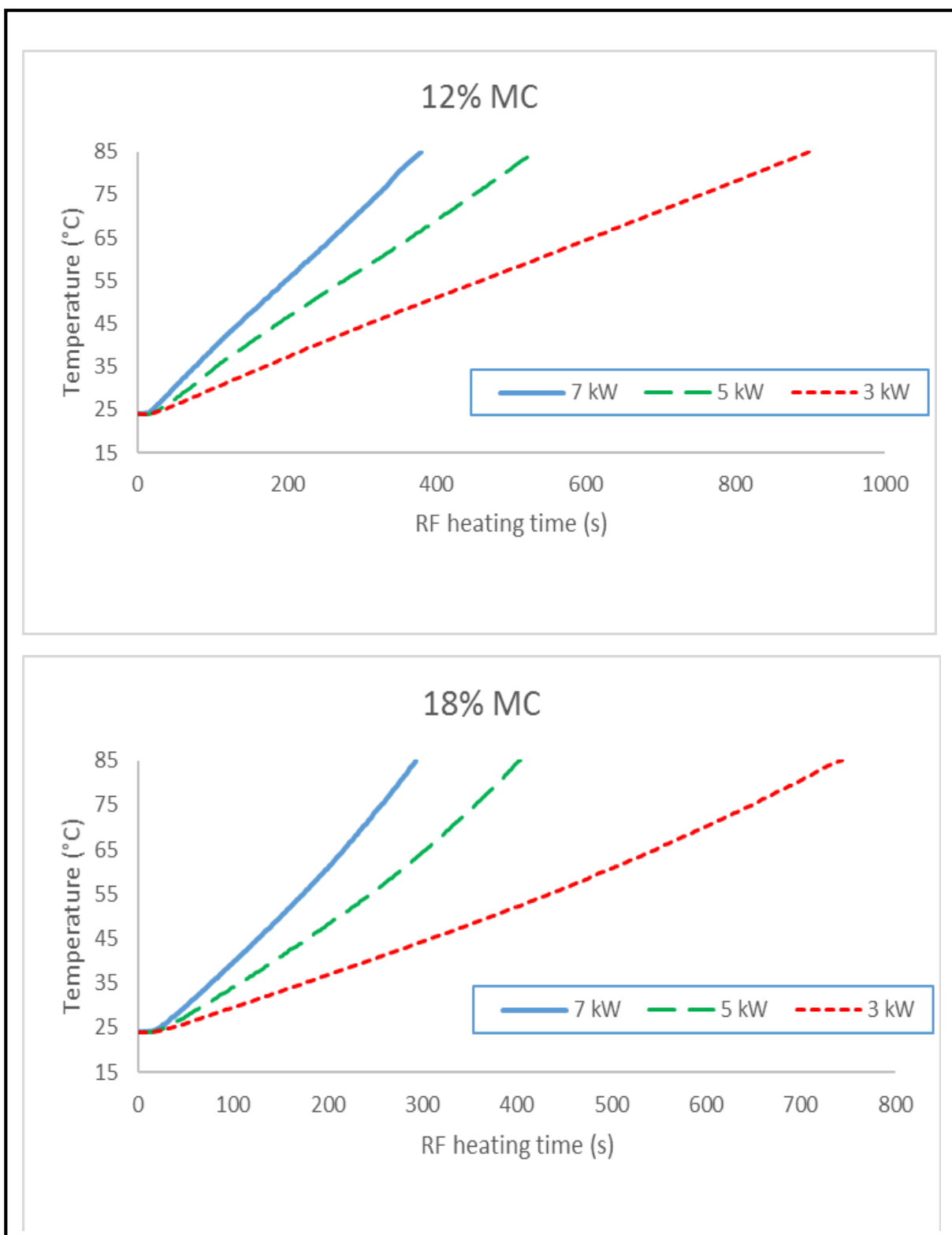


Figure 5.6. The temperature histories of wheat samples at 3 power levels (7 kW, 5 kW, and 3 kW) and 2 MCs (12% and 18%).

Table 5.3.The regression models for the temperature of the bulk wheat sample in the hottest spot as a function of RF heating time at different power levels.

Moisture Content (%w.b.)	Power (kW)	Regression model	R ²	Linear model	R ²
12	3	$T = -3E-06t^2 + 0.0713t + 22.918$	0.9998	$T = 0.0686t + 23.311$	0.9997
	5	$T = -7E-06t^2 + 0.1205t + 22.378$	0.9995	$T = 0.1167t + 22.716$	0.9994
	7	$T = 3E-06t^2 + 0.1635t + 22.434$	0.9996	$T = 0.1645t + 22.371$	0.9996
18	3	$T = 3E-05t^2 + 0.0601t + 23.423$	0.9998	$T = 0.0826t + 20.639$	0.9949
	5	$T = 0.0001t^2 + 0.0997t + 22.764$	0.9997	$T = 0.1533t + 19.174$	0.9916
	7	$T = 0.0002t^2 + 0.153t + 21.951$	0.9996	$T = 0.2143t + 18.968$	0.9941

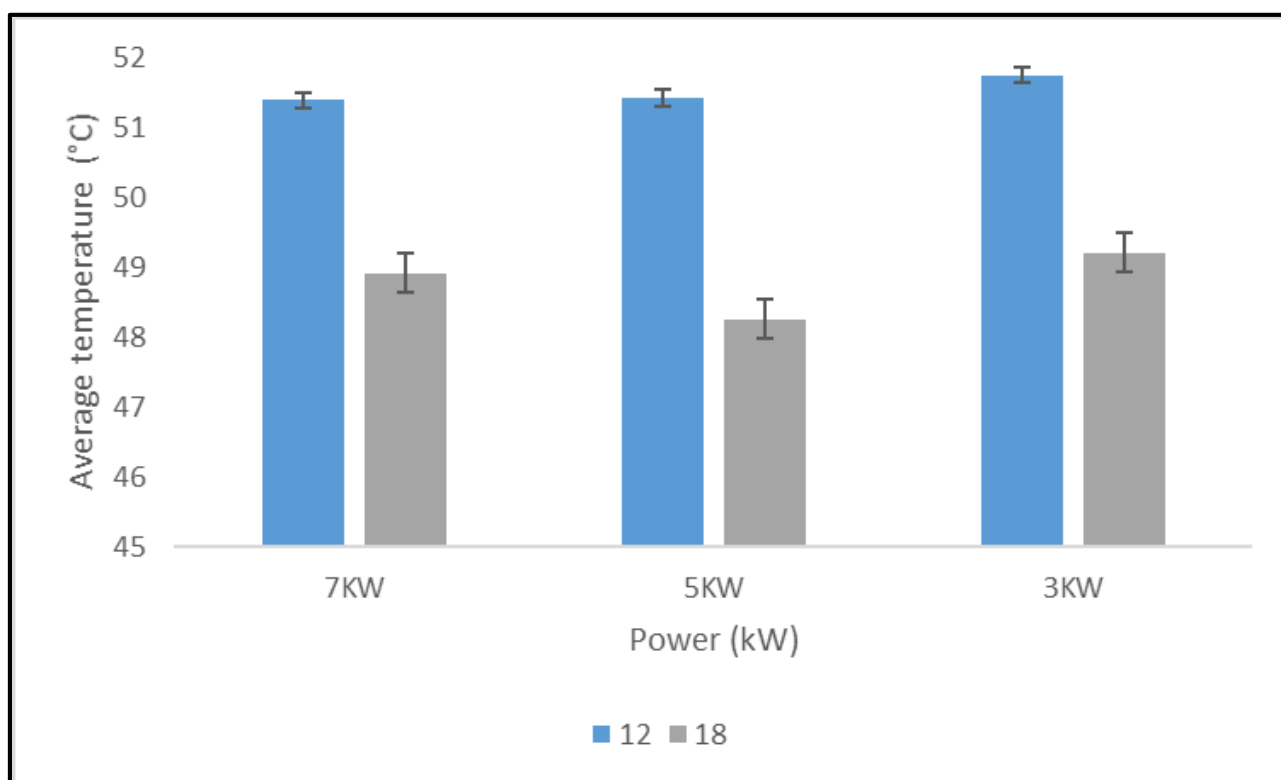


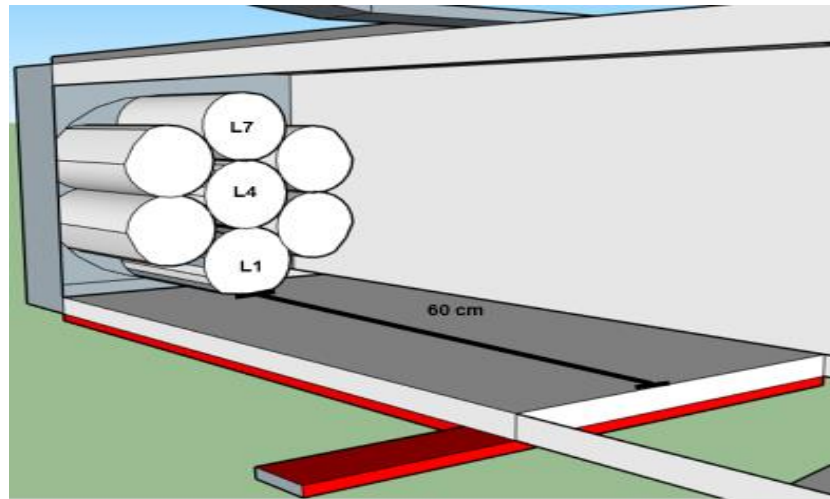
Figure 5.7. The average temperature at different power levels and 2 MCs on the temperature histories of wheat samples.

5.4.3 Temperature distribution in the parallel plate applicator of the 50-ohm RF heating system

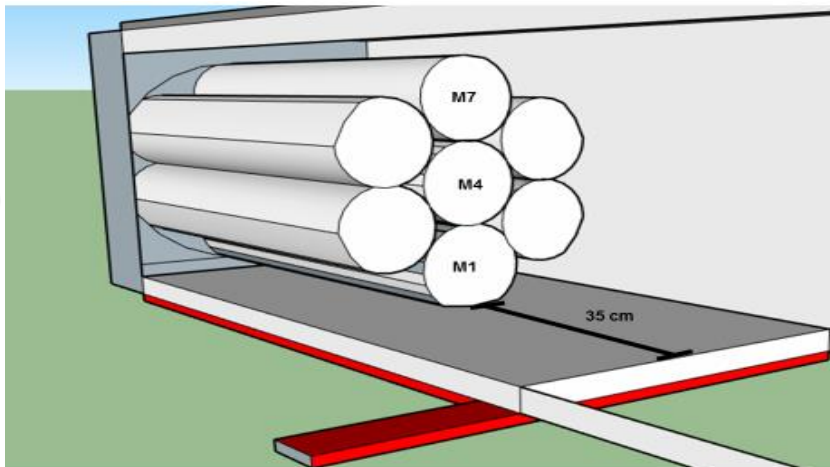
5.4.3.1 Vertical distribution of temperature of bulk wheat samples and its temperature histories at different heights from the bottom of the applicator

The location of the different measurement points for the vertical distribution of temperature assessment is visualized in Figure 5.8. In the figure, the three bags (1, 4, and 7) at the center of the applicator were divided into three sections (left, middle, and right). Each section had three points: L1, L4, and L7 (Left), M1, M4, and M7 (Middle), and R1, R4, and R7 (Right). The Fiber optic temperature sensor was placed at the centre of the bag. Therefore, the distance of bag 1 from the bottom electrode (Hot) was 8 cm and the distances for bag 4 and 7 were 18 cm and 28 cm, respectively. Figures 5.9 and 5.10 show the temperature histories of the bulk wheat samples at 12% and 18% MC. The samples were heated at 7 kW RF power and stopped when the hottest point reached 80 °C. Table 5.4 shows the vertical distribution of temperature. At all moisture contents, increasing the distance from the hot electrode decreased the temperature of the sample. This happened at all sections of the applicator. For example, at 12% MC, the temperature distribution at different sections of the applicator were: R1 = 65.3 °C, R4 = 49.2 °C, and R7 = 48.3 (Right); M1 = 69.1 °C, M4 = 52.9 °C, and M7 = 48.7 °C (Middle); and L1 = 80 °C, L4 = 57.6 °C, and L7 = 49.5 °C (Left).

(a)



(b)



(c)

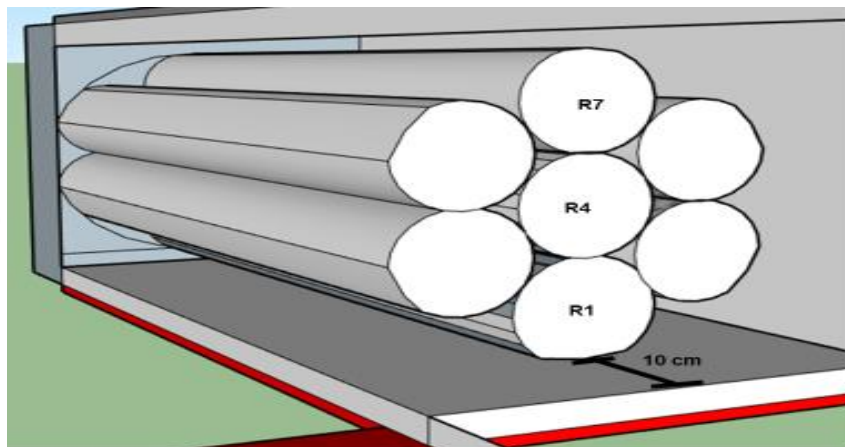


Figure 5.8. Visual presentation of measurement points of vertical distribution of temperature at different sections of the applicator: (a) Left, (b) Middle, and (c) Right.

Table 5.4. The vertical temperature distribution of bulk wheat samples at two power levels (12% and 18%) at 7 kW.

Location	Height (cm)	Temperature (°C)	Location	Height (cm)	Temperature (°C)
12% MC			18% MC		
Right section			Right section		
R1	5	65.26	R1	5	66.1
R4	15	49.23	R4	15	42.3
R7	25	48.33	R7	25	42.23
Middle section			Middle section		
M1	5	69.07	M1	5	62.3
M4	15	52.93	M4	15	47.1
M7	25	48.7	M7	25	42.36
Left section			Left section		
L1	5	80	L1	5	80
L4	15	57.67	L4	15	49.6
L7	25	49.47	L7	25	47.83

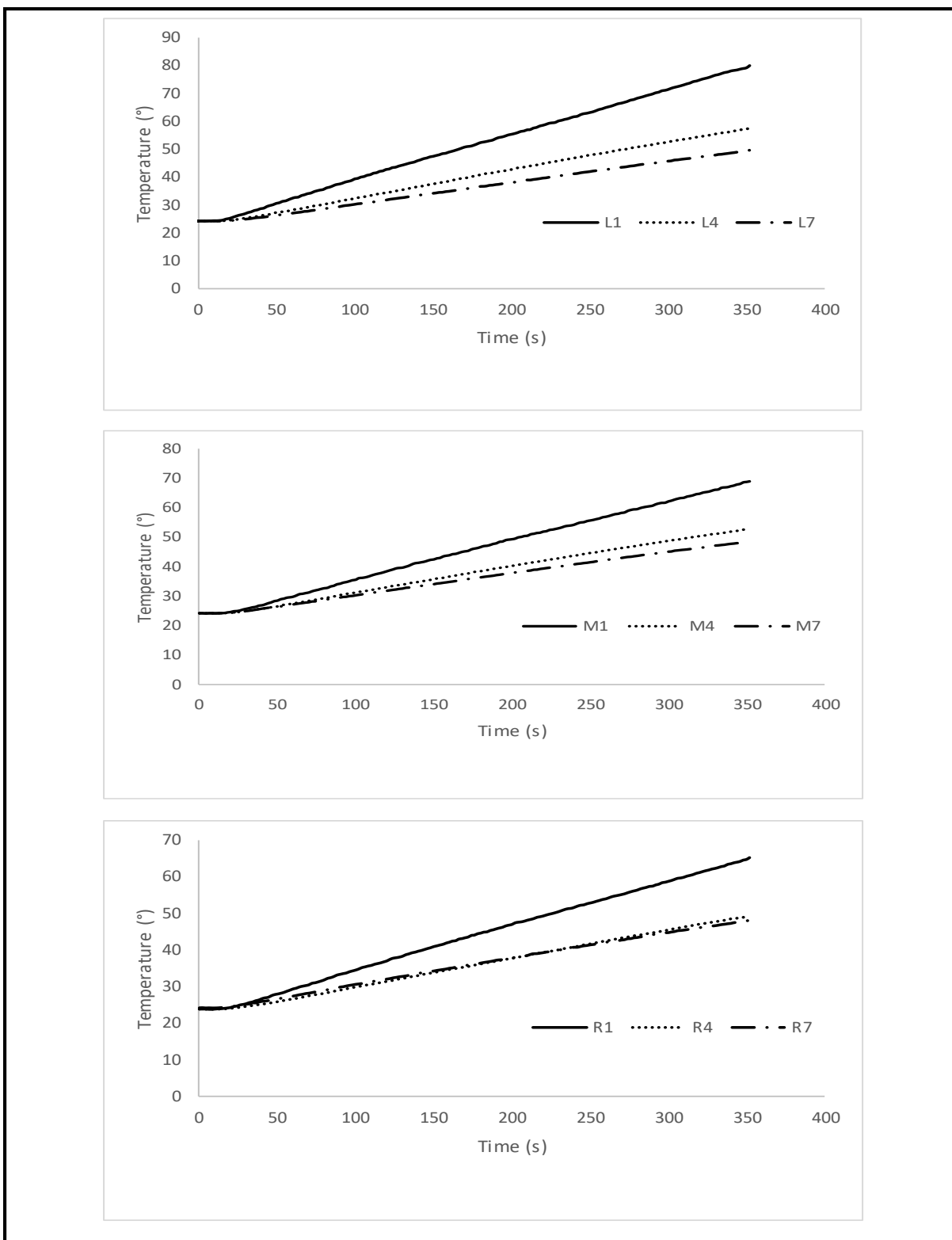


Figure 5.9. Effect of height from the hot electrode on temperature profile at 12% MC of wheat sample.

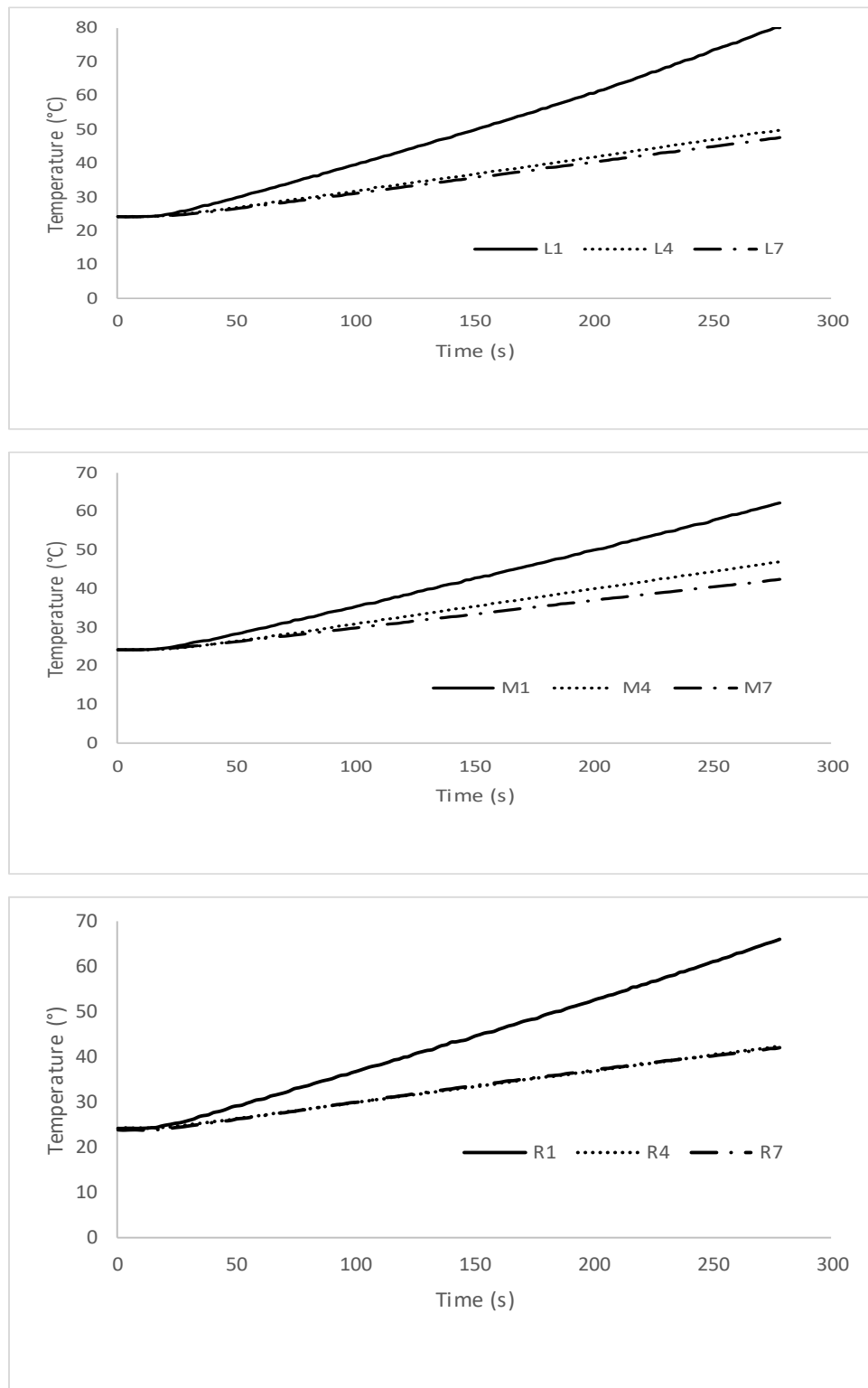


Figure 5.10. Effect of height from the hot electrode on temperature profile at 18% MC of wheat sample.

5.4.3.2 Horizontal distribution of temperature of bulk wheat samples in the applicator and its temperature histories

The assessment of horizontal temperature distribution was made using three bags (1, 4, and 7), which were chosen earlier for assessment of vertical temperature distribution. The difference was that each bag had three points for temperature monitoring. Table 5.5 shows the horizontal distribution of temperature of bulk wheat samples treated with 7 kW RF energy at two moisture contents. At 12% MC, the temperature of the sample increased when increasing the distance from the point where the AMN was connected to the electrode. Going closer to that point decreased the temperature of the sample. The heating rate was lower in the right section of the applicator compared to that in the left section. It is also important to note that the right section, at the end of the electrode, was covered by polypropylene and the other end was an open tube. Based on the results and Figure 5.11, in most cases the heating rate was lower in the right section of the applicator. This was attributed to the higher electric field strength at the corners and edges of the electrodes.

Table 5.5. Temperature distribution at the horizontal of bulk wheat samples treated at 7 kW and 2 moisture content levels (12% and 18%.

Location	Distance (cm)	Temperature (°C)	Location	Distance (cm)	Temperature (°C)
12% MC			18% MC		
Bag 1			Bag 1		
L1	10	80	L1	10	80
M1	35	69.07	M1	35	62.3
R1	60	65.26	R1	60	66.1
Bag 4			Bag 4		
L4	10	57.63	L4	10	49.6
M4	35	52.93	M4	35	47.1
R4	60	49.23	R4	60	42.3
Bag 7			Bag 7		
L7	10	49.47	L7	10	47.83
M7	35	48.7	M7	35	42.36
R7	60	48.33	R7	60	42.23

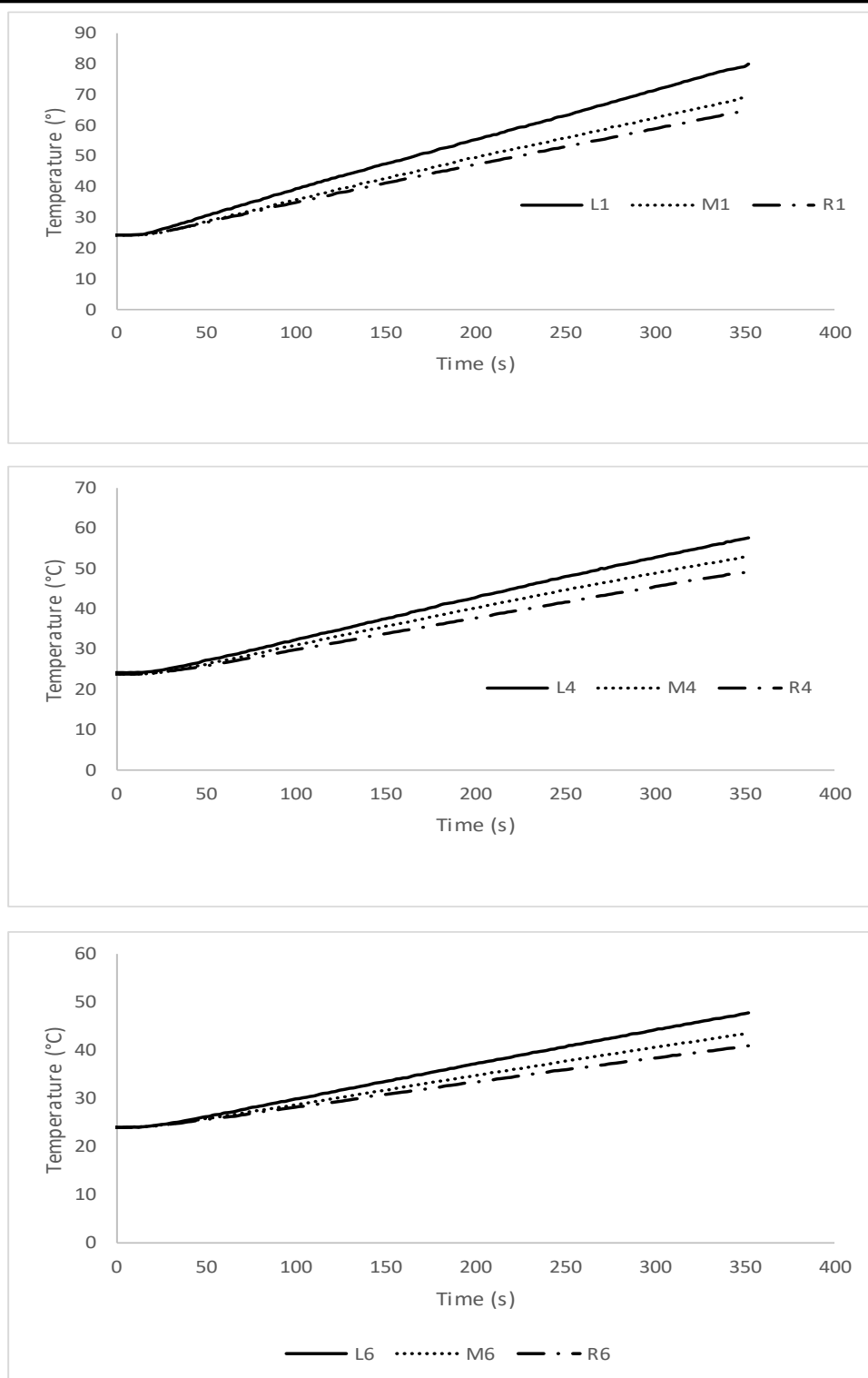


Figure 5.11. Effect of horizontal distance from the feed point on the temperature profile at 12% MC of the wheat samples at 7 kW.

5.4.3.3 Effect of distance from the wall on the temperature distribution of the bulk wheat samples

The wall of the applicator was a tubular channel (30 cm in diameter), which is made of polypropylene. Shrestha et al. (2013) reported that there was a lower temperature close to the wall of the container compared to the centre of the holder. Similar results have been reported for many studies. Table 5.6 shows the temperature distribution of the samples as a function of the distance from the wall (wall distance). The results agreed with the reports that being closer to the wall decreased the temperature of the sample. This was because of heat losses from the outer surfaces of the tubular channel.

Table 5.6. Temperature distribution as a function of distance from the wall of the tubular channel at 7 kW and 12% MC of the wheat samples.

Applicator section	Height	Location	Wall distance	Temperature (°C)	Heating rate (°C/min)
Right	10 cm	R2	5 cm	47.93	4.08
		R2.5	15 cm	57.245	5.66
		R3	5 cm	51.1	4.62
	20 cm	R5	5 cm	40.9	2.88
		R5.5	15 cm	48.78	4.22
		R6	5 cm	42.06	3.08
Middle	10 cm	M2	5 cm	51.63	4.71
		M2.5	15 cm	61	6.30
		M3	5 cm	51.06	4.61
	20 cm	M5	5 cm	43.7	3.36
		M5.5	15 cm	50.815	4.57
		M6	5 cm	45.1	3.59
Left	10 cm	L2	5 cm	54	5.11
		L2.5	15 cm	68.815	7.63
		L3	5 cm	56.4	5.52
	20 cm	L5	5 cm	47.83	4.06
		L5.5	15 cm	53.55	5.03
		L6	5 cm	48.06	4.10

5.4.4 Heating uniformity of the applicator

Heating uniformity is important in RF heating systems. It is known that heating using RF energy is more uniform than MW energy because of its higher penetration depth. However, non-uniform heating still has been a problem with RF heating systems. It was reported with conventional type of RF heating system that non-uniform heating of the samples existed. Shrestha et al. (2013) used a conventional RF heating system for disinfestation and reported the presence of non-uniform heating. The 50-ohm RF heating system is a more advanced type of RF technology. It was reported that the latter type of RF heating system was more advantageous than the former because of the flexibility to design the applicator based on the desired application. The 50-ohm RF heating was applied to disinfestation for the first time with the current study. The problem of extremely non-uniform heating by the applicator should be avoided in disinfestation. Insect pests are able to migrate to the colder spots if non-uniform heating exists. Therefore, proper assessment of the heating uniformity of the applicator should be done, and suggestions should be provided for the improvement of RF heating uniformity for successful disinfestation.

5.4.4.1 Temperature distribution of bulk wheat samples in the applicator

Figures 5.12 and 5.13 are visual presentations of the distribution of temperature in bulk wheat samples at 7 kW and two moisture contents (12% and 18%). At all moisture contents and power levels, the hottest spot was found at the 1st bag in the left section of the applicator, which was 5 cm above the hot electrode and 60 cm away from the end

where the AMN and the hot electrode connected. The coldest spot was found in the 6th bag at the right section of the applicator, 25 cm away from the hot electrode.

The effects of power and moisture content on the hottest and coldest spots in the applicator are shown in Table 5.7. At 12% MC, increasing the power level, decreased (not significantly) the coldest spot temperature of the sample ($p = 0.78$). For example, in heating the wheat samples with 12% MC at 3 kW and stopping when 80°C at the hottest spot was reached, the coldest temperature was 41.33°C. When increasing the level of power to 5 kW and 7 kW, the coldest spot temperatures were 41.26°C and 40.9°C, respectively. However, again the difference was not significant. Similarly at 18% MC, the coldest spot temperature was not affected significantly when changing the power level from 3 kW to 7 kW ($p = 0.58$). The temperature of the coldest spot inside the applicator changed slightly from 0.6°C to 1.73°C. On the other hand, moisture content had a significant effect on the temperature of the coldest spot ($p \leq 0.01$).

Table 5.7. The temperature difference between the hottest and coldest spot in the designed applicator for 50-ohm RF heating system at different power levels and 2 MCs (12% and 18%).

Moisture content (%, w.b.)	Power level (kW)	Hottest temperature (°C)	Coldest temperature (°C)	Temperature difference
12	3	80	41.33	38.67
	5	80	41.26	38.74
	7	80	40.9	39.1
18	3	80	37.0	43
	5	80	36.4	43.6
	7	80	38.13	41.87

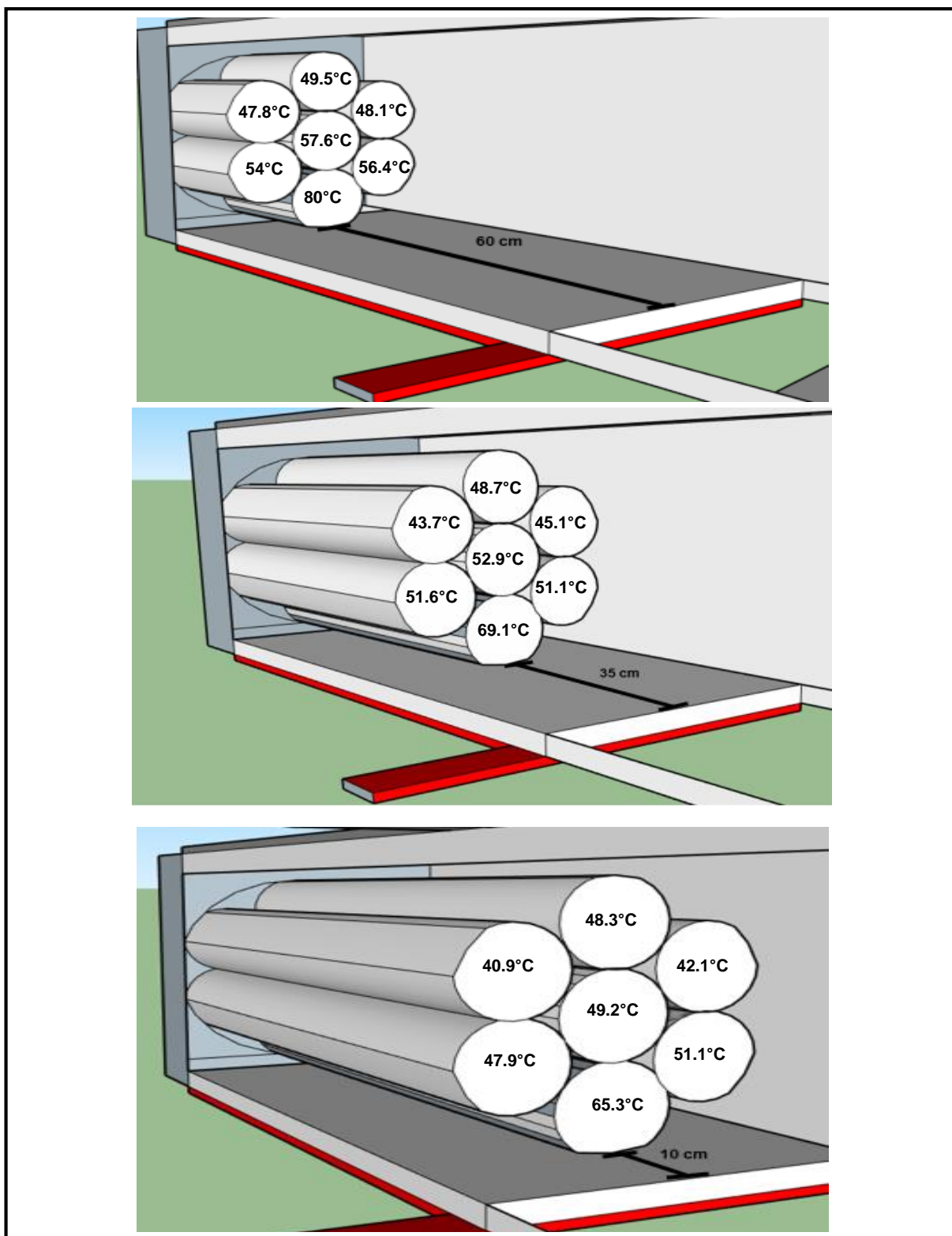


Figure 5.12. Temperature distribution of bulk wheat samples in the RF applicator at 7 kW and 12% MC.

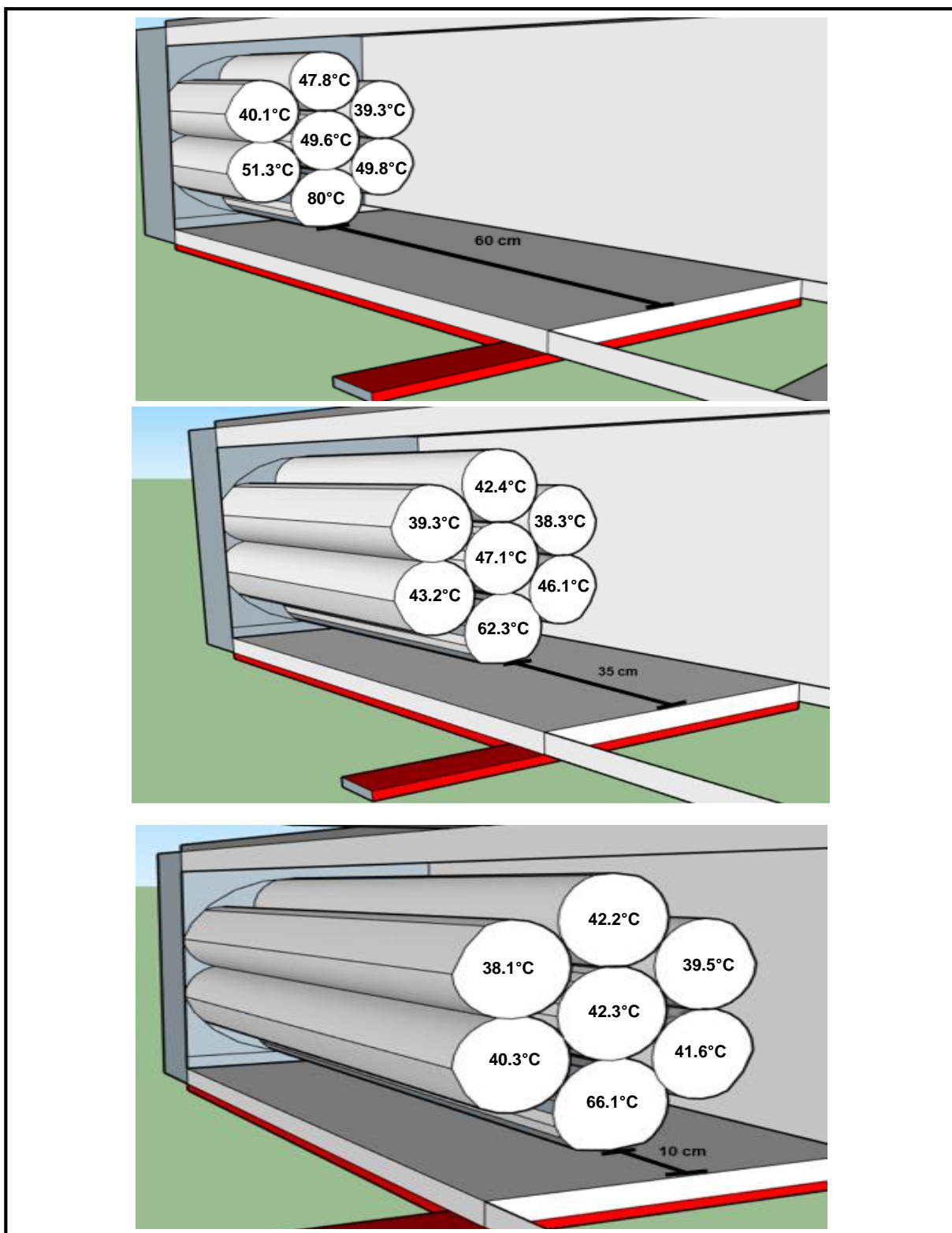


Figure 5.13. Temperature distribution of bulk wheat samples in the RF applicator at 7 kW and 18% MC.

5.4.4.2 Uniformity index values

The uniformity index (UI) is one way to assess the heating uniformity of an RF heating system. The lower the UI, the more uniform the RF heating. Table 5.8 shows the heating uniformity of the applicator at 7 kW and two moisture contents. At 12% MC, the UI of the right and middle sections of the applicator were very close, 0.29 and 0.28. The difference between their standard deviations and average temperatures were just 0.35°C and 2.48°C, respectively. The overall uniformity index of the applicator at 12% MC was 0.32, which was lower than the uniformity index at 18% MC. This means that RF heating was more uniform at lower moisture.

Table 5.8. Heating uniformity of the designed applicator for 50-ohm RF heating system at 7 kW and two MCs (12% and 18%).

Moisture Content (% w.b.)	Applicator's section	Standard Deviation	Average Temperature (°C)	Uniformity Index (UI)	UI in the entire applicator
12	Right	7.40	49.26	0.29	0.32
	Middle	7.75	51.74	0.28	
	Left	10.39	56.20	0.32	
18	Right	9.01	44.31	0.44	0.45
	Middle	7.47	45.53	0.35	
	Left	12.60	51.12	0.46	

5.4.4.3 Electric field strength assessment in relation to heating uniformity

According to Huang et al. (2018), many factors affect the heating uniformity of the applicator. These factors include the design of the RF applicator (electrode shape and configuration, the position of the inductance and feeding strips, materials of the

applicator, and air gap), dielectric properties, material size and position, thermal properties, etc. There are several interacting factors that can influence heating uniformity, but the major factor is the distribution of the electromagnetic field during RF heating of the samples (Huang et al. 2016a, 2016b; Wang et al. 2007a). The higher the electric field intensity, the higher the heating rate (Shrestha et al. 2013; Shrestha and Baik 2013). Thus, the higher power dissipation on the material, the higher the increase in temperature. Huang et al. (2018) reported the behaviour of the electric field between the parallel plate electrodes (Figure 5.14). When there was no sample present between the two electrodes (hot and ground), the electric field strength was uniform. When alternating charges (+,-) at the top electrode (hot electrode) were present, the opposite electrode at the bottom generates opposite alternating charges. Therefore, there was an attraction of charges called the electric field. In the figure, when there was no sample, the electric field was free to go to the less resistance region (conductor). However, when there was a sample placed at the bottom electrode with an air gap at the top electrode, the electric field strength was not uniform. The presence of air in the applicator is not desirable in RF heating. Air is an insulator and it has more resistance and fewer charges present. Thus, the electric field is trying to avoid the air and go to the dielectric materials or to a conductor electrode. So, the electric field coming from the corners and edges of the electrodes moves to the closer materials with more charges (dielectric or conductive materials). As seen in the figure, the closest part of the sample was the top corners and edges, resulting in an intensification of the electric field there and non-uniform heating occurred. Nonetheless, when the sample was placed at the centre of the applicator with an equal gap from the top and bottom electrodes, the electric field from the corners and

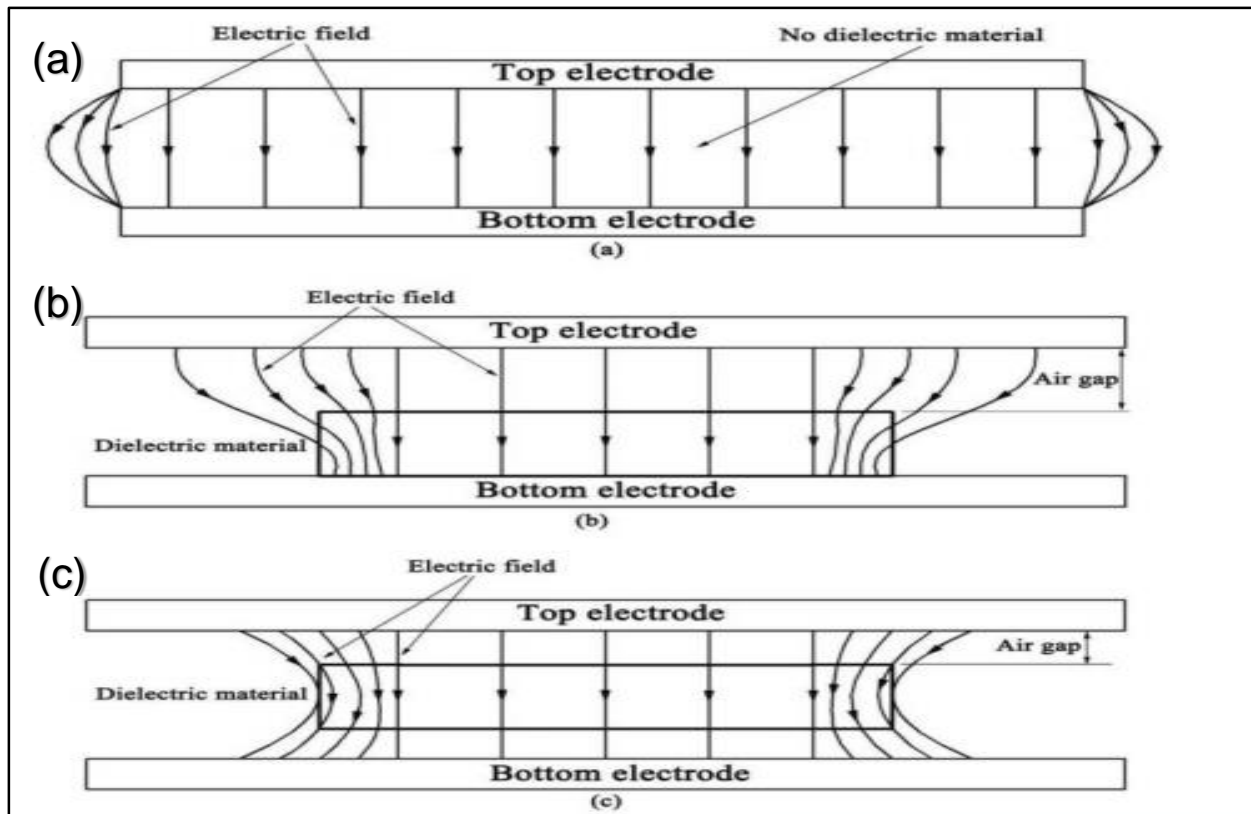


Figure 5.14. The intensity of the electric field between the parallel plate electrodes in the applicator (a) no sample, (b) sample was placed at the bottom (ground electrode), (c) sample was placed at the center of the applicator (Huang et al., 2018).

edges of the electrode was moving equally, going to the closest part of the dielectric materials. However, when the electrode size was smaller than the sample, there was less uniformity of heating compared to when the sample size was equal to that of electrodes. Llave et al. (2015) reported that when the size of the electrode was larger than the sample, the electric field intensity was higher in the corner of the sample closest to the electrodes. This was attributed to the intensification of the electric field from the edges and corners of the electrodes going to the samples. Using electrodes smaller than the sample, irregular temperature distribution was observed (Llave et al. 2015). However, when the electrodes were of same size as the sample material, there was a

more uniform distribution of temperature (Llave et al. 2014). Nonetheless, the higher electric field strength at both corners and edges of the sample was still present.

Figure 5.15 shows the locations of the hottest and coldest spots in the applicator for a pilot-scale 50-ohm RF heating system. The hot electrode was placed at the bottom of the applicator and the ground electrode was put at the top for easier connection to the automatic matching network (AMN). In most cases, the hot electrode is positioned at the top of the sample in a conventional RF heating system. In the figure, the location of the hottest spot in the applicator can be seen in the left section of the applicator. At the same time, the location with the lowest temperature (coldest spot) was present. The coldest spot was located in the right section of the applicator. The left section of the applicator where the tubular channel is open is shown in Figure 15a. In the right section of the applicator (Figure 15b), the channel was covered by a polypropylene material. It can be seen that the feed point was located at where the coldest spot was found. The location of the connection (feed point) of the hot electrode and AMN or the supplier of RF energy matters in dielectric heating. At higher frequency, the distribution of voltage in the hot electrode area works as a cosine function. It is up and down the value of voltage from the feed point to the end, dependent on the length of the electrode (Wilson 1987). The voltage values at the feed point were lower than at the other end. This was attributed to a voltage drop after the inductor. This means that lower electric field strength at the feed point compared to the other end of the electrode. Therefore, the results confirmed the lower heating rate in the left section of the applicator. Figures 5.16 and 5.17 show the comparison of temperatures at the different sections of the applicator. It can be seen that the temperatures at all points of the left section and the middle section

of the applicator indicated more uniform temperature distribution going horizontally at all moisture contents, compared to the temperatures from the middle to the right section. At 35 cm from the feed point, the temperature distribution was uniform. This suggests that putting the connection of the AMN at the middle of the electrode improves the temperature distribution in the horizontal direction. The problem of the non-uniform vertical temperature distribution was caused by an air gap between the samples. Bag 1 had the highest temperature at all sections of the applicator because the bag had no air gap against the hot electrode. In contrast, with the other bags, a space for air existed.

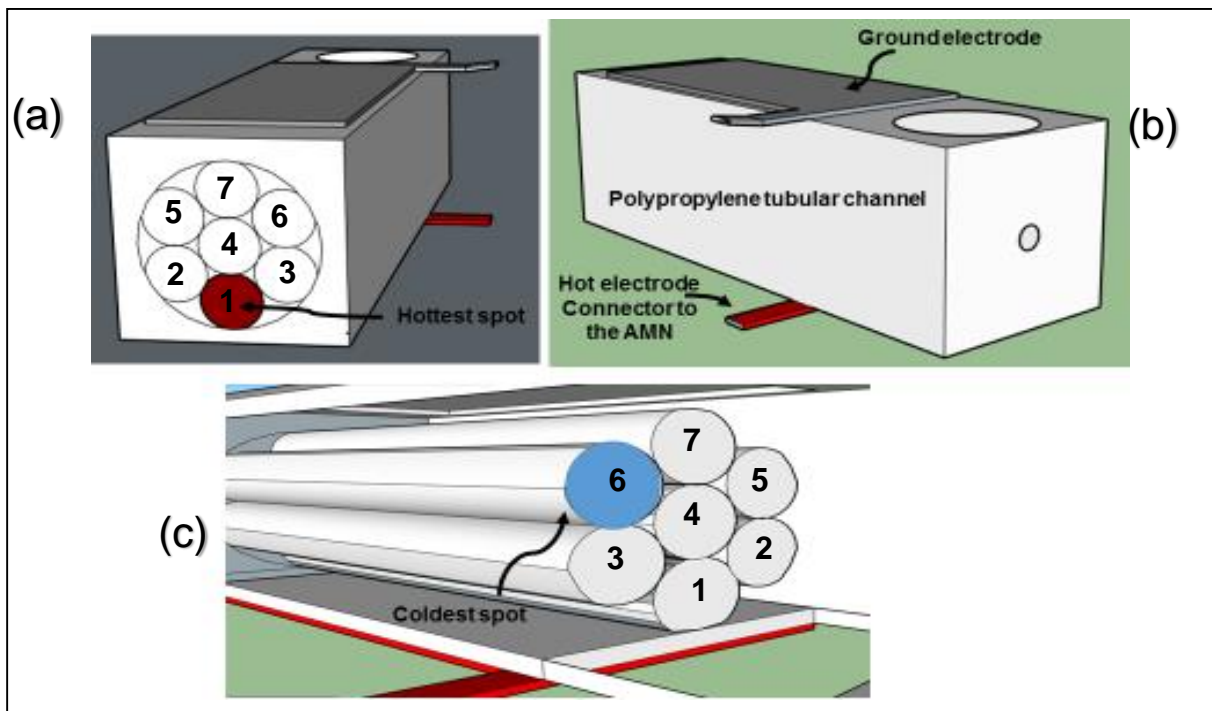


Figure 5.15. Visual presentation of the location the hottest and coldest spot of the applicator: (a) Hottest spot location at the right section of the applicator (b) View of the left section of the applicator outside the tubular channel (c) Inside look of the tubular channel pointing the coldest spot at the left section of the applicator.

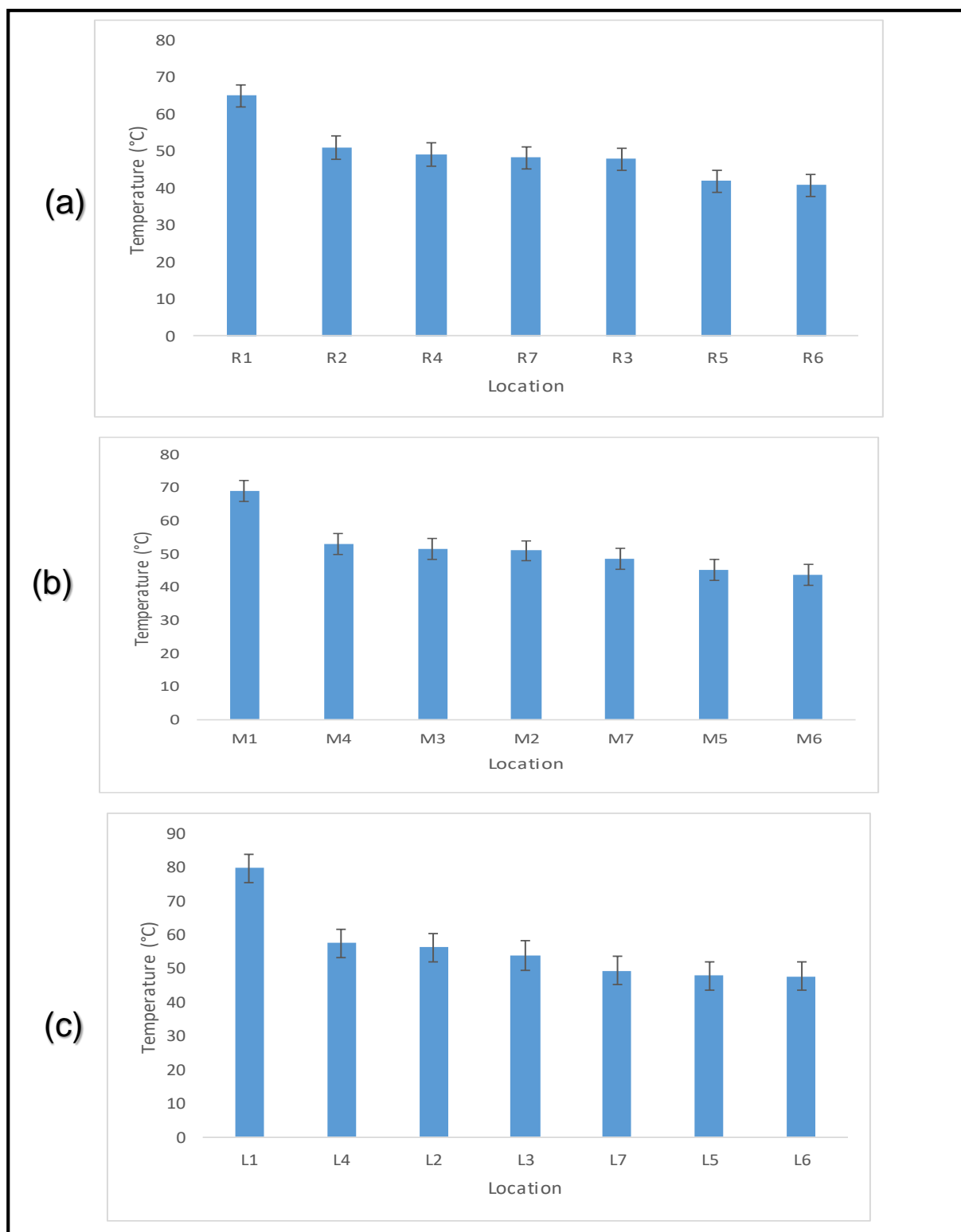


Figure 5.16. Temperature distribution of wheat samples at 12% MC treated at 7 kW RF power in the applicator: (a) Right (b) Middle (c) Left.

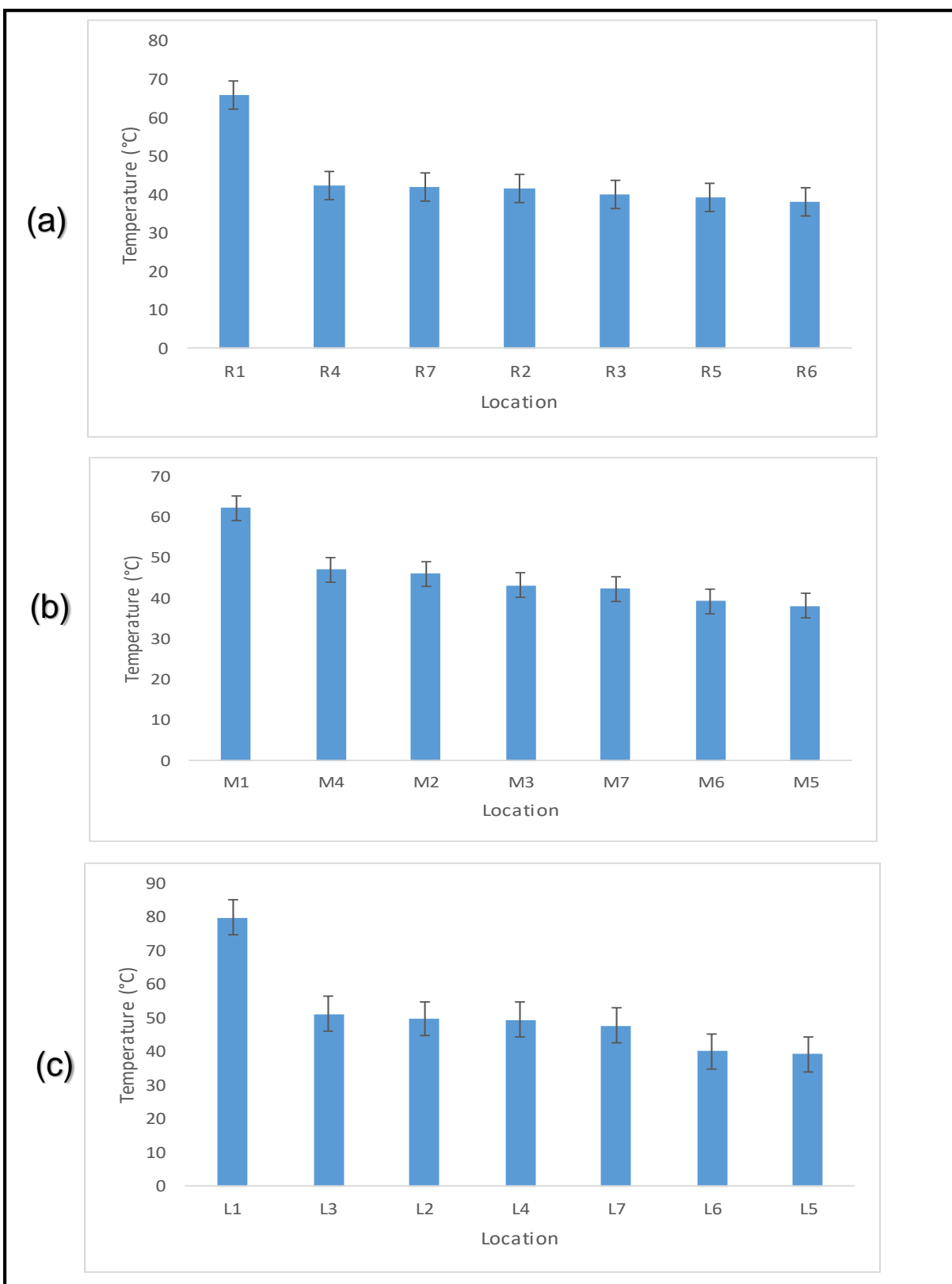


Figure 5.17. Temperature distribution of wheat samples at 18% MC treated at 7 kW RF power in the applicator: (a) Right (b) Middle (c) Left.

5.5 Conclusions and recommendations

The heating rate of the bulk wheat samples using a 50-ohm RF heating system increased when increasing the power and moisture content. The temperature histories of wheat samples at all moisture content and power levels were linear with R^2 ranging from 0.9916 to 0.9997. The temperature distribution of the applicator was observed vertically, horizontally, and at a distance from the wall. The temperature increased in the horizontal direction; the lowest temperature was found at the feed point and the highest at the other end of the electrode. For the vertical temperature distribution, the temperature decreased when increasing the distance from the hot electrode and increasing the air gap. The hottest spot was found in the left section in the applicator and the coldest spot was observed at the top of the feed point location. The effect of power and moisture content on the hottest and coldest spot difference in the applicator also was observed. At all moisture content, the difference between the hottest and coldest spot was not significantly affected by power level. However, it was significantly affected by moisture content. Nonetheless, the non-uniform temperature distribution was caused by the behaviour of electromagnetic energy as a function of the position of the feed point and the presence of an air gap in the sample. Therefore, in improving the heating uniformity in batch and continuous processes, it is suggested the connection between the AMN and hot electrode (feed point) should be placed at the middle of the electrode (35 cm) because the horizontal distribution of the temperature was more uniform from the feed point to 35 cm away. Other suggestions to overcome the non-uniform vertical temperature distribution: the polypropylene tubular channel could be placed vertically to load the samples easily (no bags) with the help of gravity, which

would avoid the presence of an air gap in the materials. Lastly, mixing or rotating the materials during RF heating would be expected to improve heating uniformity.

5.6 References

Farag, K. W., F. Marra, J.G. Lyng, D.J. Morgan and D.A. Cronin. 2010. Temperature changes and power consumption during radio frequency tempering of beef lean/fat formulations. *Food Bioprocess Technology* 3(5): 732-740.

Farag, K., J. Lyng, D. Morgan and D. Cronin. 2011. A comparison of conventional and radio frequency thawing of beef meats: Effects on product temperature distribution. *Food Bioprocess Technology* 4(7): 1128-1136.

Gao, M., J. Tang, R. Villa-Rojas, Y. Wang and S. Wang. 2011. Pasteurization process development for controlling salmonella in in-shell almonds using radio frequency energy. *Journal of Food Engineering* 104(2): 299-306.

Gao, M., J. Tang, Y. Wang, J. Powers and S. Wang. 2010. Almond quality as influenced by radio frequency heat treatments for disinfestation. *Postharvest Biology and Technology* 58: 225–231.

Guo, W., S. Wang, G. Tiwari, J. Johnson and J. Tang. 2010. Temperature and moisture dependent dielectric properties of legume flour associated with dielectric heating. *LWT Food Science and Technology* 43: 193–201.

Huang, Z., F. Marra and S. Wang. 2016a. A novel strategy for improving radio frequency heating uniformity of dry food products using computational modeling. *Innovative Food Science and Emerging Technologies* 34:100–111.

Huang, Z., B. Zhang, F. Marra and S. Wang. 2016b. Computational modelling of the impact of polystyrene containers on radio frequency heating uniformity improvement for dried soybeans. *Innovative Food Science and Emerging Technologies* 33:365–380.

Huang, Z., F. Marra, J. Subbiah and S. Wang. 2018. Computer simulation for improving radio frequency (RF) heating uniformity of food products: A review, *Critical Reviews in Food Science and Nutrition* 58(6): 1033-1057.

Jones, P. and A. Rowley. 1996. Dielectric Drying. *Drying Technol.* 14: 1063–1098.

Kim, S.Y., H.G. Sagong, S.H. Choi, S. Ryu and D.H. Kang. 2012. Radio-frequency heating to inactivate *Salmonella Typhimurium* and *Escherichia coli* O157:H7 on black and red pepper spice. *International Journal of Food Microbiology* 153(1-2): 171-175.

Koral, T. 2004. Radio frequency heating and post-baking. *Biscuit World* Iss. 7(4): 1-6.

Koral, T. 2014. Industrial radio-frequency heater. In *Radio-frequency heating in food processing principles and applications*, Awuah, G.B.; Ramaswamy, H.S.; Tang, J., Ed.; CRC: New York, 93–118.

Lagunas-Solar, M., Z. Pan, N. Zeng, T. Truong, R. Khir and K. Amaratunga. 2007. Application of radiofrequency power for non-chemical disinfestation of rough rice with full retention of quality attributes. *Applied Engineering in Agriculture* 23(5): 647-654.

Lee, N.H., C. Li, X.F. Zhao and M.J. Park. 2010. Effect of pretreatment with high temperature and low humidity on drying time and prevention of checking during radio-frequency/vacuum drying of Japanese cedar pillar. *Journal of Wood Science* 56(1): 19-24.

Llave, Y., S. Liu, M. Fukuoka and N. Sakai. 2015. Computer simulation of radiofrequency defrosting of frozen foods. *Journal of Food Engineering* 152:32–42.

Llave, Y., Y. Terada, M. Fukuoka and N. Sakai. 2014. Dielectric properties of frozen tuna and analysis of defrosting using a radio-frequency system at low frequencies. *Journal of Food Engineering* 139:1–9

Macana, R.J., T.T. Moirangthem and O.D. Baik. 2018a. 50-ohm RF technology based applicator design and fabrication for disinfestation of insect pests in stored grains. ASABE Annual International Conference, Detroit, Michigan, July 29-August 1, 2018.

Macana, R.J., T.T. Moirangthem and O.D. Baik. 2018b. Principles and guidelines for installation of 50-ohm RF heating system for disinfestation of insect pests in stored grains. ASABE Annual International Conference, Detroit, Michigan, July 29-August 1, 2018.

Macana, R.J., T.T. Moirangthem and O.D. Baik. 2018c. Shielding effectiveness of electromagnetic energy from 50-ohm radio frequency heating system for disinfestation of stored grains. . ASABE Annual International Conference, Detroit, Michigan, July 29-August 1, 2018.

Macana, R.J., T.T. Moirangthem, and O.D. Baik. 2018e. Mortality of insect pests in stored grains using 50-ohm radio frequency heating system at pilot-scale. CSBE/SCGAB 2018 Annual Conference, Guelph, Ontario, July 22-25, 2018.

Macana, R.J. and O.D. Baik. 2017. Disinfestation of insect pests in stored agricultural materials using microwave and radio frequency heating: A review, *Food Reviews International* 34(5): 483-510

Nelson, S. 1996. Review and assessment of radio-frequency and microwave energy for stored-grain control. *Transaction of the ASAE* 39: 1475–1484.

Pan, L., S. Jiao, L. Gautz, K. Tu and S. Wang. 2012. Coffee bean heating uniformity and quality as influenced by radio frequency treatments for postharvest disinfestations. *Transaction of the ASAE* 55: 2293–2300.

Shrestha, B. and O.D. Baik. 2013. Radio Frequency Selective Heating of Stored-Grain Insects at 27.12 MHz: A Feasibility Study. *Biosystems Engineering* 114: 195–204.

Shrestha, B., D. Yu and O.D. Baik. 2013. Elimination of *Crystolestes Ferrungineus* in Wheat by Radio Frequency Dielectric Heating at Different Moisture Contents. *Progress of Electromagnetic Research* 139: 517–538.

Wang, Y., L. Zhang, J. Johnson, M. Gao, J. Tang, J. Powers and S. Wang. 2014. Developing hot air-assisted radio frequency drying for in-shell *Macadamia* nuts. *Food Bioprocess Technology* 7(1): 278-288.

Wang, S., J. Yue, J. Tang and B. Chen. 2005. Mathematical modelling of heating uniformity for in-shell walnuts subjected to radio frequency treatments with intermittent stirrings. *Postharvest Biology and Technology* 35: 97–107.

Wang, Y., Y. Li, S. Wang, L. Zhang, M. Gao and J. Tang. 2011. Review of dielectric drying of foods and agricultural products. *International Journal of Agricultural and Biological Engineering* 4: 1–19.

Wang, S., M. Monzon, J. Johnson, E. Mitcham and J. Tang. 2007a. Industrial-scale radio frequency treatments for insect control in walnuts: I: Heating uniformity and energy efficiency. *Postharvest Biology and Technology* 45(2): 240-246.

Wang, S., M. Monzon, J. Johnson, E. Mitcham and J. Tang. 2007b. Industrial-scale radio frequency treatments for insect control in walnuts: II: Insect mortality and product quality. *Postharvest Biology and Technology* 45(2): 247-253.

Wang, S., J. Tang, J. Johnson, E. Mitcham, J. Hansen, G. Hallman, S. Drake and Y. Wang. 2003. Dielectric properties of fruits and insect pests as related to radio frequency and microwave treatments. *Biosystems Engineering* 85: 201–212.

Wang, S., J.N. Ikediala, J. Tang, J.D. Hansen, E. Mitcham, R. Mao and B. Swanson. 2001. Radio frequency treatments to control codling moth in in-shell walnuts. *Postharvest Biology and Technology* 22: 29 –38.

Wilson, T. L. 1987. Radio-frequency dielectric heating in industry, Report No. EM-4949; Electric Power Research Institute (EPRI): Palo Alto.

Zhou, L. and S. Wang. 2016. Verification of radio frequency heating uniformity and *Sitophilus oryzae* control in rough, brown and milled rice. *Journal of Stored Products Research* 65: 40–47.

CHAPTER 6

General discussion

This chapter ties up all of the findings of the five chapters to discuss the achievements of disinfestation using electromagnetic energy. General conclusions of all the findings and recommendations for future studies were provided in this chapter to have a successful disinfestation of insect pests in stored agricultural materials using 50-ohm RF heating system.

6.1 Disinfestation using electromagnetic energy from a 50-ohm RF heating system

Radio frequency (RF) electromagnetic energy has greater penetration depth, higher energy efficiency, and a higher selective heating effect than microwave (MW) electromagnetic energy, although RF heating is slower than MW heating. RF heating has several advantages over conventional heating because this method is volumetric, fast, and chemical free.

The disinfestation of rusty grain beetle in stored wheat was possible without degrading the quality of the host materials using the advanced type of RF heating system. The results confirmed the feasibility check for RF disinfestation using the dielectric properties of the materials. The dielectric loss factor was the dominant factor affecting the power dissipation and temperature increase rate of the material (Shrestha and Baik

2013). The higher the dielectric loss factor, the faster heating on the material. The dielectric loss factor of the rusty grain beetle was 2085% to 2230% higher than the stored wheat. Hence, the insects were killed first before damaging the quality of the host grain (Macana and Baik 2017; Huang et al. 2015; Shrestha et al. 2013; Wang et al. 2003; Nelson and Charity 1972). This feasibility check for selectivity of heating with dielectric properties was only a rough estimation without considering other properties of the materials and heat transfer from hotter insect bodies to colder wheat grains during RF heating.

The 50-ohm radio frequency heating system was promising as an alternative method for disinfestation of insect pests in stored grains. However, the heating uniformity in the applicator and limited sources and knowledge about the installation of this technology were still a big challenge. The non-uniform heating of RF energy creates hot spots and cold spots in the applicator. It is a challenge to minimize the temperature difference between the hot and cold spots in the applicator, which can increase the chance of the insects surviving.

6.2 General conclusions

Successful installation and application of the 50-ohm RF heating system requires an understanding of the technology and solving problems encountered such as arcing and fire, RF leakage and tuning the system. Tuning the system is important in order to maximize the advantages of 50-ohm RF technology. The RF generator is designed to transfer maximum power to the load with the help of the matching network. The matching network converts the impedance of the load into 50-ohms so that the generator sees

similar impedance during processing. Thus, maximum power is applied to the load and no power is reflected to the generator. The arcing in an RF heating system can cause a fire that can damage the components of the system, materials to be processed, and even the entire building. The unrounded edges and corners of the electrodes and no gap between the wood table and hot electrode caused arcing at higher RF power levels because of the high electric field intensities on those portions of the electrodes. The RF leakage could interfere the function of the matching network and other surrounding digital devices. High exposure to RF leakage could result to thermal effects in our body especially to parts which are heat sensitive. RF leakage could be avoided by proper shielding of the applicator.

The disinfestation of rusty grain beetle in stored wheat grains using the advanced type of RF heating system is promising with 100% mortality rates. The complete mortalities of all life stages of the insects were achieved at an 80°C target temperature at all moisture contents of the wheat samples. The mortalities of the adult insects were numerically simulated and the results were in good agreement with the experimental mortalities with the estimated kinetic parameters. The kinetics of the thermal death of the insect pests would be useful for designing RF applicators for controlling insects in stored grains. On the other hand, the qualities of the host wheat grains were not degraded significantly at certain moisture contents after 50-ohm RF disinfestation. The effect of 50-ohm RF energy on the moisture content, bulk and particle densities, and porosity were significant. The changes, nonetheless, were advantageous for drying purpose. The colour, milling, and predictors for baking quality of the wheat grains were not significantly affected by 50-ohm RF energy when treated up to 60°C, 70°C, and 80°C at all moisture

contents (12%, 15%, and 18%), except for mixing development time (MDT), peak to height (PKH), and peak-bandwidth (PBW). The MDT and PKH were significantly affected at all moisture contents. The PBW was affected significantly at 18% MC but not at 12% and 15% MC. Nonetheless, their values were still in the most desirable range for baking. The germination of wheat kernels was not significantly affected when treated up to 60°C to 80°C at 12% MC of the samples. The germination rates at different end temperatures were 91.1% at 60°C followed by 90% at 70°C, 88.9 at 80°C, and 88.9% at the control.

There was non-uniform heating in the designed applicator at different RF power levels and moisture contents of the bulk wheat samples. The temperature increased in the horizontal direction starting from the feed point where the matching network and hot electrode were connected. With respect to vertical temperature distribution, the temperature decreased when increasing the distance from the hot electrodes and increasing the air gap. The temperature differences between the hottest and coldest spots at 3 kW to 7 kW RF power levels were 38.6°C to 39.1°C at 12% MC and 41.9°C to 43.6°C at (18% MC).

Therefore, in general, it can be concluded that disinfestation of rusty grain beetle in stored wheat grains using 50-ohm RF energy was possible and did not degrade important qualities of wheat. However, non-uniform heating and problems encountered during the installation and application of this technology should be resolved.

6.3 General recommendations

The following can be suggested for a successful disinfestation of insects in stored agricultural materials using the 50-ohm RF heating system. First, during the installation

of this technology, collaboration with the RF supplier and RF experts and understanding the important components (RF generator, 50-ohm coaxial cable, automatic matching network, and RF applicator), impedance matching relating to basic electrical parameters (voltage standing wave ratio, impedance, capacitance, inductance, and frequency), and solving problems encountered were needed for a successful installation. Second, suggestions for prevention of arcing and fire during application and installation of the 50-ohm RF heating system: a) make sure all parts are clean with no arc producing materials (carbon soot, sharp metals, over dehydrated materials) in the RF applicator; b) in running the RF generator, the empty applicator should be avoided because the components of the applicator might melt and arc because of overheating; and c) avoid direct contact between the hot electrode and dielectric materials as this might result in overheating of the product and arcing. Third, with respect to non-uniform heating in the designed RF applicator, the non-uniform temperature distribution was caused mainly by the behaviour of electromagnetic energy as a function of the position of feed point, and the presence of an air gap in the samples. Thus, it is suggested: a) the connection between the hot electrode and the matching network (feed point) should be placed at the mid-point of the electrode (35 cm) because the horizontal distribution of the temperature was more uniform from the feed point to 35 cm away; and b) mixing materials using the RF transparent auger system with smaller air gaps will improve heating uniformity during RF heating. Fourth, the disinfestation economics using the 50-ohm RF heating system need to be evaluated for practical and effective application of this technology for disinfestation of insects in stored grains.

6.4 References

- Huang, Z., L. Chen and S. Wang. 2015. Computer simulation of radio frequency selective heating of insects in soybeans. *International Journal of Heat and Mass Transfer* 90: 406-417.
- Macana, R.J. and O.D. Baik. 2017. Disinfestation of insect pests in stored agricultural materials using microwave and radio frequency heating: A review, *Food Reviews International* 34 (5): 483-510.
- Nelson, S. and L. Charity. 1972. Frequency dependence of energy absorption by insects and grain in electric fields. *Transactions of the ASAE* 6: 1099-1102.
- Shrestha, B. and O.D. Baik. 2013. Radio frequency selective heating of stored-grain insects at 27.12 MHz: A feasibility study. *Biosystems Engineering* 114: 195-204.
- Shrestha, B., D. Yu and O.D. Baik. 2013. Elimination of *Cryptolestes ferrugineus* in wheat by radio frequency dielectric heating at different moisture contents. *Progress in Electromagnetics Research* 139: 517-538.
- Wang, S., J. Tang, R. Cavalieri and D. Davis. 2003. Differential heating of insects in dried nuts and fruits associated with radio frequency and microwave treatments. *Transactions of the ASAE* 46(4): 1175-1182.